Aus der

Medizinischen Klinik und Poliklinik IV

Klinik der Universität München

Direktor: Prof. Dr. Martin Reincke

Linezolid and BTZ043 Combined Activity against M. smegmatis as a Precursor Model for New Combined Antimicrobial Treatment of M. tuberculosis

Dissertation

zum Erwerb des Doktorgrades der Medizin

an der Medizinischen Fakultät

der Ludwig-Maximilians-Universität zu München

vorgelegt von

Alexandra Burger

aus

Frankfurt am Main

Jahr

2025

Mit Genehmigung der Medizinischen Fakultät
der Universität München

Berichterstatter:	PD Dr. Andreas Wieser
Mitberichterstatter:	PD Dr. Sabine Hofmann-Thiel
	Prof. Dr. Holger Rüssmann
Mitbetreuung durch die promovierte Mitarbeiterin:	Dr. Anna-Cathrine Neumann-Cip
Dekan:	Prof. Dr. med. Thomas Gudermann
Tag der mündlichen Prüfung:	13.11.2025

Table of Contents

Summary

Annually, tuberculosis causes the death of more than 1 million people worldwide. The curative standard treatment regimen recommended by the World Health Organization since 2010 requires a quadruple combination therapy of antibiotics for two months and a double combination therapy for four months, altogether a minimum therapy of six months. A new four-month therapy regimen recommendation has been released by the WHO in 2022, which is based on a quadruple therapy for two months and triple combination for the last two months. In either treatment option, the length of the treatment complicates the lives of these patients and causes enormous social and financial burdens. Additionally, therapy-related drug side effects are common. Multidrug-resistant and extensively drug-resistant infections pose an additional threat, impeding the global end-tuberculosis strategy. The combined mechanism of action of the antibiotics is still poorly understood. Knowledge of the pharmacodynamics of the antibiotics is essential for optimized and personalized therapeutic schemes, which yet need to be developed. To address this pivotal problem, we studied the effect of the combination of the second-line antituberculotic agent linezolid and the new antimicrobial agent benzothiazinone (BTZ043) on the surrogate organism *M. smegmatis* as a model for *M. tuberculosis*. Based on current knowledge of the individual mode of action, we hypothesized that combining a protein synthesis inhibitor with an inhibitor of mycobacterial cell wall synthesis will eventually lead to synergy in killing *Mycobacteria*. We investigated the pharmacodynamics of linezolid and benzothiazinone individually in *M. smegmatis* using stable carbon isotope labeling in matrix-assisted laser desorption ionization – time of flight mass spectrometry (MALDI-TOF MS). These results provide evidence that linezolid displays an effect on protein metabolism within the first hour of application and suggest that full or nearly-full effectiveness is reached after 3 hours of exposure. This was in contrast to benzothiazinone, which reveals its earliest onset of action beginning at 3 hours and its full or nearly-full effectiveness presumably at 7.5 hours or later. Further, we investigated the CFU count and bacterial reduction under increasing antimicrobial compound concentrations and various exposure times, first individually and then in combination. Our *in vitro* results support the theory that linezolid and benzothiazinone applied in an optimized scheme demonstrate synergistic effects against *M. smegmatis.* The results showed that a continuous linezolid trough level of 2 x MIC (c = 1.0 µg/mL) combined with a short exposure to a high concentration of benzothiazinone at 20 x MIC (c = 94.6 ng/mL) after a 3-hour pre-incubation period with linezolid is sufficient for an efficient combination of the two agents.

This challenges the imperative usage of a continuous high-dosage administration of benzothiazinone when administered in combination with other antimicrobial agents. Last, our analysis was complemented by micrographs taken with the scanning electron microscope. Our results revealed morphological changes in *M. smegmatis* exposed to the combination of linezolid and benzothiazinone that supported the hypothesis that a short benzothiazinone exposure is not inferior to a continuous exposure in a combined application. Ultimately, our experimental evidence of the effect of the combined antibiotic agents on *Mycobacteria* and their metabolic dynamics deepens our understanding of linezolid and benzothiazinone and provides a promising basis for future research on improved tuberculosis therapeutic schemes.

Zusammenfassung

Weltweit verursacht die Tuberkulose noch immer den Tod von über 1 Millionen Menschen jedes Jahr. Die kurative Standardtherapie der Tuberkulose erfordert eine Kombination aus vier Antibiotika, die anfänglich über zwei Monate eingenommen werden muss und mit zwei Antibiotika über weitere vier Monate fortgeführt wird, sodass sich der Behandlungszeitraum über sechs Monate erstreckt. Eine neue Empfehlung für eine viermonatige Kombination wurde von der WHO im Jahre 2022 veröffentlicht, welche auf einer zweimonatigen Kombination aus vier Antibiotika und einer weiteren zweimonatige Phase aus drei Antibiotika beruht. In beiden Fällen geht die lange Dauer der Therapie für die Patienten nicht nur mit großen psychosozialen Belastungen einher, sondern stellt aufgrund der Verbreitung der Tuberkulose in insbesondere ressourcenarmen Ländern für viele Patienten eine enorme finanzielle Bürde dar und weist zudem viele Arzneimittelnebenwirkungen auf. Weiterhin werden Infektionen mit multi-resistenten und extrem-resistenten Stämmen eine immer größere Herausforderung für die Therapie und gefährden die WHO-Strategie zur weltweiten Ausrottung der Tuberkulose.

Obwohl die Wirkmechanismen der einzelnen Antibiotika inzwischen recht gut erforscht sind, sind die derzeitigen Kenntnisse über die *kombinierten* Wirkmechanismen der Antibiotika unzureichend. Für die Entwicklung individuell angepasster Therapieschemata ist ein tieferes Verständnis über die Pharmakodynamik kombinierter Antibiotikatherapien jedoch unerlässlich. Wir beschäftigten uns mit dieser wichtigen Thematik, indem wir die kombinierte Wirkung der Antibiotika Linezolid und Benzothiazinone (BTZ043) an *M. smegmatis* als Modell für *M. tuberculosis* untersuchten. Linezolid ist ein Antibiotikum, welches bereits fest in der Zweitlinientherapie bei Infektionen mit resistenten Tuberkulose-Stämmen eingesetzt wird, während sich BTZ043 als neuer Wirkstoff gegen *M. tuberculosis* noch in der klinischen Testphase befindet. Aufgrund der Kenntnisse über die individuellen Wirkmechanismen beider Substanzen vermuteten wir, dass die Hemmung der Protein-Biosynthese durch Linezolid, kombiniert mit der Inhibition der mykobakteriellen Zellwandsynthese (BTZ043) zu einer synergistischen antibiotischen Wirkung am Modellorganismus *M. smegmatis* führen würde. Wir untersuchten deswegen zunächst die Wirkung der einzelnen Antibiotika auf den Proteinmetabolismus von *M. smegmatis* anhand stabiler Kohlenstoffisotopenmarkierung in der *matrix-assisted laser desorption ionization – time of flight mass spectrometry* (MALDI-TOF MS). Die Ergebnisse dieser Experimente zeigten, dass Linezolid bereits innerhalb der ersten Stunde nachweisliche Effekte auf den Proteinmetabolismus zeigt, und legten nahe, dass der maximale oder fast-maximale Effekt

nach drei Stunden Exposition eintritt, während der Wirkungsbeginn von BTZ043 auf die beobachteten Analyten frühestens nach drei Stunden nachweisbar ist und ein Wirkmaximum bei 7.5 oder mehr Stunden vermuten lässt. Weiterhin untersuchten wir das bakterielle Wachstum unter dem Einfluss von Linezolid und Benzothiazinone anhand der KBE-Auszählung und Berechnung des Reduktionsfaktors bei zunehmenden Konzentrationen und verschiedenen Expositionszeiten, einzeln und in der Kombination. Die Ergebnisse der *in-vitro* Experimente unterstützen die Hypothese, dass die beiden Antibiotika, in einem optimierten Schema angewandt, synergistisch gegen *M. smegmatis* wirken. Unterstützt durch die Ergebnisse in der MALDI-TOF MS Analyse fanden wir heraus, dass eine effiziente Kombination der beiden Wirkstoffe eine sehr hohe, jedoch lediglich kurzzeitige Benzothiazinone-Dosis in 20-facher MIC (c = 94,6 ng/mL) erfordert, wenn die Kultur vorher mit einem kontinuierlichen, niedrigen Linezolid-Spiegel in 2-facher MIC (c = 1,0 µg/mL) mit einer Vorinkubationszeit von drei Stunden präinkubiert wurde. In der Zusammenschau wird dadurch in der kombinierten Anwendung mit anderen Antibiotika die Notwendigkeit einer kontinuierlichen, hochdosierten Verabreichung von Benzothiazinone, wie bisher angenommen, in Frage gestellt. Die Analyse wurde schließlich durch mikroskopische Aufnahmen mit dem Rasterelektronenmikroskop (REM) von *M. smegmatis* unter dem Einfluss der beiden Antibiotika ergänzt. Die morphologischen Veränderungen von *M. smegmatis*, welcher der Kombination der beiden Antibiotika ausgesetzt war, unterstützen die Annahme, dass die kurze, hochdosierte Benzothiazinone-Konzentration in der kombinierten Anwendung mit Linezolid einer kontinuierlich hochdosierten Exposition nicht unterlegen ist.

Schlussendlich bieten unsere Ergebnisse ein tieferes Verständnis für die kombinierte Wirkung von Linezolid und Benzothiazinone auf Mykobakterien und ihren Metabolismus, und liefern eine vielversprechende Grundlage für die zukünftige Forschung und Entwicklung verbesserter Therapieschemata für die Tuberkulose.

1 Introduction

1.1 Tuberculosis

1.1.1 Epidemiology

Tuberculosis is an infectious disease, with an estimated 10.0 million new cases among the world population in 2018 (World Health Organization, 2019). Despite available antimicrobial chemotherapy and its declining incidence, it is the deadliest of all infectious diseases caused by a single agent, causing the death of up to 1.3 million people worldwide in 2016 (World Health Organization, 2017). Tuberculosis accounts for 33% of deaths of HIV-coinfected patients globally (World Health Organization, 2019). One third of the world population is estimated to be a carrier of a latent tuberculosis infection with only 5% to 10% of infected patients developing active tuberculosis (World Health Organization, 2017). Since being discovered in 1882 by Robert Koch, it is known that tuberculosis is caused by the bacillus *Mycobacterium (M.) tuberculosis* (Sakula, 1982). Tuberculosis primarily affects the lungs (pulmonary tuberculosis), but can disseminate to nearly every organ in the human body and cause extrapulmonary tuberculosis (Brodhun, Altmann, Hauer, Fiebig, & Haas, 2015; Golden, 2005; Suárez et al., 2019).

1.1.2 Transmission

Transmission occurs primarily through inhalation of infectious droplet nuclei which are produced by coughing, sneezing, shouting, singing or any other forceful expiratory maneuver (Turner & Bothamley, 2014). It is thought that transmission occurs via clustering in space or over time (Churchyard et al., 2017). While there is a lot of evidence showing that there is a high risk of transmitting drug-susceptible and drug-resistant tuberculosis via close contacts and in households (G. J. Fox, Barry, Britton, & Marks, 2013; Shah, Yuen, Heo, Tolman, & Becerra, 2013), it is now thought that in high burden areas transmission is more likely to happen outside the household in public transport, schools, workplaces and healthcare facilities (Andrews, Morrow, Walensky, & Wood, 2014; Martinez et al., 2017; Yates et al., 2016). There is historical evidence supporting that socioeconomic conditions such as better nutrition and high living standards are key factors in improved tuberculosis control (Hermans, Horsburgh, & Wood, 2015; Lienhardt et al., 2012). Even though childhood vaccination with *Bacillus Calmette-Guerin* (BCG) was part of immunization programs in 153 countries around the world in 2018 (World Health Organization, 2019), its efficacy against pulmonary tuberculosis in adults remains poor (Skeiky & Sadoff, 2006).

1.1.3 Pathogenesis

After inhalation, *M. tuberculosis* growth takes place preferentially in well-ventilated upper parts of the lung, specifically in alveolar macrophages (J. L. Flynn, Chan, & Lin, 2011; Suárez et al., 2019). In the immunocompetent patient, host immune cells, especially macrophages and T-lymphocytes, deal with the infectious agent by forming large cell granulomas which macroscopically appear like small nodes of 1 mm to > 2 cm (J. L. Flynn et al., 2011). Granulomas are marked by an epithelioid lining border consistent of merged macrophages, followed by a lymphocytic cuff and inner necrotic and acellular region, the caesum (J. L. Flynn et al., 2011; Williams & Williams, 1983). It is now known that the granulomas are dynamic structures constituting both an innate immune response and a complex acquired immune response (Ehlers & Schaible, 2013; O'Garra et al., 2013; Orme & Basaraba, 2014). Granulomatous lesions are considered heterogenous in morphology, structure and host outcome (Cadena, Fortune, & Flynn, 2017; Ehlers & Schaible, 2013). It has long been assumed that the bacteria are contained in the granuloma and are inhibited from spreading throughout the lung and the body (J. A. L. Flynn, 2004). However, the protective versus pathological character of the granuloma for the host has been discussed in various studies (Orme & Basaraba, 2014). It could be shown that existing granulomas containing bacteria are not closed off from the environment, and rather seem to attract cells that carry bacteria from a new infection (Cosma, Humbert, & Ramakrishnan, 2004; J. A. L. Flynn, 2004). The infection can proceed into a latent tuberculosis infection where the bacillus is kept under control by being "locked" into its lesions (Williams & Williams, 1983) and years can pass with no diagnostic test revealing signs of active tuberculosis (Suárez et al., 2019). In immunodeficient patients, especially HIV-infected patients, or in patients with other vulnerability factors such as malnutrition, immunosuppressant medications such as corticosteroids or infliximab, genetic predisposition, diabetes and tobacco use, the latent state can transition into an active tuberculosis at any time (Horsburgh, 2014; Schurz, Daya, Möller, Hoal, & Salie, 2015; World Health Organization, 2017). Further studies reveal that *M. tuberculosis* may survive in other loci of the body without typical formation of granuloma and can create an extrapulmonary outburst even without lung involvement (Barrios-Payán et al., 2012).

1.1.4 Clinical Presentation

Active pulmonary tuberculosis most typically presents with cough, hemoptysis, fever, night sweats, weight loss, and general weakness (Suárez et al., 2019). However, it can also present itself with many other symptoms, depending on which organ is affected (Schaberg et al., 2017).

The worst-case scenario is the miliary tuberculosis where the mycobacteria have disseminated systematically into extrapulmonary organs such as liver, kidney, spleen, bones and skin, setting up multiple macroscopically white foci causing an eminent threat to the life of the patient (Golden, 2005). Equally dangerous is tuberculous meningitis or even septic acute tuberculosis (Golden, 2005). Miliary tuberculosis and tuberculous meningitis are commonly seen in HIV-infected patients and children (Ahmad et al., 2018; Dodd, Yuen, Sismanidis, Seddon, & Jenkins, 2017; Golden, 2005; Suárez et al., 2019).

1.1.5 Diagnosis and Treatment

To confirm the diagnosis of an active tuberculosis disease it is requisite to provide microscopical, biomolecular or cultural evidence of *M. tuberculosis* (Schaberg et al., 2017; World Health Organization, 2019). Among these techniques, cultural evidence is the gold standard for diagnosis and therefore, should always be pursued when suspecting an infection with *M. tuberculosis* (Schaberg et al., 2017). Cultural evidence may become positive only after several weeks and often, multiple sputum cultures are necessary (Suárez et al., 2019). If pulmonary tuberculosis is suspected, morning sputum smear is the most important sample material (Schaberg et al., 2017). Recently confirmed by the WHO, the Xpert MTB/RIF, a molecular test, allows sensitive detection of tuberculosis and rifampin resistance from sputum smear within hours (Boehme et al., 2010). A highly infectious, open pulmonary tuberculosis can be excluded if three separately collected sputum samples are negative for acid-fast bacilli in microscopy (Schaberg et al., 2017; Suárez et al., 2019). To exclude an open pulmonary tuberculosis, three separately collected, negative sputum cultures are required (Suárez et al., 2019). However, depending on the suspected infection site, retrieval of material through broncho-alveolar lavage, from urine, cerebrospinal fluid, blood or through biopsy of the lung lesion, bone marrow, skin, gastric or intestinal mucosa may be necessary (Schaberg et al., 2017). A biopsy of a granuloma showing the histopathological structure of a caseating granuloma with central necrosis and a lymphocytic cuff is pathognomonic for tuberculosis (Dheda et al., 2005; Dheda, Schwander, Zhu, Van Zyl-Smit, & Zhang, 2010).

Tuberculosis is typically diagnosed by chest X-ray and multiple sputum cultures in search for acid-fast bacilli (Schaberg et al., 2017). Under certain circumstances, for example, if lesions are not clearly identifiable in the chest X-ray, other imaging such as computer tomography of the chest may become necessary (Schaberg et al., 2017). In some countries, the tuberculin skin test (TST) and Interferon-Gamma-Release Assays (IGRAs) are used for initial assessment, even

though it could be shown that in low- and middle-income settings, they have no value in diagnosing active TB – especially in HIV-coinfected adults (Metcalfe et al., 2011). The IGRA is routinely being used to detect latent tuberculosis infection (LTBI) especially in persons who have been in close contact to patients with contagious pulmonary tuberculosis infection (Suárez et al., 2019). Its specificity in diagnosing LTBI, estimated among individuals in settings with low tuberculosis incidence (high-income settings) is known to be high (Menzies, Pai, & Zwerling, 2008). LTBI is defined as an *M. tuberculosis* infection with persistence of viable bacteria without symptoms or clinical evidence (O'Garra et al., 2013; Schaberg et al., 2017). Persons with LTBI are not infectious and they are usually detected by a positive result on immunological testing such as IGRA and/or TST (Mack et al., 2009; Pai et al., 2014). Both tests are based on cellular immune response, and as such, are incapable of distinguishing between LTBI and active disease (Pai & Menzies, 2007). A total of 5 % to 10 % of IGRA positive cases will develop active tuberculosis disease during their lifetime (O'Garra et al., 2013; Vynnycky & Fine, 2000). It has been acknowledged that within the two seemingly binary states of LTBI and active tuberculosis, in fact, there is a spectrum of host responses with a highly dynamic diversity of pathologies (Barry et al., 2009; Cadena et al., 2017; Ehlers & Schaible, 2013).

Since 2010, the WHO guidelines have recommended that patients infected with active, drug-susceptible tuberculosis require antimicrobial treatment with the quadruple therapy consisting of isoniazid, rifampicin, pyrazinamide and ethambutol for two months in the initial phase and treatment with rifampicin and isoniazid for the following four months in the continuation phase (Kerantzas & Jacobs, 2017; World Health Organization, 2019). This treatment is well-known and is based on the TB treatment studies performed by the British Medical Research Council in the second half of the 20th century (W. Fox, Ellard, & Mitchison, 1999; WHO consolidated guidelines on tuberculosis, 2022). It has been approximated that up to 85 % of patients have a successful treatment outcome undergoing this standard therapy (WHO consolidated guidelines on tuberculosis, 2022). But the lengthy treatment poses a high burden to patients' lives and health systems (World Health Organization, 2017). Trying to reduce treatment time to less than six months had not been successful in the past (Gillespie et al., 2014; Johnson et al., 2009). Recently though, a study was performed that demonstrated that the efficacy of a 4-month rifapentine-based regimen containing moxifloxacin was noninferior to the standard 6-month regimen (Dorman et al., 2021). This regimen consists of two months with isoniazid, rifapentine, moxifloxacin and pyrazinamide, followed by two months of isoniazid, rifapentine and

moxifloxacin and was published as a conditional recommendation with moderate certainty of evidence in 2022 (WHO consolidated guidelines on tuberculosis, 2022). Due to factors such as the substantially higher costs of the 4-month regimen and higher pill burden, further research is required on resource implications, cost-effectiveness and overall feasibility (WHO consolidated guidelines on tuberculosis, 2022). One indicator for treatment success is time to first culture-negative sputum (Eurosurveillance editorial Team, 2013; Lange et al., 2014). Thereby, two individual cultures must be taken at least 30 days apart and when both appear negative, the date of the first sputum sample is determined as the date of culture conversion (Lange et al., 2014).

1.1.6 Challenges

Particularly challenging is the worldwide increase of cases of multidrug-resistant tuberculosis (MDR-TB), defined as tuberculosis with resistance to the two most effective first-line antimicrobial agents isoniazid and rifampin (World Health Organization, 2019). MDR-TB requires treatment with a second-line regimen (World Health Organization, 2019). Including all the incident cases of tuberculosis that were resistant to at least rifampin in 2018 (MDR/RR-TB), a rough 484,000 cases could be estimated. About 50% of these cases (MDR/RR-TB) occurred in India, China and the Russian Federation (World Health Organization, 2019). Globally, there were about 214,000 deaths from MDR/RR-TB in 2018 (World Health Organization, 2019). Regimens for treating MDR-TB include therapies of 20 months duration and longer, posing an additional challenge to treatment success rates (D Falzon et al., 2011; D Falzon et al., 2017). It was suggested that the optimal number of drugs in the initiation phase were five, and four in the continuation phase (Ahmad et al., 2018). It was recommended by the WHO to start these regimens with a combination of bedaquiline, fluoroquinolones and linezolid plus one or more agents likely to be effective (World Health Organization, 2022). The successful treatment rates of MDR-TB cases range from 54 % to 61% (Ahmad et al., 2018; World Health Organization, 2017) indicating that treatment options are still suboptimal**.** Another challenge poses the group of patients with extensively drug-resistant tuberculosis (XDR-TB), defined as MDR-TB plus resistance to at least one of the fluoroquinolones and one injectable agent used in MDR-TB treatment, such as amikacin (World Health Organization, 2019). 13,068 cases of XDR were reported by 81 countries in 2018, whereas it must be mentioned that only 59% of notified MDR/RR-TB patients were tested for XDR-TB (World Health Organization, 2019), so the real numbers are most likely much higher. The five countries reporting most cases were Belarus, India, the

Russian Federation, South Africa and Ukraine (World Health Organization, 2019). Among patients with XDR-TB, the highest failure and relapse rates were found (Ahmad et al., 2018) with a treatment success rate of approximately 39% in 2018 (World Health Organization, 2019). Meanwhile, the oxazolidinone linezolid has been widely used in drug-resistant tuberculosis and has taken the place as a core element in antimicrobial treatment of MDR-TB (Ahmad et al., 2018; World Health Organization, 2022).

Although the influence of antimicrobials for the treatment of tuberculosis caused by *M. tuberculosis* has been studied since 1944 (Kerantzas & Jacobs, 2017), it remains unclear when or if the combination of antimicrobial therapy kills *M. tuberculosis* and the patient is *de facto* cured from the infection.

1.2 *Mycobacteria*

Mycobacteria are a genus of the family *Mycobacteriaceae* of the suborder *Corynebacterinea*e belonging to the phylum *Actinobacteria* (Fuchs et al., 2014). Even though there are roughly more than 190 identified species, a majority is represented by environmental, non-pathogenic mycobacteria that can be found in soil, and decomposing biological matter (King et al., 2017). Mycobacteria are widely known for their pathogenic species *M. tuberculosis, M. bovis* and *M. leprae* (King et al., 2017). By sequencing their 16S RNA, mycobacteria can phylogenetically be classified into rapidly-growing species such as *M. fortuitum* clade, *M. smegmatis*, *M. chelonae* clade and *M. abscessus* clade, and slowly-growing species (> 16 hours doubling time) such as mycobacteria from the *Mycobacterium-tuberculosis* complex, *Mycobacterium avium* complex and the *Mycobacterium kansasii* clade (Fuchs et al., 2014; Stahl & Urbance, 1990). Mycobacteria are obligatory aerobic, rod-shaped, acid-fast, non-motile bacteria and characterized by a uniquely complex cell wall which consists of a cell membrane, an inner layer and an outer layer (Cook et al., 2009; Hett & Rubin, 2008). Generally, mycobacteria are classified as gram-positive organisms despite carrying both gram-negative and gram-positive traits (Hett & Rubin, 2008). While mycobacteria do not retain Gram stain, DNA-based taxonomy categorizes mycobacteria as gram-positive organisms as most mycobacterial genes show high resemblance to genes in other gram-positive bacteria such as *Bacilli* (Hett & Rubin, 2008). The inner layer of the cell wall forms an insoluble complex with three different components: from inwards directly next to the cell membrane towards outwards, we can find a thick peptidoglycan layer similar to that seen in gram-positive bacteria, which is covalently linked to arabinogalactan (Hett & Rubin, 2008). Arabinogalactan is a polysaccharide which serves as an anchor to the last main component, the

mycolic acids (Hett & Rubin, 2008). Mycolic acids consist of 60 to 90 carbons per chain and are the primary determinant for the impermeability of the cell wall (Hett & Rubin, 2008). They account for the natural resistance of mycobacteria to many antibiotics as they are little permeable to hydrophilic compounds (Hett & Rubin, 2008). Intercalated within the lipid environment follows the outer compartment, a layer consisting of embedded lipids and proteins, which can also function as signaling molecules of mycobacteria (P. J. Brennan, 2003). It is thought that hydrophilic solutes enter the cell primarily through porins (Cook et al., 2009; Niederweis et al., 1999). In contrast to other rod-shaped bacteria which grow at the center, it is known that mycobacteria grow at their tips and undergo snapping cell division (Daniel & Errington, 2003; Thanky, Young, & Robertson, 2007). This was concluded from demonstrating that nascent peptidoglycan, the integral cell wall element, could be visualized at the of poles of mycobacteria (Hett & Rubin, 2008).

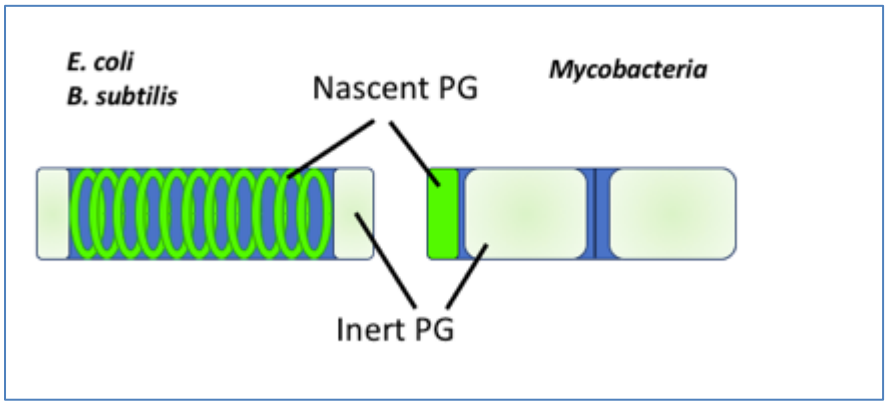

Figure 1-1: Localization of nascent and inert peptidoglycan (PG) in different bacteria.

Adapted from Journals.ASM.org (Hett & Rubin, 2008).

The challenges that the cell wall faces during cell division resemble the “Achilles heel” of the mycobacteria which could explain the lack of growth during latency and presumably their ability to survive host inflammatory mediators and antibiotic treatment (Hett & Rubin, 2008). A reversed correlation between virulence and growth rate has been hypothesized as all pathogenic strains are thought to be slow growers, but the theory remains unproved (Hett & Rubin, 2008).

In vitro doubling time of *M. tuberculosis* ranges from 12 hours to 54 hours (Gill et al., 2009; James, Williams, & Marsh, 2000; Larsen, Biermann, & Jacobs, 2007). It takes 3 to 6 weeks to determine growth on solid media (Merkov, 2006). Previously, it has been assumed that in chronic tuberculosis, mycobacterial growth reaches a static equilibrium with non-replicating

persistence (Muñoz-Elías et al., 2005; Rees & Hart, 1961). In a study initiated to better understand the replication of pathogens during latency, this assumption has been challenged by showing in the mouse model that substantial ongoing replication still takes places during latent infection (Gill et al., 2009). This assumption is further supported by the fact that isoniazid, the first-line agent to treat latent tuberculosis, was not effective against non-replicating bacilli *in vivo* (Kanai, 1966). Optimal growth medium for mycobacteria comprises either glycerol or glucose as a carbon source (Larsen et al., 2007).

The saprophyte *M. smegmatis* is widely used as a surrogate organism in order to outflank the difficulty cultivating *M. tuberculosis* or *M. bovis* BCG (Gill et al., 2009; R. Wang, Prince, & Marcotte, 2005). In contrast to *M. tuberculosis*, it is non-pathogenic, has a doubling time of 3 to 4 hours, and forms colonies in 3 to 4 days (Akinola, 2013; Fuchs et al., 2014; Merkov, 2006). In a variety of studies, *M. smegmatis* has been used as a prior screen for the efficacy of compounds against *M. tuberculosis* (Lu & Drlica, 2003). Due to their similar resistance/susceptibility profile in terms of MIC, it has been suggested that *M. smegmatis* may serve as a highly specific screening surrogate to select compounds that are active against MDR-TB (Chaturvedi, Dwivedi, Tripathi, & Sinha, 2007).

1.3 Bacterial Growth and Susceptibility Studies

1.3.1 Minimal Inhibitory Concentration

The Minimal Inhibitory Concentration (MIC) is defined as the lowest concentration of a compound to prevent growth/multiplication of the bacteria under defined laboratory conditions (Pankey & Sabath, 2004; Wiegand, Hilpert, & Hancock, 2008). It can be identified by various methods such as agar and broth dilution methods, or photometry (Wiegand et al., 2008). It is an *in vitro* parameter to classify a microorganism as drug-susceptible or resistant to a certain antibiotic agent and can be used to monitor microbial drug resistance (Wiegand et al., 2008). The MIC value does not provide information about the mode of action (or information on bactericidal vs. bacteriostatic activity) and the value alone is sometimes a poor predictor of *in vivo* efficacy of the antibiotic compound (Wiegand et al., 2008).

1.3.2 Bacterial Killing and Logarithmic Reductions

Logarithmic (log) reductions on the base of 10 are a standard to quantify disinfection and refer to the efficiency of a compound to reduce a pathogen (EPA, 2012). Log reductions are commonly denoted by the reduction factor. The greater the reduction factor, the more effective is the compound in bacterial killing. Log reductions of a pathogen are determined by plating the

bacteria exposed to the compound and comparing the CFU count to either a reference group that was grown without antimicrobial exposure (wild type) or to the original bacterial burden ("Log and Percent Reductions in Microbiology and Antimicrobial Testing | Microchem Laboratory," n.d.). A log reduction of 1 refers to a 10-fold reduction ($1:10^1$) or 90%. The reduction factor is the value to which the power of the number was raised, or else the number of log reductions.

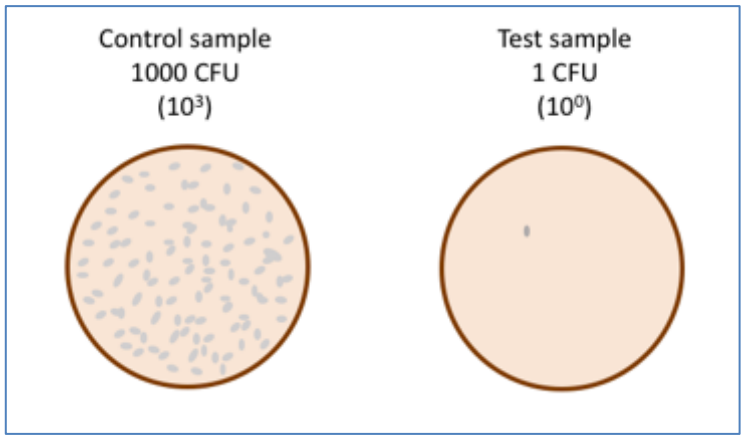

Figure 1-2: Log reduction.

Example for log reductions and reductions factor. Test sample 1 CFU; control 1000 CFU. Relation is $1/1000 = 1/10^3$, hence 3 log reductions. Reduction factor is 3.

Categorizing a compound as bacteriostatic or bactericidal may provide valuable information, but for prediction of clinical efficacy it is requisite to consider pharmacodynamic and pharmacokinetic data (Pankey & Sabath, 2004). Furthermore, the distinction between the two may appear clear under strict *in vitro* laboratory conditions, but terming a particular compound bactericidal or bacteriostatic may apply only to the tested bacteria (and not against all bacteria) and in a certain concentration range, it may be also inconsistent in the clinical context (Pankey & Sabath, 2004).

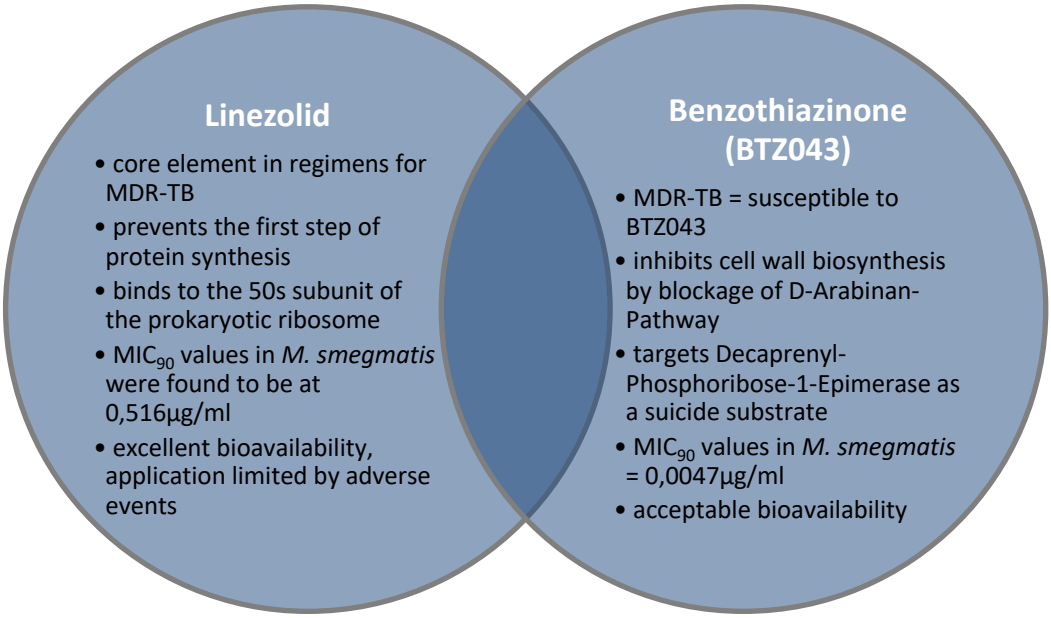

1.4 Linezolid

Linezolid, sold by the commercial name "Zyvoxid", was released to the market in April 2000 and is an Oxazolidinone traditionally used as a reserve chemotherapeutic agent in infections with resistant *Staphylococcus aureus* strains and other gram-positive cocci (Champney & Miller, 2002). Its mechanism of action has been examined in various studies and it is understood that linezolid binds to the ribosomal 50S subunit of the prokaryotic ribosome, thereby inhibiting the formation of ternary complex between t-RNA, 30S subunit and mRNA which is requisite for the initiation of translation (Champney & Miller, 2002; Lin, Murray, Vidmar, & Marotti, 1997; Matassova et al., 1999; Shinabarger et al., 1997; Swaney, Aoki, Ganoza, & Shinabarger, 1998). Most MDR- and XDR-TB strains are still susceptible to linezolid, which is why linezolid has become part of the core of second-line regimen for MDR and XDR-TB (Ahmad et al., 2018; Dennis Falzon et al., 2017) where it has shown excellent efficacy (Agyeman & Ofori-Asenso, 2016; Chaiprasert et al., 2014; Lee et al., 2012; Riccardi, Pasca, & Buroni, 2009; Sotgiu et al., 2012). Linezolid is a synthetic agent of excellent oral bioavailability, its oral bioavailability being nearly equivalent to intravenous bioavailability, and good pulmonary and soft tissue penetration (Boselli et al., 2005; Conte, Golden, Kipps, & Zurlinden, 2002; Dehghanyar et al., 2005; Stalker & Jungbluth, 2003; Welshman, Sisson, Jungbluth, Stalker, & Hopkins, 2001). Its pharmacokinetic profile has been well-investigated, finding that linezolid is rapidly absorbed, reaches its C_{max} after 1-2 hours usually and is found 30% protein-bound in plasma (Stalker & Jungbluth, 2003). For treatment of XDR-TB or MDR-TB, different modes of administration are being discussed, such as applying 300 mg or 600 mg per day (Koh et al., 2009; Lee et al., 2012; Song et

al., 2015; Sotgiu et al., 2012). Lower concentrations are better tolerated but may bear the risk of selecting linezolid-resistant *M. tuberculosis* strains (Lee et al., 2012). A mechanism of resistance could first be examined in *M. smegmatis* and in *M. tuberculosis in vitro* isolates where mutations in the ribosomal protein L3 or the 23S rRNA (the linezolid binding site) were found to create MICs of 64 µg/mL and higher, whereas another mechanism of resistance – supposedly non-ribosomal – was assumed in resistant strains with MICs of 4 - 8 µg/mL (Hillemann, Rüsch-Gerdes, & Richter, 2008; Sander et al., 2002). DNA sequencing of clinical isolates in resistant tuberculosis cases later indeed also revealed L3 or 23S rRNA mutations (Lee et al., 2012). Other presumed mechanisms of resistance in mycobacteria are efflux pumps, response regulators or target-modifying enzymes (Hett & Rubin, 2008). Generally, the antibiotic efficacy of oxazolidinones have previously been described as time-dependent (Pankey & Sabath, 2004).

General side effects of linezolid include but are not limited to nausea, dizziness, headaches, vomiting, diarrhea, and tiredness (Roger, Roberts, & Muller, 2018; Sotgiu et al., 2012). Most common specific adverse reactions are related to prolonged administration of more than 28 days which is the originally recommended maximum administration period of linezolid and which is commonly exceeded when used for treatment of MDR- or XDR-TB (Lee et al., 2012). These specific adverse events include optic- or peripheral neuropathy, serotonin syndrome, lactic acidosis and anemia or thrombocytopenia due to myelosuppression (Boak et al., 2014; Kenreigh et al., 2016; Kishor, Dhasmana, Kamble, & Sahu, 2015; Leader, Hackett, Allan, & Carter, 2018; Roger et al., 2018; Zhang et al., 2015). These specific adverse events were reported to go along with a trough level of > 2 µg/mL over at least three weeks (Song et al., 2015). The underlying cause of the neuropathy and observed thrombocytopenia by linezolid is seen in the structural resemblance between bacterial and human mitochondrial ribosomes, ultimately leading to mitochondrial dysfunction by the inhibition of mitochondrial protein synthesis (De Vriese et al., 2006; Garrabou et al., 2017; Nagiec et al., 2005; Soriano, Miró, & Mensa, 2005; Srivastava et al., 2017). The side effects were often so severe that therapy had to be discontinued; with adverse effects usually disappearing or stabilizing with discontinuation of treatment (Kenreigh et al., 2016; Tang et al., 2015; Zahedi Bialvaei, Rahbar, Yousefi, Asgharzadeh, & Samadi Kafil, 2017). Due to especially long treatment times and limited tolerability of linezolid, the administration of linezolid for XDR-TB and MDR-TB cases is a balancing act between efficacy, tolerability and safety (Agyeman & Ofori-Asenso, 2016; Maartens & Benson, 2015; Sotgiu

et al., 2012; Tang et al., 2015; Zhang et al., 2015). An optimal clinical regimen is yet to be determined (Boak et al., 2014; Roger et al., 2018).

1.5 Benzothiazinone

A novel group of antimycobacterial drugs, the 1.3-benzothiazin-4-ones, has entered the tuberculosis treatment drug pipeline. One of the most popular compounds is known as BTZ043, here referred to as benzothiazinone (World Health Organization, 2019).

BTZ043 inhibits the mycobacterial cell wall synthesis by targeting the enzyme decaprenylphosphoryl-β-D-ribose 2'-Epimerase (DprE1) (Makarov et al., 2009). DprE1 is an enzyme involved in the arabinose pathway (Makarov et al., 2009) as it catalyzes the reaction of decaprenylphosphoryl-β-D-ribofuranose (DPR) to decaprenylphosphoryl-β-D-arabinose (DPA), and thus providing D-arabinose which is the only donor source for the production of arabinogalactan, an essential component of the mycobacterial cell wall (Mikušová et al., 2005).

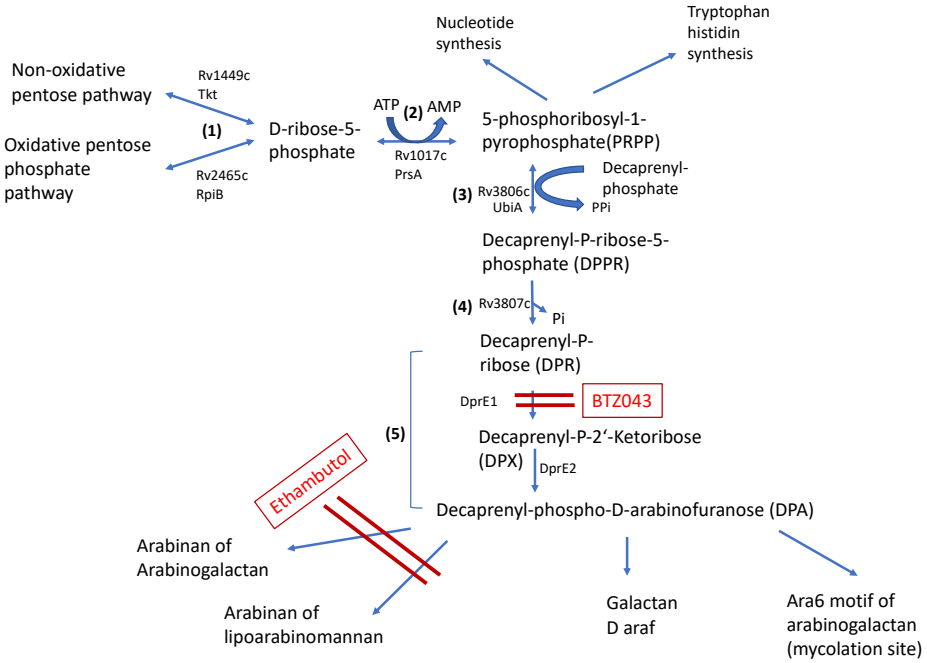

Figure 1-3: Decaprenyl-Phospho-D-arabinofuranose pathway.

Schematic representation of the Decaprenyl-Phospho-D-arabinofuranose biosynthetic pathway. Adapted from (Kolly et al., 2014; Wolucka, 2008). Presumably, the biosynthesis of Decaprenyl-phospho-D-arabinofuranose takes place in five steps. (1) D-ribose 5-phosphate (R5P) is isomerized of D-ribulose 5-phosphate from the oxidative pentose phosphate pathway by Rv2465c (RpiB; (Roos et al., 2004; Roos, Mariano, Kowalinski, Salmon, & Mowbray, 2008) or produced by the transketolase Rv1449c (Tkt) from intermediates of the non-oxidative pentose phosphate pathway (Fullam, Pojer, Bergfors, Jones, & Cole, 2012). (2) R5P and ATP are catalyzed by the phosphoribosyl pyrophosphate synthetase (Rv1017c) into 5-phosphoribosyl 1-pyrophosphate (PRPP) and AMP (PrsA; (Luke J. Alderwick et al., 2011; Lucarelli et al., 2010). (3) UbiA (Rv3806c) catalyzes the reaction of activated PRPP and the decaprenyl phosphate acceptor to 5′-phosphoribosyl-monophospho-decaprenol (DPPR; (Huang et al., 2005; Scherman et al., 1996). (4) Rv3807c produces decaprenyl-phosphoribose (DPR) by removing the 5′-phosphate group of

DPPR. (5) DPR is then 2′-epimerized to DPA in two steps via a decaprenyl phospho-2′-keto-D-arabinose (DPX) intermediate Rv3790 (DprE1) andRv3791 (DprE2)(Mikušová et al., 2005).

Arabinogalactan is crucial for cell wall integrity because it covalently links the mycolic acids of the outer cell wall surface to the peptidogalactan of the inner cell wall surface (L.J. Alderwick, Birch, Mishra, Eggeling, & Besra, 2007; Mikušová et al., 2005).

It is thought that BTZ043 is activated through reduction of its nitro group by DprE1 (Neres et al., 2012; Trefzer et al., 2010) and covalently binds to the cysteine residue 378 (Makarov et al., 2009; Sarah M. Batt, Talat Jabeen, Veemal Bhowruth, Lee Quill, Peter A. Lund, Lothar Eggeling, Luke J. Alderwick, Klaus Fütterer, 2012; Trefzer et al., 2010) in *M. tuberculosis* (corresponding cysteine 394 in *M. smegmatis* (Neres et al., 2012)) situated in the active site of the molecule DprE1, eventually destroying its catalytic function and inhibiting the enzyme irreversibly as a suicidal substrate (Trefzer et al., 2012). It blocks the enzyme in a near-quantitative manner, meaning in a ratio of nearly 1:1 (Trefzer et al., 2012), which could explain its exceptionally high potency with MICs ranging at 1ng/mL for *M. tuberculosis* and 4ng/mL for *M. smegmatis,* respectively (Makarov et al., 2009).

It is thought that the lipophilic character of BTZ043 is crucial to its high efficacy, as a correlation has been described between lipophilicity and antimycobacterial activity (Patrick J. Brennan & Nikaido, 1995; Makarov et al., 2009; Yajko, Sanders, Nassos, & Hadley, 1990). Although other studies reveal that PBTZ169, a more hydrophilic version of benzothiazinones, may have an improved pharmacological profile and efficacy in animal models (Makarov et al., 2014). Neres et al. could show in 2012 that fluorescently labeled benzothiazinone and DprE1 appear to accumulate at the poles of mycobacteria, so it can be concluded that this must be the active growing site of mycobacteria, providing us with another hint to assume the mycobacterial property to grow at their poles (Daniel & Errington, 2003; Thanky et al., 2007).

BTZ043 is a new agent in the antituberculotic drug pipeline with a bactericidal effect and high potency. It has shown to act additively with other antituberculotic agents and even in synergy with bedaquiline (Lechartier, Hartkoorn, & Cole, 2012). Currently, BTZ043 is still being tried in studies, but it could already be shown that isolates from MDR-TB strains were susceptible to BTZ043 (Pasca et al., 2010), making it a promising candidate of new antituberculotic drug regimens. No adverse events could be observed when administering BTZ043 to mice over one month (Makarov et al., 2009), whereas in embryos of zebrafish defects in notochord development have been observed (Makarov et al., 2014); and side effects in the human patient yet remain to be tested. The efficacy of BTZ043 as an antimicrobial agent has been compared to

first-line antituberculotic compounds when observed over long periods of time (Makarov et al., 2009). Some studies describe its mechanism of action as rather time-dependent than dose-dependent (Makarov et al., 2009), but there remain other assumptions that BTZ043 may behave rather dose-dependently (Batt et al., 2012). The pharmacodynamic and pharmacokinetic profiles of benzothiazinone thus provide reason for further investigation.

1.6 Matrix-Assisted Laser Desorption/Ionization Time of Flight Mass Spectrometry

1.6.1 General

Mass spectrometry is an analytical technique used to analyze the masses of molecules. The basic principle of mass spectrometry is to generate ionized compounds, to measure their mass to charge ratio and to quantify them (Budzikiewicz, 1969). Various mass spectrometry techniques exist, based on different ionization and detection systems (Budzikiewicz, 1969). In 1975, mass spectrometry has first been described to be used in diagnostic identification of microbes (Anhalt & Fenselau, 1975). Nowadays, mass spectrometry is routinely being used in laboratories worldwide as a method for rapid analysis and identification of bacteria and fungi. The most widely-known method is matrix-assisted laser desorption/ionization time of flight mass spectrometry (MALDI-TOF MS) (Carbonnelle et al., 2011; Jung et al., 2014; Seng et al., 2009). MALDI-TOF MS is a mass spectrometry method in which MALDI is used as the source of ionization and the time of flight is analyzed (Karas, Bachmann, & Hillenkamp, 1985). Applying this method, peptides and proteins of organisms can be analyzed in mass spectra, enabling identification of bacteria and fungi by comparing the spectra to a data base (Cherkaoui et al., 2010). Mass spectrometry has had a large impact on identification of microorganisms as it can be used for immediate detection of species and is more cost-effective and faster in comparison to conventional biochemical methods (Cherkaoui et al., 2010; Seng et al., 2009; Tan et al., 2012; Tran, Alby, Kerr, Jones, & Gilligan, 2015; Wieser, Schneider, Jung, & Schubert, 2012). Different approaches with MALDI-TOF MS are being evaluated for its potential use to detect bacterial susceptibility and resistance and underlie further exploration (Jung et al., 2014; Moreno et al., 2018).

1.6.2 Technique

The sample is co-crystallized with MALDI matrix on the target plate and is placed in the MALDI sampling chamber (Hillenkamp & Karas, 1990). Short laser pulses cause thermal desorption and ablation of the co-crystallized sample material on the MALDI target (Hillenkamp & Karas, 1990).

The matrix molecules rapidly and efficiently absorb the laser irradiation as they have strong optical absorption at the wavelength of the laser (Tanaka et al., 1988). This creates a hot plume of gases and ionization of the matrix molecules, and consecutively the ionization of the analytes. The ionized molecules are then accelerated by an electrical field of several kilovolts into the ion optics and drift tube of the mass spectrometer. In the drift path, the molecules are separated according to their mass to charge ratio. A detector at the end of the drift path measures the time of flight (TOF) (Wolff & Stephens, 1953). Heavier molecules of the same charge reach lower speed as the transferred total energy is only proportional to the charge. A single charge Q (z = +1) can be assumed for the majority of molecules and their mass can be determined by the time of flight (Karas, Glückmann, & Schäfer, 2000). Usually, molecules acquire a single charge, but in a few cases, molecules can be charged twice or three times (Karas et al., 2000). In the end, a spectrum of signals in dependence of mass to charge is obtained (Wolff & Stephens, 1953). The signal strength thereby depends on the number of molecules reaching the detector with the respective mass to charge ratio. Ionization efficiency however, depends on numerous different parameters and cannot be considered to be constant. This is the reason why the quantitative nature of MALDI-TOF MS itself is limited (Szájli, Fehér, & Medzihradszky, 2008).

1.6.3 Carbon Isotope Labeling

Mass spectrometry enables the detection of masses. By measuring the mass, it is not only possible to identify molecules, it is further possible to distinguish between different isotopes of the same molecules. Carbon isotopes are universally present in carbon containing molecules, which makes it a suitable isotope for mass spectrometric measurement. Carbon isotope labeling has been applied as an additional tool to mass spectrometry in order to add the dimension of time to the method. Carbon isotope labeling is routinely used in the radiocarbon method, also known as ^{14}C dating (Hajdas et al., 2021; Libby, 1955). ^{14}C is an instable, thus radioactive carbon isotope with a half-life period of 5730 years and is incorporated into organisms like other carbon isotopes (Hajdas et al., 2021). Same as other elements, elemental carbon underlies a natural distribution of isotopes. The natural amount of ^{12}C represents 98.89% of all carbon isotopes and the natural amount of the stable isotope ^{13}C is 1.11% (Meija et al., 2016). The fraction of the unstable ^{14}C isotopes in relation to its stable pendants decreases over time. A vital organism with a functioning metabolism is characterized by its uptake of carbon molecules – including the universally distributed amount of unstable ^{14}C carbon isotopes. Therefore, through

mass spectrometry, the fractional number of radioactive ^{14}C isotopes in relation to stable carbon isotopes can be determined, and thus, the age of organic molecules of a vital organism can be estimated from the moment that its metabolism ceased (Hajdas et al., 2021; Libby, 1955). The principle of carbon isotope labeling can also be applied by artificially adding stable isotopes in order to trace the passage of the isotope through a metabolic pathway. Metabolic labeling with the stable ^{13}C isotope has been used in SILAC (stable-isotope labeling by amino acids in cell culture), a simple and accurate approach to quantitative proteomics through mass spectrometry (Mann, 2006). The principle of SILAC is based on growing two bacterial cultures, one with a medium that contains normal amino acid and another with a medium that comprises a ^{13}C-labeled and thus, heavier amino acid (Mann, 2006). For this approach it is prerequisite that the bacteria are auxotroph to the respective amino acid, which can either be achieved by using an essential amino acid or by knocking out synthesis pathways to produce the respective (non-essential) amino acid. In the mass spectra, the incorporation of the labeled amino acid into a bacterial protein or peptide presents itself with a known m/z shift compared to bacterial protein with amino acids of naturally distributed isotopes (Jung et al., 2014; Mann, 2006). SILAC thus adds a time dimension to proteomics and enables the evaluation of dynamic incorporation of proteins (Mann, 2006). However, mycobacteria require rather complex growth media and are very difficult to make auxotrophic for amino acids, which impedes their combination with the methodology in SILAC. Thus, it has not found use in mycobacteria so far.

2 Joint Objective

A combination therapy of four antimicrobial agents administered for two months followed by the administration of two antimicrobial agents for four months is necessary for successful treatment of *M. tuberculosis* (World Health Organization, 2019). Recently, a new four-month combination regimen with more than two antibiotics has been put forward by the WHO as a conditional recommendation (WHO consolidated guidelines on tuberculosis, 2022). Particularly challenging are the emerging cases of XDR-TB and MDR-TB which require prolonged treatment times and innovative combination schemes (World Health Organization, 2019). Combination therapy is known to increase clinical effectiveness due to stronger antimycobacterial effects and hindering the evolution of drug resistance. However, no satisfying answers have been found on how and when antimicrobial compounds interact in their combination and the combined mode of action remains difficult to predict. A new possible combination of antimicrobial agents in the anti-tuberculosis drug pipeline is linezolid and benzothiazinone. Linezolid is a protein biosynthesis inhibitor, blocking the initiation process of mRNA translation and has routinely been used in infections with gram-positive cocci (Champney & Miller, 2002; Shinabarger et al., 1997; Swaney et al., 1998). Benzothiazinone lead compound BTZ043, a new substance of unsatisfactorily explored pharmacodynamics and -kinetics, is a cell wall synthesis inhibitor with an irreversible mechanism of action due to its nature as a suicide substrate (Makarov et al., 2009; Trefzer et al., 2012). It binds non-covalently to the active site of DprE1, which is known as an enzyme in the metabolism of arabinose to maintain the cell wall in mycobacteria by forming mycolic acids (Makarov et al., 2009). In this thesis, an exciting new direction through an experimental approach is pursued to explore the combined mode of action of linezolid and benzothiazinone lead compound BTZ043. We specifically hypothesize that linezolid administered together with benzothiazinone is an effective *in vitro* antimicrobial combination in fighting *M. smegmatis* as a model organism for *M. tuberculosis.* We investigate on how a synergistic effect can be shown and which pharmacodynamics are required to achieve synergy. To address this question, it is essential to devote ourselves to the question of when and at which concentration the initial effect of linezolid as a single agent can be shown and whether this information can be used for the development of an optimized combined antimicrobial scheme. Further, we study the pharmacodynamic traits of benzothiazinone against *M. smegmatis.* To verify and possibly substantiate the main hypothesis, the surrogate organism *M. smegmatis* is investigated based on three different methods that form the main pillars of the project: (1) examining the

protein metabolism of mycobacteria exposed to linezolid and benzothiazinone by observing protein profiles obtained through MALDI-TOF MS using a stable-isotope traced nutrient, (2) cultivating, plating and counting the CFU of *M. smegmatis* under various growth conditions and (3), revealing the effect of the antibiotic agents on *M. smegmatis* through scanning electron microscopy.

3 Materials and Methods

3.1 Materials

Table 1: Equipment

Equipment	Model	Manufacturer	Comment
Pipettes and tubes	Eppendorf reference	Eppendorf AG, Hamburg, Germany	
Photometer	Ultrospec 3100 pro	Amersham Biosciences, Little Chalfont, United Kingdom	Optical density
Centrifuges	3K30 Sigma laboratory centrifuge	Sigma Laborzentrifugen GmbH, Osterode am Harz, Germany	
	1K15 Sigma laboratory centrifuge	Sigma Laborzentrifugen GmbH, Osterode am Harz, Germany	
	Thermo Scientific™ Heraeus™ Megafuge 1.0R	Fisher Scientific GmbH, Schwerte, Germany	
	LLG Labware	Lab Logitistics Group GmbH, Meckenheim, Germany	
Matrix-assisted laser desorption and Ionization – Time of flight mass spectrometer (MALDI-TOF MS)	Microflex LT	Bruker Daltonics, Bremen, Germany	Software used for analysis is the program FlexControl
Target	MicroScout MFP Target with 96 spots; polished steal BC	Bruker Daltonics, Bremen, Germany	
Safety workbench	HBB2436	BDK - Luft- und Reinraumtechnik GmbH, Sonnenbrühl, Germany	
Incubators	Certomat H	Sartorius Lab Instruments GmbH & Co. KG, Goettingen, Germany	
Analytical balances	Sartorius BP 61	Sartorius Lab Instruments GmbH & Co. KG, Goettingen, Germany	
Bunsen burner	Fireboy plus	Integra Biosciences AG, Zizers, Switzerland	
Scanning Electron Microscope	Zeiss Sigma VP Field Emission Scanning Microscope	Carl Zeiss Microscopy GmbH, Jena, Germany	
Vortexer	VF2	Bachofer Laborgeräte, Reutlingen, Germany	
Ground shaker	Certomat H	Sartorius Lab Instruments GmbH & Co. KG, Goettingen, Germany	
	Certomat U und Certomat HK	B Braun Biotech International GmbH, Melsungen, Germany	
Vacuum station	PALL	Pall Corporation, Port Washington, New York, USA	

Table 2: Chemicals

Chemical	Origin
Tween 80	Sigma-Aldrich, St. Louis, Missouri, USA
Methanol ≥ 99.9%	Carl Roth GmbH & Co. KG, Karlsruhe, Germany
Acetonitrile ≥ 99.0%	Fluka/ Sigma-Aldrich, St. Louis, Missouri, USA
Formic Acid 98 - 100%	Fluka/ Sigma-Aldrich, St. Louis, Missouri, USA
Formaldeyhde solution 36.5 - 38% in H_2O	Sigma-Aldrich, St. Louis, Missouri, USA
Glycerol ≥ 99.5%	Carl Roth GmbH & Co. KG, Karlsruhe, Germany
Aqua Ampuwa	Fresenius Kabi GmbH, Bad Homburg, Germany
Trifluoroacetic acid ≥ 99.0%	Sigma-Aldrich, St. Louis, Missouri, USA
a-Cyano-4-hydroxycinnamic acid (MALDI matrix) ≥ 99.0%	Sigma-Aldrich, St. Louis, Missouri, USA

Table 3: Buffers and Solutions

Phosphate Buffered Saline (PBS)	80g NaCl 2g KCl 17.8g NaH2PO4-2H20 (sodium phosphate dihydrate) 2.4gKH2PO4 (potassium dihydrogen phosphate) In 800ml H_20 dest completely dissolved and pH 7.3 Fill up to 1 liter Autoclave or sterile-filter	For 10x PBS
Elution buffer for MALDI	Acetonitrile Formic Acid Aqua	800 µl (50%) 560 µl (35%) 240 µl (25%)
Matrix dissolvent	Acetonitrile (makes 50% of dissolvent) Aqua (47.5% of dissolvent) Trifluoroacetic acid (2.5% of dissolvent)	

Table 4: List of Bacterial Strains

Species	Origin	Intended use / comment
Mycobacterium smegmatis	Mc^2155 (Snapper, Melton, Mustafa, Kieser, & Jr, 1990)	Surrogate organism for antimicrobial treatment
Mycobacterium bovis Bacillus Calmette-Guerin (BCG)	ATCC 1173P2 (American Type Culture Collection, 2023; Calmette, Guerin, & Boquet, 1927)	Surrogate organism for antimicrobial treatment

Table 5: Growth Media

Type	Composition	Origin
Blood Agar	Columbia Sheep W/5% SB	Becton Dickinson, Franklin Lakes, New Jersey, USA

Bouillon Base	Middlebrook 7H9	Sigma-Aldrich, St. Louis, Missouri, USA
Middlebrook OADC Enrichment	Sodium Chloride 8.5g Bovine albumin 50.0g Dextrose 20.0g Catalase Oleic acid 0.6mL	Becton Dickinson, Franklin Lakes, New Jersey, USA
Tween 80	Tween 80	Sigma-Aldrich, St. Louis, Missouri, USA
Glycerol	Glycerol 100%	Carl Roth GmbH & Co. KG, Karlsruhe, Germany

Table 6: Antimicrobial Substances

Antibiotic substance	Abbreviation	Solvent	Stock solution	Origin
Benzothiazinone (BTZ043)	BTZ	DMSO	8300 µg/mL	Hans Knöll Institut, AG Florian Kloß, Jena, Germany
Linezolid ≥ 98%	LZD	Methanol	5000 µg/mL	Sigma-Aldrich, St. Louis, Missouri, USA

3.2 Methods

3.2.1 Growth Medium

One bottle of 20mL OADC enrichment and 100 µL Tween 80 (0.05%) are added to 180 mL of Middlebrook 7H9. The medium is autoclaved and then stored at room temperature. The cultures are incubated at 37° C at 140 rpm unless indicated differently.

3.2.2 Photometry

For calibration, 1000 µl of media are pipetted into the cuvette and the Optical Density (OD) is measured at a wavelength of λ = 600 nm. This value is subtracted from the OD_{600} of the consecutively measured sample values. The OD of the sample values is also measured by pipetting 1000 µL of a well-vortexed sample into the cuvette and measuring the OD_{600}. The data is only reliable in the linear range of the instrument, in this case between OD_{600} of 0.1 – 2.0. Dilution of the sample with sterile medium was required if the sample density exceeded the linear region. Photometry was used as a rough estimate of the expected CFU count.

3.2.3 Cryo Conservation of *M. smegmatis* Aliquots

20 µL of *M. smegmatis* type Mc^2155 are inoculated in 5 mL Middlebrook 7H9, OADC enrichment and 0.05 % Tween 80 and placed on the ground shaker. 5 mL of 40% glycerol solution are added (glycerol dissolved in AQ Bidest; then sterile-filtered with a pore size of 0.4 5µm), so that the final glycerol concentration is 20%. Into each Eppendorf tube 100 µL of mid-log culture are

aliquoted and frozen at -80°C. For thawing, the samples are placed outside the freezer on a small plastic rack on ice, and spaces are left in the rack between the Eppendorf tubes. After approximately 45 minutes, the samples are ready for careful mixing.

3.2.4 Bacterial Overnight Culture

The *M. smegmatis* aliquot is thawed on ice until it is completely fluid. Carefully vortex the aliquot. 40 µL of the sample are pipetted into an Erlenmeyer flask with baffles with 20 mL of Middlebrook 7H9 enriched with OADC Middlebrook and 0.05% Tween 80. In order to produce a culture of an OD_{600} = 0.3 - 0.6, the culture is incubated for 17 hours prior to experiments.

3.2.5 Defining Minimal Inhibitory Concentration (MIC)

Strains are grown in medium to density of OD_{600} = 0.1 and are confronted with various concentrations of a chemotherapeutic agent (here linezolid and benzothiazinone). The OD_{600} is measured after 16 hours. The sigmoidal curve, defined by two asymptotes, represents the bacterial susceptibility to concentrations in logarithmic echelons. All experiments were conducted using concentrations of 90% inhibition unless explicitly indicated otherwise.

3.2.6 Equalizing the Starting Optical Density (OD)

For all experiments unless indicated otherwise, we used a start OD of the culture OD_{600} = 0.1. This was in order to create identical growth conditions for every experiment with *M. smegmatis* and to ensure measurements in the linear growth phase. The OD of the overnight culture was determined via photometry and the respective volume of the culture taken and diluted in growth medium. To calculate the respective volume, following formula was used:

$$volume_{required} = OD_{aim} : OD_{measured\ in\ culture} \times volume_{aim}$$

The calculated volume of culture was extracted under sterile conditions with a glass pipette, centrifuged in a plastic falcon at 10,000 rpm for 10 minutes at 20 °C. The supernatant was discarded, and the pellet re-dissolved in the required volume of growth medium.

3.2.7 Serial Dilution

Serial dilutions were used for plating a series of a sample to determine the bacterial burden. To create the 10^{-1} dilution (1:10), 50 µL of sample are pipetted into an Eppendorf tube with 450 µL of fresh PBS and then vortexed thoroughly. For the 10^{-2} dilution, 50 µL of the 10^{-1} diluted sample are pipetted into 450 µL fresh PBS and then vortexed thoroughly. Steps are repeated until the desired dilution is reached.

3.2.8 Plating and Colony Forming Units (CFU) Count

50 µL of well-vortexed and ice-cooled sample are placed with a pipette into 450 µL of PBS buffer and vortexed for 1 minute. Careful vortexing and cautious pipetting of the dilution series increases the consistency of the value ranges. 50 µL of the serially diluted sample are pipetted onto Columbia sheep blood agar and spread with sterile spatula on the entire blood plate evenly in all directions in a 45° angle to the surface until the solution is evenly spread and absorbed into the agar plate. The lid on the plate is closed and plates are stacked upside down. The procedure is repeated with increasing serial dilutions of the sample (see 3-28). All plates are placed in the incubator at 37 °C. After three days, the plates are removed from the incubator and colony forming units (CFU) are counted either directly or on the following day. The respective plates are placed in the refrigerator to inhibit further growth at 4 - 7°C. The mean number of CFU per sample of the plated dilutions are calculated. All experiments are performed in triplicates.

3.2.9 Washing

This washing protocol was created to simulate the sudden drop of a defined antibiotic concentration in the culture medium after a certain exposure duration, as seen in a peak exposure concentration. The washing step intended to minimize the concentration of BTZ043 after exposing *M. smegmatis* to BTZ043 at a certain concentration for either 0.5 hours, 2 hours, or 4 hours. As the original linezolid concentration in the culture medium was maintained while the concentration of BTZ043 decreased; the sample with linezolid retained its original concentration of linezolid *during* and *after* the washing process. The washing was performed on control batches in parallel as well.

To prepare the washing step, antibiotic solutions with defined concentrations are created before. For the washing step of the wildtype control (without any antibiotic treatment), pure medium of M7H9 with OADC supplement and 0.05% Tween 80 are provided without addition of an antibiotic compound. The glass tubes are taken off the ground shaker, the entire 2 mL are removed rapidly with a disposable pipette (to decrease pipetting time) and then placed in 2 mL-Eppendorf tubes. The samples are centrifuged at 10,000 rpm for 6 min at 4° C. The 4°C were chosen in order to inhibit further growth during the centrifugation time. After centrifugation, the supernatant is swiftly removed until only the pellet is visible, then the pellet is redissolved in 500 µL of the respective dilution (culture medium, or culture medium and linezolid at c = 1.032 µg/mL). The centrifugation step is repeated. Again, the supernatant is removed

and the pellet re-dissolved in either 1000 µL medium or medium with antibiotic solution, and vortexed. All contents of the Eppendorf tubes are added to a fresh glass culture tube, in which 1000 µL of the respective antibiotic solution (or pure growth medium) is already prepared.

3.2.10 Reduction Factor

The reduction factor is calculated by the decadal logarithm of the relation of the wildtype CFU count to the treated CFU count. For example:

Average CFU count/mL in the wildtype = 1 000 000 = 1 x 10^6 → log (10^6) = 6

Average CFU count/mL in the treated group = 10 000 = 1 x 10^4 → log (10^4) = 4

The logarithms are subtracted from each other, thus receiving a reduction factor of 6 - 4 = 2. A reduction factor of 2.0 means that the CFU of the manipulated bacteria resembled the fraction $1/10^2$ of the wildtype CFU, thus a ratio of 1 : 100.

3.2.11 Growth of *M. smegmatis* with ^{13}C Tracer Nutrient

All experiments begin with an overnight culture with a starting OD = 0.1. Antibiotic dilutions for linezolid and benzothiazinone are prepared in multiples of their MICs. 8.52 µl of each control nutrient and tracer nutrient are pipetted into tubes with 500 µl culture, vortexed thoroughly and placed to further 3000 µl of culture in the glass tubes. Antimicrobial compounds are added to respective tubes and all samples placed on the ground shaker at 140 rpm. 500 µL samples were taken after 1 hour, 3 hours, 5 hours, 7.5 hours, 12 hours and 25 hours and frozen in Eppendorf tubes at -20°C. Samples are thawed the next day and prepared following the MALDI preparation protocol (page 3-30), then measured with MALDI-TOF MS Microflex.

3.2.12 MALDI-TOF MS Sample Preparation

A GHP filter plate with the pore size of 0.2 µm is placed on the vacuum station. The samples are filled into the wells of the filter plate. If the volume exceeds 350 µL, the samples are placed carefully with the vacuum suction turned on. The entire fluid is let to be sucked through. The pressure is released and 300 µL AQ Bidest (sterile-filtered) pipetted into each well. After 5 minutes, the suction is activated and the water is sucked through. This washing step is repeated twice.

The GHP filter plate is placed on ice with a base or stand underneath to protect the membranes from contamination. Into each well, 100 µL ice cold acetone are pipetted, left for 5 minutes on the ice, then placed on the vacuum station and the suction is turned on. The filter plate is then removed and carefully beat on a tissue, placed on the vacuum station under suction one last time.

The filter plate is removed and placed in the incubator with its stand for 7 minutes. The acetone needs to evaporate completely.

The filter plate is then placed on the collecting 96-well plate. 20 µL elution buffer (15 % AQ Bidest; 35 % formic acid; 45 % acetonitrile) are filled into each well; the plate is protected with Parafilm und the cover sealed for 5 minutes. Then the whole plate is centrifuged with the collecting plate at 4000 rpm for 3 minutes at 20 °C. 1.4 µL of eluate are pipetted from the collecting plate onto the MALDI target. The target is left to dry entirely in the incubator at 37°C.

The MALDI matrix is prepared by adding MALDI matrix to matrix dissolvent in an Eppendorf tube. The compound is dissolved using an ultrasonic bath and vortexed thoroughly. 1 µL of MALDI matrix is pipetted onto the previously dried samples. The samples are left to dry entirely on the target in the incubator at 37 °C. This protocol was elaborated by our research group.

3.2.13 Measuring with MALDI-TOF MS

The target is inserted into the mass spectrometer (Microflex LT, Bruker Daltonics) and remotely controlled using the program FlexControl.

The mass spectrometer uses a class III B-laser emitting laser pulses of 355 nm UV-light and has an imaging resolution of 10 µm. We used the program FlexAnalysis to visualize the mass spectra. In order to quantify peaks in the mass spectrum and to visualize the peak shift, our lab group developed an in-house script in collaboration with analytical chemistry of TUM (Haisch group). The program written on MathLab (with special acknowledgement to PD Dr. med. Andreas Wieser and Prof. Dr. Christoph Haisch) ran the following mode: MALDI-dTF-SAIFpNS_170927_3 with d3T250FS4AI0FpNS.

3.2.14 SEM Sample Preparation

The samples require fixation and dehydration for the micrographs of mycobacteria with the SEM. *M. smegmatis* samples are fixed with formalin solution (final concentration 3.7%) for 5 min. The samples are centrifuged at 4500 rpm for 5 minutes at 20 °C. The supernatant is discarded and the pellet re-suspended in 3.7% formalin solution. For better quality of the micrograph background, the process is repeated and the sample re-dissolved in 200 µL 3.7% formalin solution. 5 µL are pipetted onto a small piece of aluminum foil (about 5 mm x 5 mm). The samples are left to dry in the incubator at 37°C. Ascending ethanol dehydration series with aqueous 10%, 30%, 70% and 100% ethanol are prepared. Each aluminum foil is left floating upside down on the respective alcohol/water drops for 7 minutes. Then the aluminum foil with the sample upwards is left to dry. Samples of the batch from the first day are placed in the

desiccator under nitrogen flow, and all samples are collectively measured on the second day. Acknowledgments for the elaboration of this protocol go to Sarah Sternkopf.

The micrographs are taken by the SEM (Zeiss Sigma VP Field Emission Scanning Microscope, Carl Zeiss Microscopy GmbH, Germany) in collaboration with Technische Universität München (TUM) under high vacuum, with a 3.1 mm working distance and 30 µm objective lens aperture. The images are collected using the secondary electron detector, voltage of 3 kV.

3.2.15 SEM Length and Width Measurement

The bacteria in the micrographs were visualized in Image J and measured manually using the program Fiji. The 1 µm- or 2 µm-bar in the bottom left of every micrograph was used for calibration. The pixel aspect ratio was determined using the scale bar tool followed by marking the clearly distinguishable bacteria with the 'draw line' and 'measure size' function. The measure tool was drawn through the middle of the bacteria in its longest diameter and when bent, the line passed through the middle of the segment.

Inclusion criteria for length measurement were: bacteria must be clearly distinguishable as one cell and must not cross any other bacteria underneath. Inclusion criteria for width measurement were that the bacteria must be measured at its thinnest width that was still representative for the entire cell. For critical review of the criteria, see discussion on page 5-94.

3.2.16 Statistical Analysis

Data was statistically analyzed by Microsoft Excel and GraphPad Prism 6. Groups of $n = 9$ and larger where tested for their consistency with an ideal Gaussian distribution using D'Agostino-Pearson omnibus normality test (recommended by GraphPad Prism)[1]. Groups were tested for outliers beforehand. All values, including outliers, are illustrated in diagrams. If Gaussian distribution could be assumed, two groups were tested for significant difference using t-test with Welch's correction, assuming unequal standard deviation (SD). In small groups, where no Gaussian distribution could be assumed (mostly with $n = 3$ or $n = 6$), the non-parametric Mann Whitney U test was applied to test for significant difference among groups.

[1] graphpad.com/guides/prism/7/statistics

4 Results

4.1 Minimal Inhibitory Concentration

In previous experiments of our lab group, the growth behavior of *M. smegmatis* had been investigated under the influence of various antibiotic agents. Growth curves of *M. smegmatis* in the presence of linezolid and benzothiazinone were determined by photometry at a wavelength of λ = 600 nm (1-14), as can be seen in Figure 4-1.

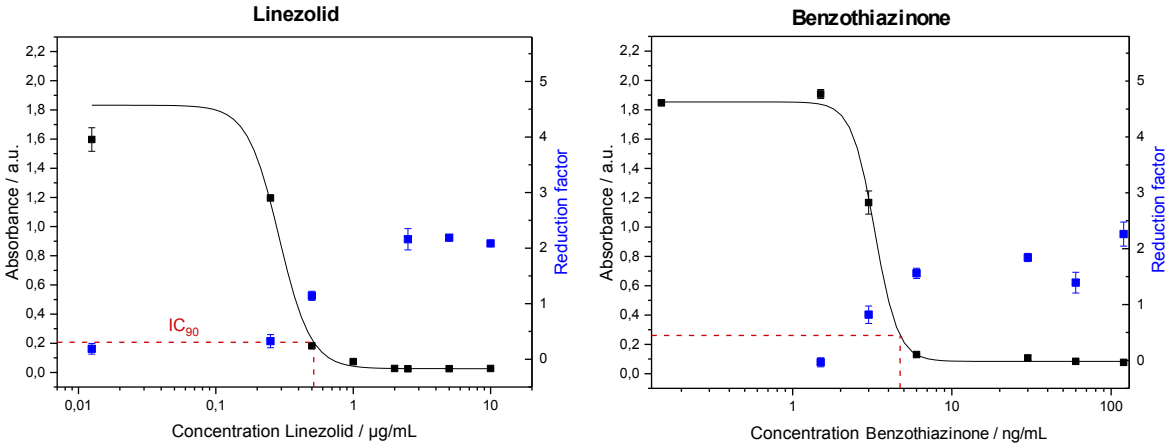

Figure 4-1: MIC curves of linezolid and benzothiazinone.

Sigmoidal curve fits were taken to calculate IC_{90} values which were then defined as MICs for this project. With special acknowledgements to Dr. Anna-Cathrine Neumann-Cip.

Through these curves, the IC_{90} values for *M. smegmatis* could be determined using the equation as defined in Table 7. The IC_{90} values were then referred to as Minimal Inhibitory concentration (MIC). The IC_{90} values were used instead of the classical MIC_{80} in order to test a higher inhibitory effect. For better understanding, concentration levels of the compounds in the experiments are marked by their multiples in relation to the respective MIC.

Table 7: MICs of the Antibiotic Compounds

Calculation for IC_{90}	LZD (µg/mL)	BTZ (ng/mL)
A1	1.83	1.85
A2	0.026	0.084
x0	0.29	3.28
p	3.77	6.02
Absorbance calculated at IC_{90}	0.21	0.26
Absorbance at IC_{90}	0.21	0.26
Concentration IC_{90}	0.52	4.73

LZD = linezolid; BTZ = benzothiazinone; logistic fit; equation: y= A2 + (A1-A2)/(1+(x/x0)^p)

4.2 The Effect of Linezolid and Benzothiazinone on *M. smegmatis* Protein Metabolism by Carbon Isotopic Labeling in MALDI-TOF MS

4.2.1 Center of Gravity

MALDI-TOF MS itself is not a quantitative method as the intensity of mass to charge (m/z) signals depends on multiple parameters (e.g. crystallization of the matrix, the distance of the laser to the matrix, competition of ionization). Even though the resolution of mass spectrometry in theory allows the exact determination of m/z signals, the MALDI process inherently features limited precision: The combination of inaccurate MALDI conditions and the overlay of isotope distributions leads to broader mass spectrum peaks. Hence, in order to provide a quantitative analysis of labeled and unlabeled protein populations, a new method was developed by our research group in collaboration with Prof. Dr. Christoph Haisch of TUM.

In mass spectra of lysed *M. smegmatis*, individual m/z signals were identified. For each peak an upper and a lower limit border was defined by our research group. The center of gravity value (COG) represents the position of an observed m/z peak in the mass spectrum. The COG, given in the unit m/z, was calculated for the area between two determined limits. Assuming a charge $z = +1$, a mass can be assigned to the corresponding peak represented by the COG (Figure 4-2). It can be assumed that every peak corresponds to a specific molecule, mostly a protein or peptide.

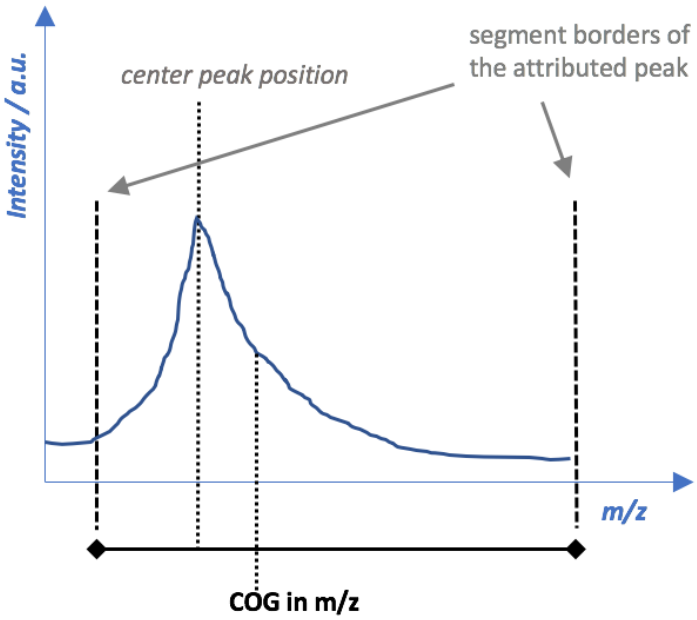

Figure 4-2: Center of gravity.

Illustration of a mass spectrum peak and the center of gravity value (COG). From the mass spectrum, the segment of a peak attributed to a certain protein, is depicted.

4.2.2 Peak Positions in Mass Spectra

For the peaks listed in Table 8, the corresponding analyte was identified in earlier work (with special acknowledgments to Dr. Anna-Cathrine Neumann-Cip). The number is the center peak position, the limits were determined individually in our research group for *M. smegmatis*. The analyte at m/z 2755 could not be assigned to a defined molecule, but it was assumed to carry sugar residues after HPLC-MS/MS analysis was performed. It is therefore named glycopeptide.

Table 8: Corresponding Peak to Respective Protein in Mass Spectra

Center peak position (m/z)	Identified protein	Function
5517	Hypothetical protein MSMEG_5081	- Unknown (12/2020)
4329	50 S L29	- Part of the ribosome thus important for protein synthesis, but also extra-ribosomal functions assumed (Fan, Tang, Yan, & Xie, 2014)
4555	50 S L27	- Part of the bacterial ribosome, knockout leads to severe defects in cell growth (Maguire, Beniaminov, Ramu, Mankin, & Zimmermann, 2005) - Assumed to stabilize peptidyl tRNA (Y. Wang & Xiao, 2012) - Impairment of A-site substrate binding in ribosomes lacking L27 (Trobro & Åqvist, 2008)
5756	Integration Host Factor	- important role in DNA damage response, nucleoid compaction and integrative recombination (Sharadamma et al., 2015; Stock & Zhulin, 2017)
4152	Hypothetical protein MSMEG_1770	- unknown (12/2020)
3160	50 S L33	- ribosomal protein
2755	glycopeptide	- could not be identified more closely
9546	PFAM16525	- haem-binding haemophore (Finn et al., 2016) - part of a heme acquisition system in mycobacteria assumedly as a source to iron uptake (Finn et al., 2016; Tullius et al., 2011)

4.2.3 Differential Center of Gravity (ΔCOG)

M. smegmatis was incubated in growth medium with either ^{13}C-traced 0.24% v/v glycerol or natural 0.24% v/v glycerol as a carbon source. Samples were taken after 1 hour, 3 hours, 7.5 hours, 12 hours, and 25 hours of incubation, then lysed and prepared for measurement by MALDI-TOF MS (3-30). The center of gravity (COG) values of eight peaks (see above) were calculated. These values change with incorporation of ^{13}C derived from the glycerol added into the medium – the mass of the protein increases with more ^{13}C being used in building new proteins, whereas the charge will stay the same. Thus, the allover mass/charge ratio of the newly synthesized protein increases. As a result, in the mass spectrum, the COG of molecules with

incorporated tracer is higher than without tracer. The difference is quantified by determining the differential center of gravity (ΔCOG) at different points in time. The ΔCOG is calculated by subtraction of the COG of the native group (glycerol) from the COG of the respective labeled group (^{13}C-traced glycerol). This allows to level out other sources for differences in mass over time. Even without labeling, the COG within the control group is not entirely constant over time due to the natural way of the bacteria to modify their proteins by posttranslational modification inside the growing cell or during extraction or to adapt to altered milieu (e.g. methylation, formylation, oxidation). Thus, all changes that are not due to tracer incorporation are eliminated as they occur simultaneously in the labeled and unlabeled analyte population. Figuratively, the ΔCOG can be understood as a measure for the position shift on the m/z graph (Figure 4-3). Due to the overlap and non-targeted nature of natural and artificial nutrient based isotope distribution, the shifted peak appears wider than the peak representing the native molecule.

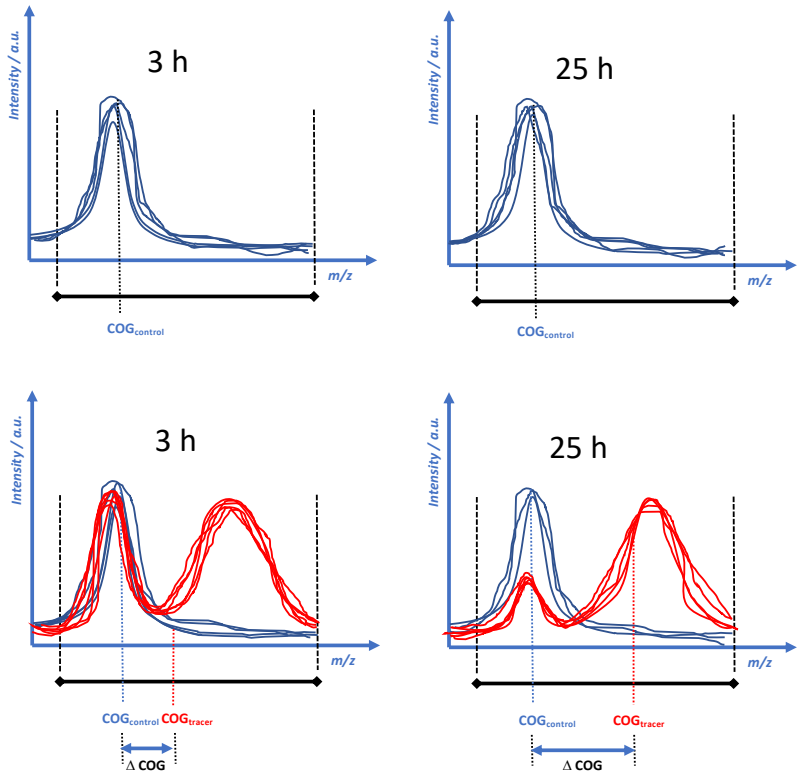

Figure 4-3: Illustration of the ΔCOG.

Left graphs exemplarily show a mass spectrum segment at 3 hours, and the graphs on the right-hand side depict the same segment at 25 hours. $COG_{control}$ = peak position of unlabeled protein; COG_{tracer} = peak position of labeled protein. Upper graph: peak of control group is shown (blue), lower graph: peak of control (blue) and labeled sample (red) are shown in overlay with the resulting ΔCOG (peak shift). In this case, the ΔCOG increases between the timepoint of 3 hours and 25 hours.

4.2.4 ΔCOG Timelines

We demonstrated the temporal evolution of the ΔCOG of the WT in order to define the ΔCOG that is maximally achievable under optimal circumstances. ΔCOG values were generated for eight defined segments of the m/z-axis in the mass spectrum, which could be allocated to seven proteins and one smaller molecule, here referred to as glycopeptide, of the *M. smegmatis* proteome (Table 8). The ΔCOG values of these proteins were generated each under natural growth conditions and under exposure to an antimicrobial compound at various timepoints. In this trial, *M. smegmatis* was either grown without antibiotic agent (wildtype WT; untreated), exposed to either linezolid in 2 x MIC (c = 1.0 µg/mL, blue, "L02") or benzothiazinone in 2 x MIC (c = 9.5 ng/mL, green, "B02"). The timeline of the WT was determined in previous studies by our research group by taking samples at eight different points in time and observing the increase of the ΔCOG. In the graph, the shift is represented by the ΔCOG (y-axis) in dependence of time (x-axis). The wildtype results (WT) of this particular trial are depicted (orange) in comparison to the sum of our previous experiments represented by the fit curve (magenta, "WT timeline") of our lab group and are shown in Figure 4-4. We observed that the ΔCOG reaches a saturation and generated an exponential fit curve with confidence bands (magenta) from the timeline. The asymptote of the curve fit, indicated in every diagram as a line intersecting the y-axis, shows the maximum value which the ΔCOG value is approaching. The asymptote value is a point of reference for the respective analyte and was defined as 100% contribution under optimal conditions in the WT. It is the state approaching 100% of maximally possible *de-novo*-synthesized proteins through this pathway in the WT. Reaching the asymptote, the sum intensity of the unlabeled molecule is below detection limit. The results of linezolid and benzothiazinone are shown in Figure 4-5 and Figure 4-6. To determine when the labeling reaches a saturation in the WT, we identified the point in time when the ΔCOG of the WT approaches the asymptote value and no more significant difference to the asymptotic value can be detected (Table 9). The timepoint of saturation for nearly all proteins lies between 7.5 hours and 25 hours. The WT control values of PFAM16525 (peak at m/z 9546) in this individual experiment visibly approach a plateau between 7.5 hours and 12 hours, nevertheless, all values are significantly different from the asymptotic value of the general WT timeline.

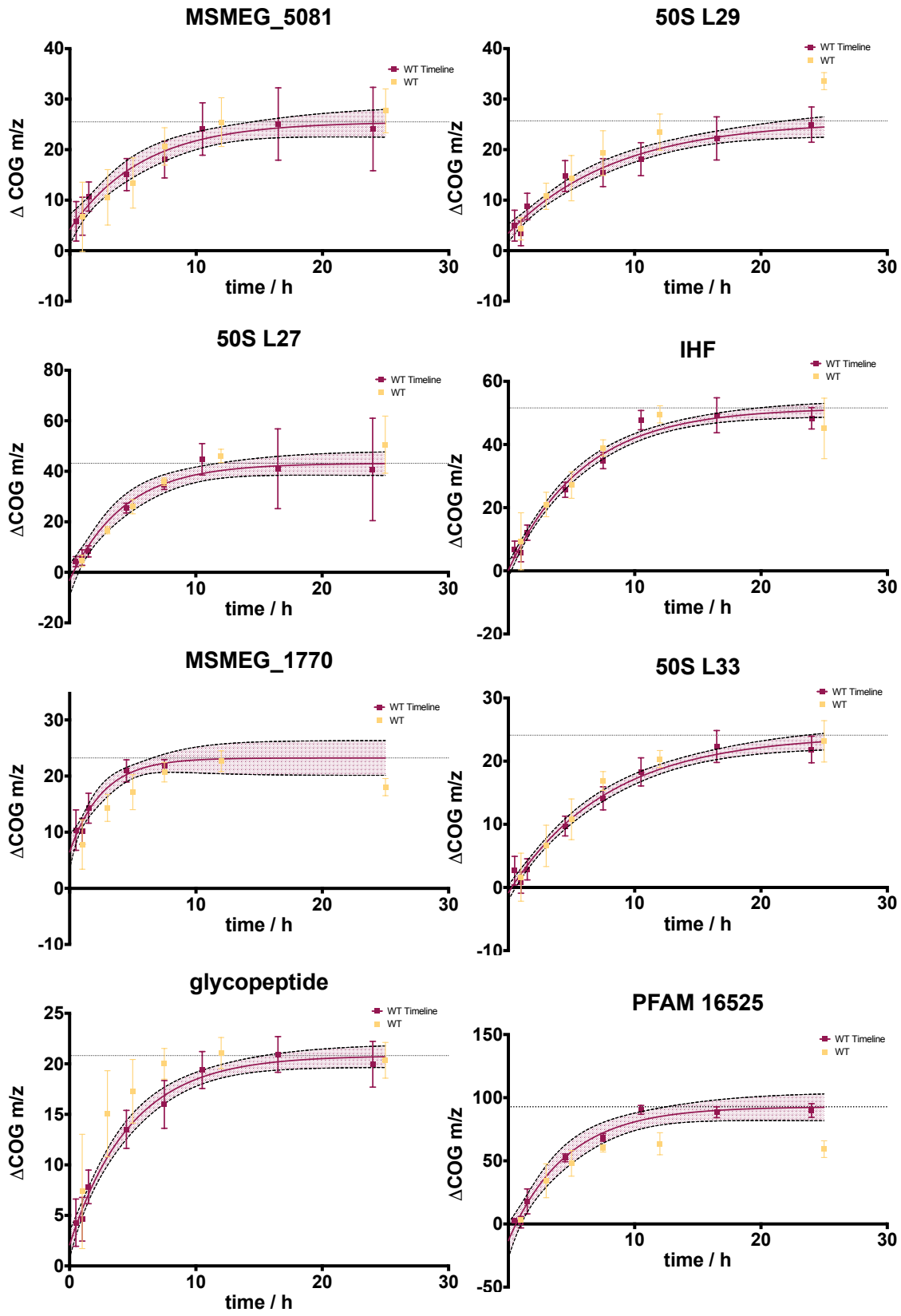

Figure 4-4 Peak shift of the wildtype

The ΔCOG in mass to charge (m/z) in dependence of time under the influence of linezolid in 2 x MIC (blue, L02). The timeline of the wildtype (WT) was determined in several experiments by our research group and is shown magenta with 95% confidence bands. ΔCOG control values of the WT

Table 9: Timepoint of Saturation of Labeling in the Wildtype

Molecule	Center peak position (m/z)	Asymptote value of the ΔCOG shift	Timepoint of saturation / hours
Glycopeptide	2755	20.81	7.5
MSMEG_5081	5517	25.49	12
50 S L29	4329	25.67	12
Integration Host Factor	5756	51.58	12
MSMEG_1770	4152	23.22	12
50 S L27	4555	43.15	25
50 S L33	3160	24.11	25
PFAM16525	9546	92.80	not reached

The timepoint of saturation was determined by T-testing the ΔCOG values of the WT of multiple timepoints in this individual experiment to the hypothetical value of the asymptote of the respective timeline until a significant difference could not anymore be detected. The ΔCOG timeline of the WT and the asymptote value were determined in several preceding experiments by our research group.

We measured the dynamics of the peak shift over time. Therefore, the ΔCOG values of different timepoints of every analyte were studied. We discovered that the mean ΔCOG of the WT after 3 hours and the respective mean after 7.5 hours of every examined analyte are significantly different from each other. Putting these mean values of ΔCOG in relation to each other results in ratios ranging from 1.32 to 2.56 (Table 10). The $\Delta COG_{7.5h}/\Delta COG_{3h}$ ratio represents an estimated relation of the amount of newly-synthesized protein at 7.5 hours to its amount at 3 hours.

Table 10: Contribution Ratio of 7.5 Hours to 3 Hours

Center peak position (m/z)	Molecule	*p*-value	$\Delta COG_{7.5h}/\Delta COG_{3h}$
5517	MSMEG_5081	0.0004	1.96 (±1.4)
4329	50S L29	0.0002	1.79 (± 0.84)
4555	50S L27	<0.0001	2.14 (± 0.28)
5756	Integration Host Factor	<0.0001	1.85 (±0.47)
4152	MSMEG_1770	<0.0001	1.45 (± 0.37)
3160	50S L33	<0.0001	2.56 (± 1.5)
2755	glycopeptide	<0.0001	1.32 (± 0.48)
9546	PFAM16525	0.0004	1.75 (± 0.77)

The ΔCOG at 7.5 hours and ΔCOG at 3 hours were compared by T-testing the mean and SD (n = 9), respectively. The p-value ranges from < 0.0001 to 0.0004. Thus, all ΔCOG values at 7.5 hours were significantly different to the ΔCOG at 3 hours of the respective analyte group. Then the contribution ratio (± SD) was calculated.

Generally, the data shown in Figure 4-5 demonstrates that no ΔCOG value of any of the eight peaks under influence of linezolid in 2 x MIC (blue) reaches the same value as the WT at the end of the experiment. *M. smegmatis* exposed to benzothiazinone in contrast (Figure 4-6), shows allover smaller divergence from the WT timeline.

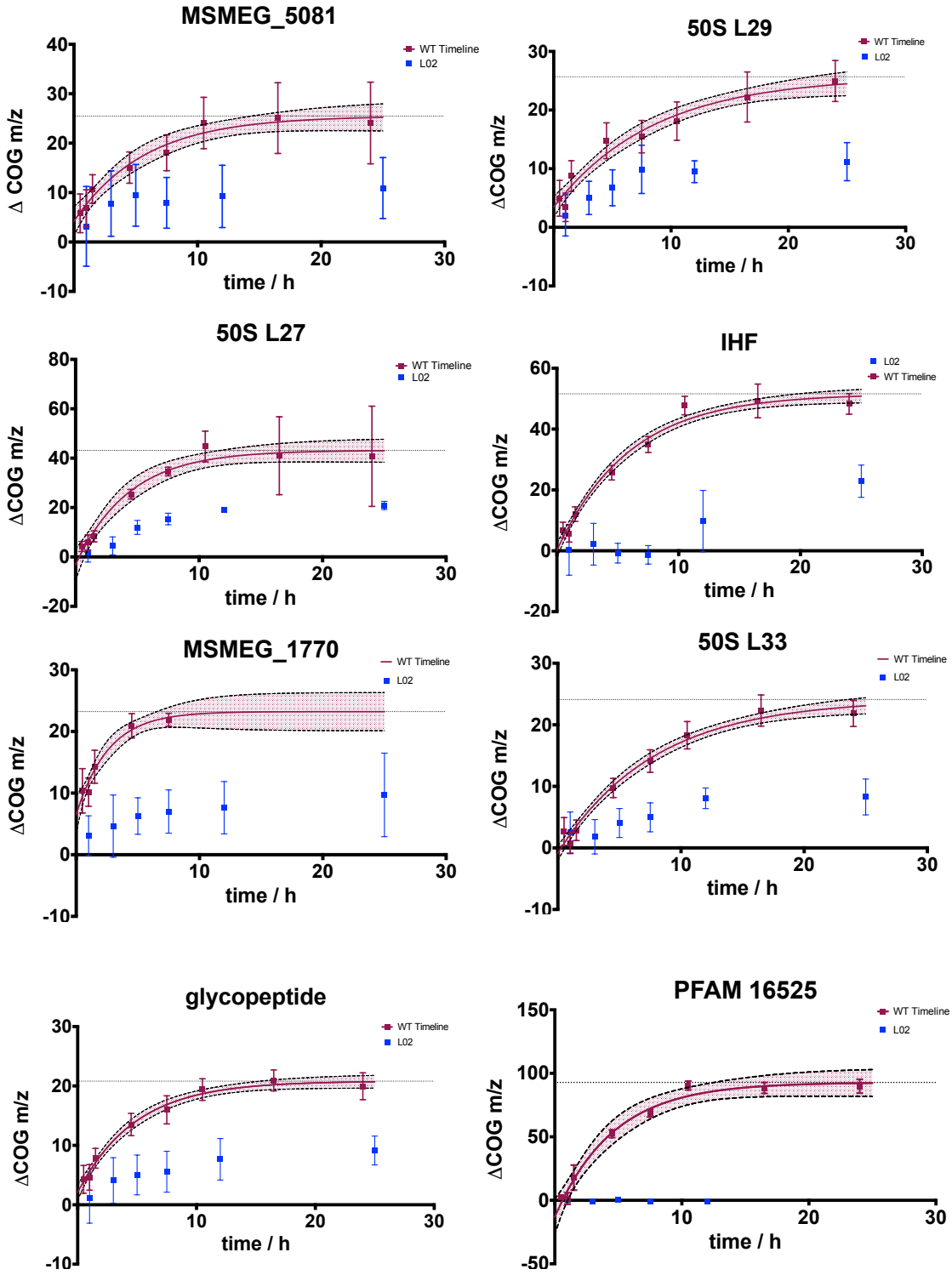

Figure 4-5: Peak shift under the influence of linezolid

ΔCOG in mass to charge (m/z) in dependence of time under the influence of linezolid in 2 x MIC (blue, L02). The timeline of the wildtype (WT) was determined in several experiments by our research group and is shown magenta with 95% confidence bands. ΔCOG control values of the WT were generated for the given timepoints but are not depicted in this graph for better overview. Peak at m/z 5517 – hypothetical protein MSMEG_5081; peak at m/z 4329 – 50 S L29; peak at m/z 4555 – 50 S L27; peak at m/z 5756 – Integration Host Factor; peak at m/z 4152 – hypothetical protein MSMEG_1770; peak at m/z 3160 – 50 S L33; peak at m/z 2755 – glycopeptide (unidentified); peak at m/z 9546 – PFAM16525.

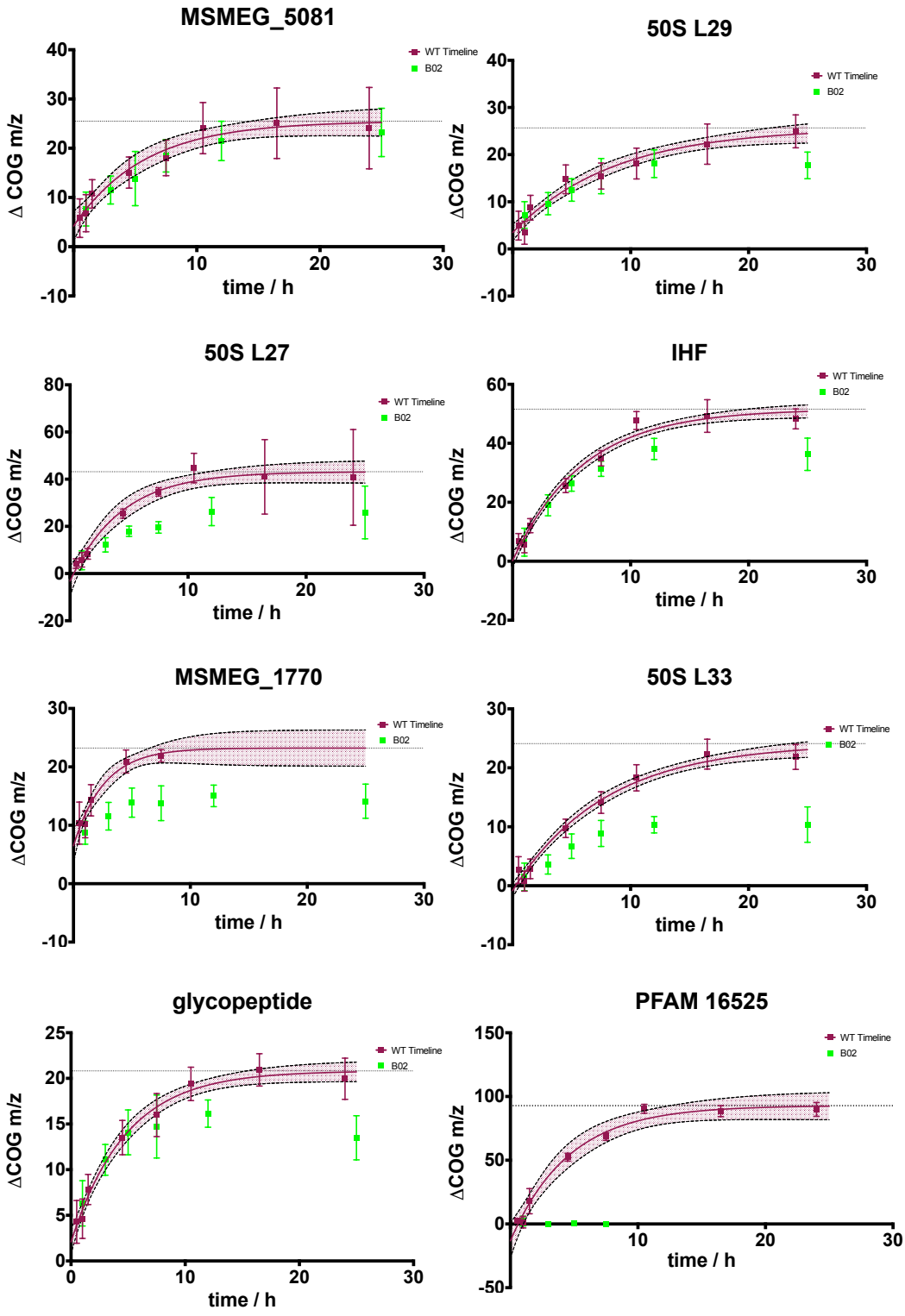

Figure 4-6: Peak shift under the influence of benzothiazinone

ΔCOG in mass to charge (m/z) in dependence of time under the influence of benzothiazinone in 2 x MIC (green, B02). The timeline of the wildtype (WT) is shown magenta with 95% confidence bands. ΔCOG control values of the WT were generated for given timepoints but are not depicted in this graph for better overview. Peak at m/z 5517 – hypothetical protein MSMEG_5081; peak at m/z 4329 – 50 S L29; peak at m/z 4555 – 50 S L27; peak at m/z 5756 – Integration Host Factor; peak at m/z 4152 – hypothetical protein MSMEG_1770; peak at m/z 3160 – 50 S L33; peak at m/z 2755 – glycopeptide (unidentified); peak at m/z 9546 – PFAM16525.

4.3 The Effect of Linezolid on the CFU Count

To test the antimicrobial activity of linezolid, *M. smegmatis* was incubated for a duration of 7.5 hours and 25 hours either with or without exposure to linezolid. The samples were then plated and the colony forming units (CFU) counted. In the following figure, the number of CFU of the *M. smegmatis* culture of the wildtype (WT) compared to *M. smegmatis* exposed to linezolid in 2 x MIC can be seen.

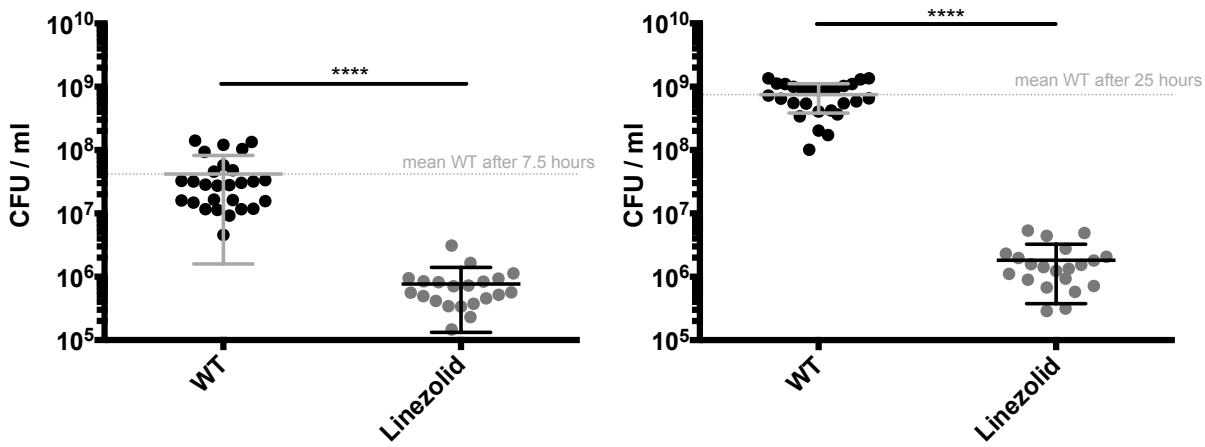

Figure 4-7: *M. smegmatis* CFU count under the influence of linezolid.

Total growth time 7.5 (left) and 25 hours (right). *M. smegmatis* was incubated with linezolid applied in 2 x MIC (c = 1.0 µg/mL). The intersecting line indicates the average CFU count of the wildtype at the same time point respectively. The y-axis starts at 10^5 CFU/mL. Bars refer to mean and standard deviation (SD). $WT_{7.5h}$ = 4.2 x 10^7 CFU/mL; WT_{25h} = 7.5 x 10^8 CFU/mL (both n = 27). Mean $Linezolid_{7.5h}$ = 7.7 x 10^5 CFU/mL; mean $Linezolid_{25h}$ = 1.8 x 10^6 CFU/mL (n = 21). A gaussian distribution could be assumed in the wildtype group, groups were compared using t-test with Welch's correction. Four stars**** refer to a $p < 0.0001$.

On each graph, the average CFU count of the *M. smegmatis* WT is plotted as a dotted line, illustrating the reference to other resulting CFU under exposure with antimicrobial agents: the mean number of CFU counted after 7.5 hours incubation was 4.2 x 10^7 (from 2.6 x 10^7 to 5.8 x 10^7 CFU/mL 95 % confidence interval of mean [95% CI]; n = 27) and 7.5 x 10^8 CFU/mL after 25 hours incubation time (95% CI from 6.0 x 10^8 to 8.9 x 10^8 CFU/mL; n = 27). When testing linezolid as a single agent, the CFU count is significantly different from the WT with a mean of 7.7 x 10^5 after 7.5 hours (4.8 x 10^5 to 1.1 x 10^6 CFU/mL [95%CI]) and 1.8 x 10^6 CFU/mL after 25 hours (1.2 x 10^6 to 2.5 x 10^6CFU/mL [95%CI]; both n = 21, both p <0.0001).

4.4 The Effect of Linezolid on Log Reductions

In the following chart, the killing of *M. smegmatis* exposed to linezolid can be seen in accordance to duration of co-incubation and concentration. The reduction factor was calculated by

the CFU count of *M. smegmatis* exposed to linezolid in relation to the respective wildtype/untreated (WT) control group (for reduction factor, see 3-30).

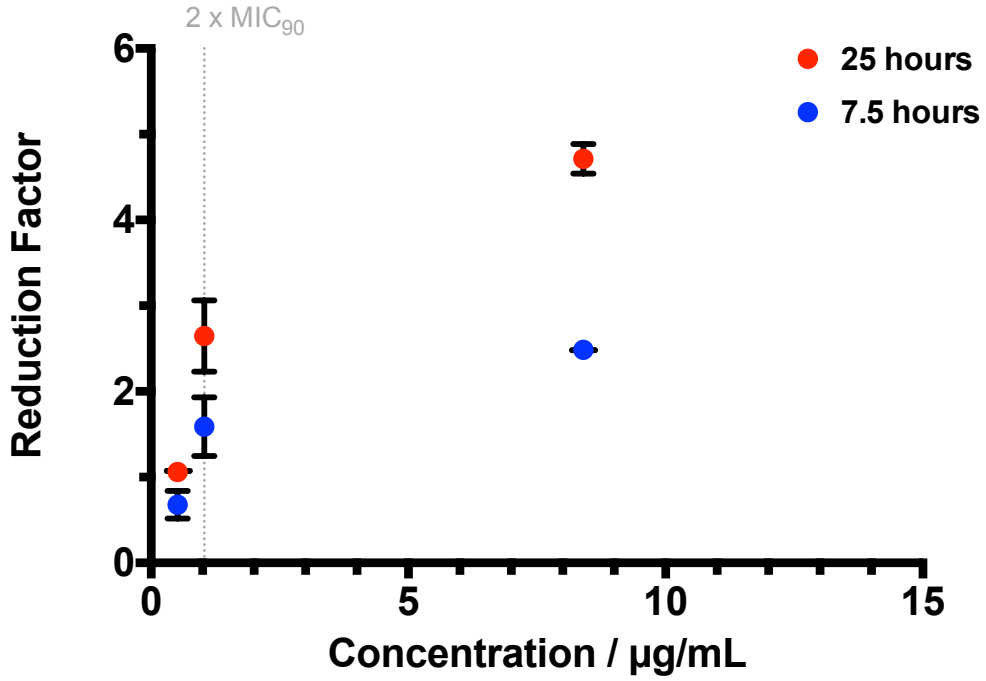

Figure 4-8: Linezolid reduction factor after 7.5 and 25 hours.

Reduction factor (RF) after 7.5 hours and 25 hours under the influence of linezolid applied in 1 x MIC (c = 0.5 µg/mL), 2 x MIC (c = 1.0 µg/mL) and 20 x MIC_{80} (c = 8.4 µg/mL). Bars refer to mean and standard deviation (SD). Duration of observation period is marked either blue (7.5 hours) or red (25 hours). Mean reduction after 7.5 hours: RF_{MIC} = 0.68 (*n* = 3), RF_{2xMIC} = 1.6 (*n* = 21), $RF_{20xMIC80}$ = 2.5 (*n* = 3). Respective reduction after 25 hours: RF_{MIC} = 1.1 (*n* = 3), RF_{2xMIC} = 2.6 (*n* = 21), $RF_{20xMIC80}$ = 4.7 (*n* = 3).

The reduction factor at this concentration and over an observation time of 25 hours reaches a value of 2.6 (*n* = 21). Exemplarily, this means the number of CFU of mycobacteria grown in the presence of linezolid stood in a ratio of 1 : $10^{2.6}$ to the CFU of the WT grown over the same time period. After a total of 7.5 hours observation (blue), the average reduction factor of *M. smegmatis* exposed to linezolid at MIC was found to be 0.68 (95% CI from 0.3 to 1.1), 1.6 at 2 x MIC (1.4 to 1.7) and 2.5 at 20 x MIC_{80} (2.3 to 2.7). After 25 hours of growth, the reduction factor was found to be 1.1 at 1 x MIC (95% CI from 0.8 to 1.3; *n* = 3), 2.6 at 2 x MIC (2.5 to 2.8; *n* = 21) and 4.7 at 20 x MIC_{80} (4.3 to 5.1; *n* = 3). Significant difference between 7.5 and 25 hours could be found at the group exposed to linezolid in 2 x MIC (*n* = 21). A trend of correlation is visible between increasing concentration and reduction factor. Furthermore, a trend is visible that longer incubation period goes along with an increase of the reduction factor (red vs. blue). Comparing the absolute number of the CFU count of *M. smegmatis* with linezolid at 7.5 hours and 25 hours growth time, the number of CFU is still significantly larger in the group that was

incubated for 25 hours (Figure 4-9). This means there is still growth despite inhibition. After 7.5 hours, the average CFU count is 7.7 x 10^5 CFU/mL (95% CI from 4.8 x 10^5 CFU/mL to 1.1 x 10^6 CFU/mL), after 25 hours it is 1.8 x 10^6 CFU/mL (95% CI from 1.2 x 10^6 CFU/mL to 2.5 x 10^6 CFU/mL).

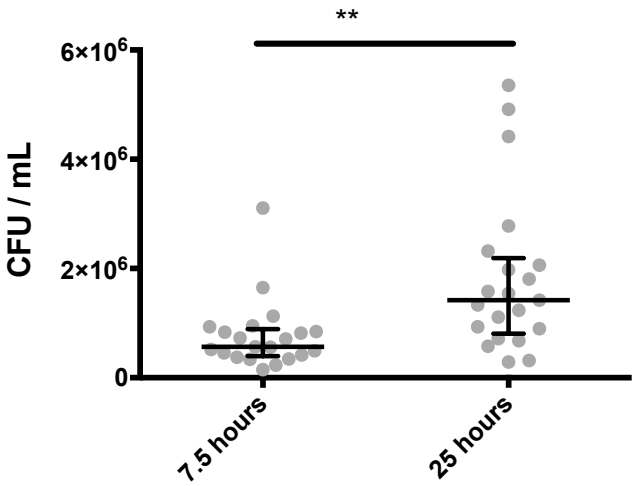

Figure 4-9: Total CFU count under the influence of linezolid after 7.5 hours and 25 hours.

Demonstrating the total CFU count of *M. smegmatis* under the influence of linezolid in 2 x MIC (c = 1.0 µg/mL) at two different points of time. The y-axis begins at 0 CFU/mL. Bars refer to median and inter-quartile range. Mean CFU count = 7.7 x 10^5 after 7.5 hours and 1.8 x 10^6 after 25 hours; *n* = 21. Two stars ** refer to a p-value < 0.01.

This permits the conclusion that *M. smegmatis* still replicates slowly between the observed time points of 7.5 hours and 25 hours and that linezolid under these circumstances is not able to completely impair *M. smegmatis* growth.

4.5 The Effect of Linezolid on *M. smegmatis* Morphology

The micrographs were taken with the scanning electron microscope (SEM) after 7.5 hours and 25 hours incubation of *M. smegmatis* with linezolid in 2 x MIC (c = 1.0 µg/mL). The samples were prepared and fixed following the SEM preparation protocol (3-31). On the basis of the micrographs taken, length and width of *M. smegmatis* were measured with the program ImageJ.

4.5.1 Morphology and Examples

The surface of the *M. smegmatis* wildtype (WT) appears smooth and the bacteria fairly straight. The mean length of the WT averages at 3.9 µm and the mean width at 0.34 µm. On visualization, their shape is found to be regular and consistent over multiple micrographs. *M. smegmatis* incubated with linezolid in 2 x MIC, appears longer than the WT and the bacteria have dents on their surface. Masses as seen in *a)* of Figure 4-10 could be detected on numerous other

photographs after 7.5 hours and 25 hours observation period. After 25 hours, the bacteria have yet increased in length and now have an average length that is more than twice the length of the WT (for length, see Figure 4-11). On multiple micrographs, cells appear distorted and cell bodies flattened. On various images, one pole area was found to be ballooned, as seen in *c)*.

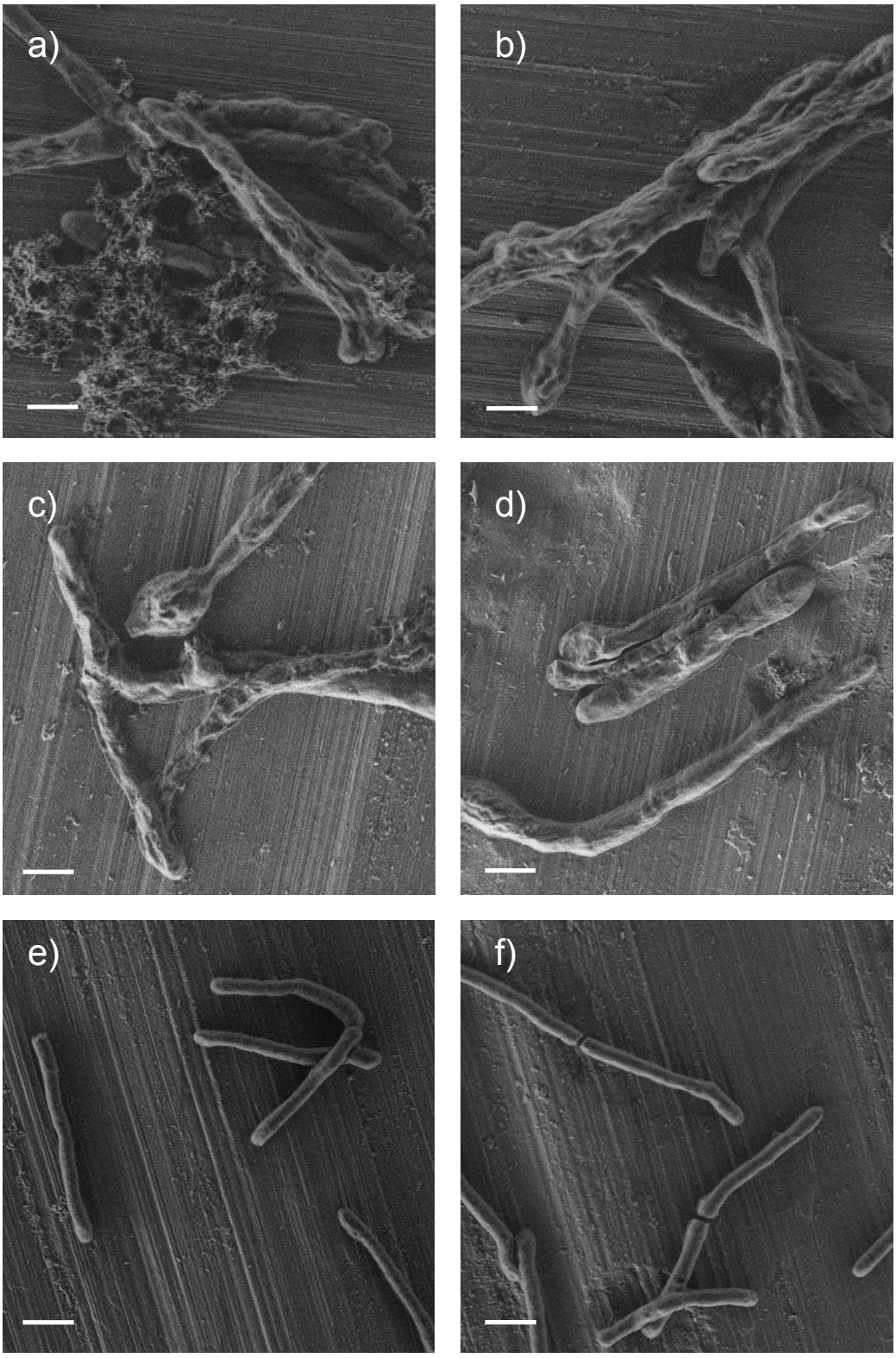

Figure 4-10: *M. smegmatis* morphology, incubated with linezolid in 2 x MIC.

Concentration of linezolid = 1.0 µg/mL (2 x MIC). Observation period in *a)* and *b)* are 7.5 hours with a mean length of 6.1 µm (n = 39) and *c)* and *d)* 25 hours with a mean length of 8.1 µm (*n* = 31). The wildtype for comparison in *e)* and *f)*. The white bar represents 1 µm.

4.5.2 *M. smegmatis* Length and Width

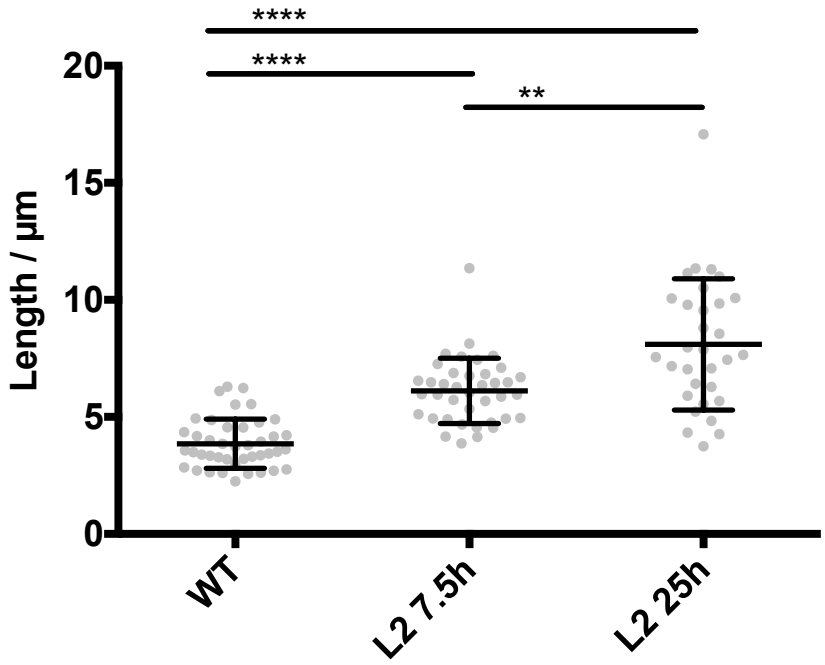

Figure 4-11: *M. smegmatis* length under the influence of linezolid.

Images were taken with the SEM, visualized in Image J and the mycobacteria were measured in their longest diameter using the program Fiji. We measured the samples after each 7.5 and 25 hours of incubation with linezolid in 2 x MIC (L2) and compared them with the wildtype (WT). N ranges from 31 to 42; mean ± SD are blotted. Length of every group was compared to the wildtype or its respective observation period by t-test with Welch's correction. Two stars ** refer to a *p*-value of < 0.001 and four stars **** to a $p < 0.0001$.

The mean length of the *M. smegmatis* WT, observed after 7.5 hours of growth, was found to be 3.9 µm (95 % CI of mean from 3.5 µm to 4.2 µm; $n = 42$). *M. smegmatis* incubated with linezolid in 2 x MIC showed a mean length of 6.1 µm (5.7 µm to 6.6 µm; $n = 39$). Significant increase in length after 7.5 hours compared to WT was $\Delta_{mean} = 2.3$µm (95% CI from 1.7 µm to 2.8 µm; $p < 0.0001$). The mean length after 25 hours incubation time with linezolid reached 8.1 µm (95 % CI from 7.1 µm to 9.1 µm; $n = 31$). The significant difference to WT length averaged at $\Delta_{mean} = 4.2$ µm (95 % CI from 3.7 µm to 5.3 µm; $p < 0.0001$). Extending the observation period from 7.5 hours to 25 hours resulted in a significant length change of $\Delta_{mean} = 2.0$ µm (95% CI from 3.1 µm to 0.9 µm; $p = 0.0008$). From all observed experiments, 8.1 µm was the maximum average length that *M. smegmatis* reached within the row of our experiments.

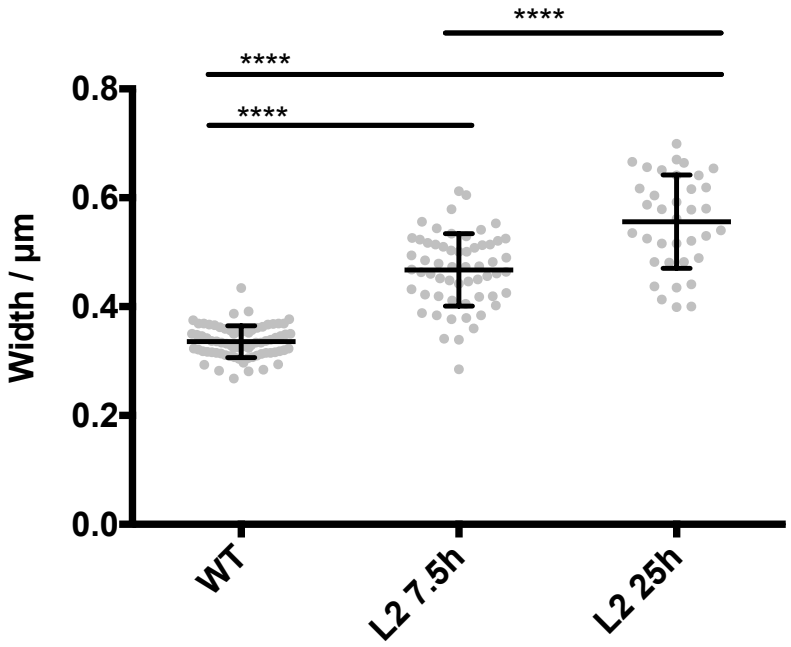

Figure 4-12: *M. smegmatis* width under the influence of linezolid.

The micrographs of *M. smegmatis* were visualized in Image J and measured in their width using the program Fiji. The WT was tested after 7.5 hours. Linezolid (L2) in 2 x MIC (c = 1.0 µg/mL). N ranges from 36 to 74, blotted are mean and SD. A gaussian distribution could be assumed. Significant difference was determined by t-tests with Welch's correction. Four stars **** refer to a $p < 0.0001$.

The mean width of the WT averaged at 0.34 µm (95% CI of mean from 0.33 µm to 0.34 µm; $n = 74$). The width of the group exposed to linezolid in 2 x MIC after 7.5 hours was found to be significantly larger than the WT width, averaging at 0.47 µm (0.45 µm to 0.48 µm; Δ_{width} = 0.13 µm [0.11 µm to 0.15 µm]; $n = 59$, $p < 0.0001$). Incubation for a total period of 25 hours with linezolid in an identical concentration resulted in an even thicker cell shape of 0.56 µm (0.53 µm to 0.59 µm; Δ_{width} = 0.22µm [0.19 µm to 0.25µm]; $p < 0.0001$). Significant difference was also detected between the mean width of *M. smegmatis* exposed to linezolid for 7.5 hours compared to 25 hours (Δ_{width} = 0.09 µm [0.06 µm to 0.12 µm]; $p < 0.0001$).

Based on the average length and width of the WT and estimating a cylindrical shape, a mean surface area of 4 µm^2 and volume of 0.3 µm^3 could be calculated. Estimating the surface with linezolid exposure in consideration of average width and length led to a calculated surface of A = 9 µm^2 after 7.5 hours and 15 µm^2 after 25 hours respectively, thus being a multiple of the surface of the WT. The volume of the bacteria incubated with linezolid could be estimated to be around 1 µm^3 (7.5 hours) and 2 µm^3 (25 hours), also being three to six times larger than the average of the WT. As the calculation of surface and volume is based on using a strictly cylindrical shape and only the average values of width and length measurements were applied, these values are provided for orientation only.

4.6 The Effect of Benzothiazinone on Log Reductions

In order to test the antimicrobial effect of benzothiazinone, mycobacteria were confronted with increasing concentrations of benzothiazinone. The mycobacteria were pre-incubated without the respective therapeutic agent for one hour and then incubated with benzothiazinone in the respective concentration. The incubation time was 7.5 hours or 25 hours in total.

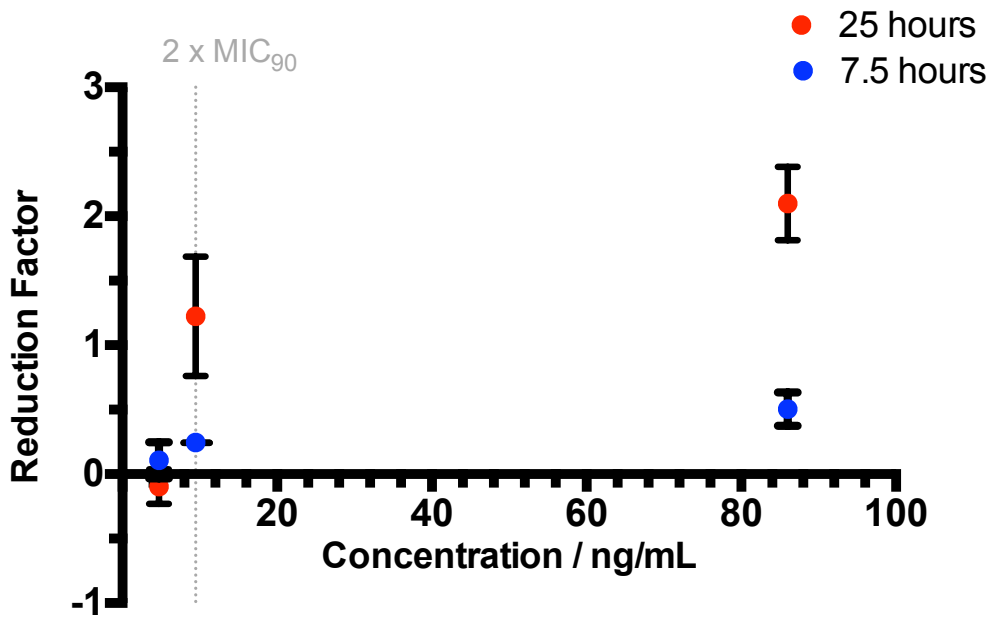

Figure 4-13: Benzothiazinone killing after 7.5 and 25 hours.

Reduction factor after 7.5 hours and 25 hours under the influence of benzothiazinone applied in 1 x MIC (c = 4.7 ng/mL), 2 x MIC (c = 9.5 ng/mL) and 20 x MIC_{80} (c = 86.0 ng/mL). Bars refer to mean and SD. Duration of observation period is marked either blue (7.5 hours) or red (25 hours). Respective reduction after 7.5 hours: RF_{MIC} = 0.11 (*n* = 3), RF_{2xMIC} = 0.25 (*n* = 3), $RF_{20xMIC80}$ = 0.50 (*n* = 3). Respective reduction after 25 hours: RF_{MIC} = - 0.1 (*n* = 3), RF_{2xMIC} = 1.2 (*n* = 3), $RF_{20xMIC80}$ = 2.1 (*n* = 3).

Incubation of *M. smegmatis* with benzothiazinone in its MIC resulted in an average reduction factor of 0.1 after 7.5 hours (95% CI of mean ranged from -0.2 to 0.5; *n* =3) and -0.1 after 25 hours of growth (95% CI of mean from -0.4 to 0.3; *n* = 3). A negative reduction factor refers to a higher number of CFU in the test group compared to the wildtype (WT). Exposure of *M. smegmatis* to benzothiazinone in 2 x MIC showed a reduction factor of 0.25 (95% CI of mean from 0.08 to 0.4; *n* = 3) after 7.5 hours and 1.2 (95% CI of mean from 0.7 to 2.4; *n* = 3) after 25 hours of observation, the latter indicating a mean reduction of approximately 1:10 compared to the wildtype. During the observation period of 7.5 hours, even the highest concentration of benzothiazinone represented by the 20 x MIC_{80}, did not exceed a reduction of 0.5 (0.2 to 0.8; *n* = 3). 25 hours of exposure to benzothiazinone at the same concentration led to a reduction of 2.1 (95% CI of mean from 1.4 to 2.8; *n* = 3), meaning that approximately 1 in 100 mycobacteria

survived. Hence, a trend is visible between increasing concentration of benzothiazinone and reduction factor. Furthermore, there is a trend of correlation between reduction factor and exposure time to benzothiazinone.

4.7 The Effect of Benzothiazinone on the CFU Count

In the following graph, the effect of benzothiazinone in increasing exposure times on the CFU count is depicted regarding a total growth time of 25 hours or 7.5 hours. The experiments were conducted following a general scheme where the pre-incubation period, in this case referring to a segment without the respective antimicrobial agent (BTZ), and the exposure time were modified. The exposure time was modified by sustaining the concentration until the end of the incubation period (long-term) or by eliminating benzothiazinone concentration levels through a specifically developed washing protocol (see 3-29) after 2 hours or 4 hours.

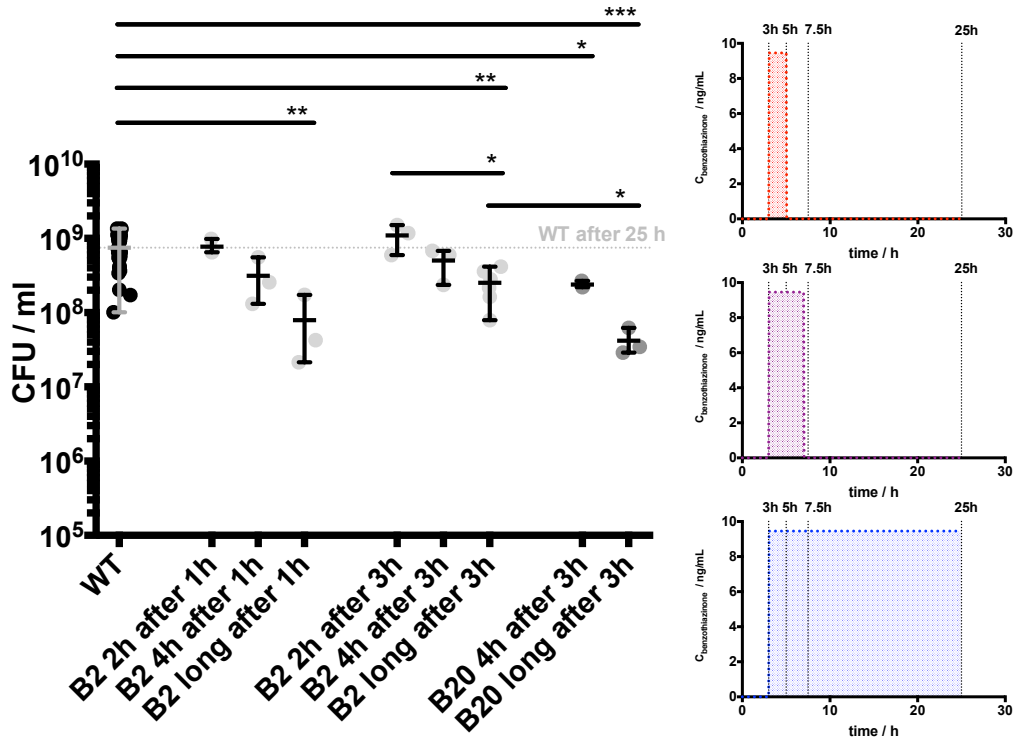

Figure 4-14: *M. smegmatis* CFU count under the influence of increasing exposure times with benzothiazinone.

Left: CFU count after 25 hours growth period with increasing benzothiazinone exposure times. Right: concentration levels of benzothiazinone with a compound-free pre-incubation period of 3 hours, increasing exposure times (2 hours, 4 hours, long = continuously). Bars refer to mean and range. "WT" (grey dotted line) indicates the mean CFU count of the wildtype; "B2" refers to benzothiazinone in 2 x MIC (c = 9.5 ng/mL); "B20" refers to benzothiazinone in 20 x MIC (c = 94.6 ng/mL). 1-hour pre-incubation period: $mean_{B2\ 2h\ after\ 1h}$ = 7.7 x 10^8 CFU/mL (*n* = 3); $mean_{B2\ 4h\ after\ 1h}$ = 3.1 x 10^8 CFU/mL (*n* = 3), $mean_{B2\ long\ after\ 1h}$ = 7.9 x 10^7 CFU/mL (*n* = 3). Benzothiazinone group with 3 hours pre-incubation period: $mean_{B2\ 2h\ after\ 3h}$= 1.1 x 10^9 CFU/mL (*n* = 3); $mean_{B2\ 4h\ after\ 3h}$ = 5.0 x 10^8 CFU/mL (*n* = 3); mean $_{B2\ long\ after\ 3h}$ = 2.5 x 10^8 CFU/mL (*n* = 6), $mean_{B20\ 4h\ after\ 3h}$ = 2.4 x 10^8 CFU/mL (*n* = 3), $mean_{B20\ long\ after\ 3h}$ = 4.2 x 10^7 CFU/mL (*n* = 3).

One star* refers to a *p*-value < 0.05; two stars** to a *p*-value < 0.01; three stars*** to a *p*-value of < 0.001 and four stars to a $p < 0.0001$. A Gaussian distribution could be assumed in the wildtype group ($n = 27$). All benzothiazinone groups had *n* ranging from 3 to 6 and were compared using the Mann-Whitney U test.

M. smegmatis WT reached an average of 7.4×10^8 CFU/mL (95% CI of mean ranging from 6.0×10^8 CFU/mL to 8.9×10^8 CFU/mL; $n = 27$) after 25 hours incubation time. *M. smegmatis* exposed to benzothiazinone in 2 x MIC for 2 hours or for 4 hours after 1-hour pre-incubation showed no significant difference compared to the CFU count of the WT (7.7×10^8 CFU/mL [n = 3] and 3.1×10^8 CFU/mL [$n = 3$]; $p = 0.8453$ and $p = 0.0724$). Significant loss in CFU was observed when *M. smegmatis* was exposed to benzothiazinone for the rest of the experiment ("long", in this case referring to 24 hours after 1-hour pre-incubation) under otherwise identical conditions (mean = 7.9×10^7 CFU/mL; $\Delta_{CFU} = 6.6 \times 10^8$; $p = 0.002$).

Parallel observations were made regarding the experiment with a pre-incubation period of 3 hours: Exposure times with benzothiazinone in 2 x MIC for 2 hours and 4 hours do not cause a significant change of the CFU count in comparison to the WT (mean = 1.1×10^9CFU/mL [n=3] and mean = 5.0×10^8 CFU/mL [$n = 3$]; $p = 0.1547$ and $p = 0.3867$, respectively). In contrast, benzothiazinone added after 3 hours for the long period, meaning until the end of the experiment (total exposure time 22 hours), demonstrated significantly less CFU in comparison to the WT (2.5×10^8 CFU/mL [$n = 6$]; $\Delta_{mean} = 4.9 \times 10^8$ CFU/mL; $p = 0.0014$). The same group also showed significant difference in *M. smegmatis* exposed to benzothiazinone for 2 hours under otherwise identical growth conditions ($\Delta_{mean} = 8.5 \times 10^8$ CFU/mL; $p = 0.024$). Hence, there is a trend of a negative correlation between the exposure time of benzothiazinone and the respective CFU count.

M. smegmatis exposed to benzothiazinone in higher concentrations, now 20 x MIC, shows significant CFU loss by applying the compound for 4 hours (mean = 2.4×10^8CFU/mL [$n = 3$]; $\Delta_{mean} = 5.0 \times 10^8$ CFU/mL; $p = 0.026$). For reference, *M. smegmatis* exposed to benzothiazinone in only 2 x MIC, an exposure time of 4 hours did not result in a significantly reduced CFU count. *M. smegmatis* exposed to benzothiazinone in 20 x MIC after 3 hours preincubation showed a significantly lower CFU count than *M. smegmatis* exposed to 2 x MIC under otherwise identical growth conditions ($\Delta_{mean} = 2.1 \times 10^8$ CFU/mL; $p = 0.0238$).

The data visualized in the graph and elucidated in the text illustrate that both concentration and duration of exposure to benzothiazinone are factors that influence the inhibition of

M. smegmatis. In conclusion, the effect of benzothiazinone on *M. smegmatis* applied as a single agent shows time and dose dependency.

4.8 The Effect of Increasing Benzothiazinone Exposure Times on Log Reductions

The concentration of benzothiazinone in all data groups on the following graph is 2 x MIC and the total observation time is 7.5 hours, equivalent to two *M. smegmatis* lifecycles. Due to a specifically developed washing protocol, benzothiazinone exposure times could be modified (2 hours, 4 hours or "long" = continuously) after a pre-incubation period of either 1 hour or 3 hours. Pooling these groups by their pre-incubation period or inversely, by their time since exposure to benzothiazinone in 2 x MIC of either 4.5 hours or 6.5 hours, respectively, led to the following observation (right graph, Figure 4-15).

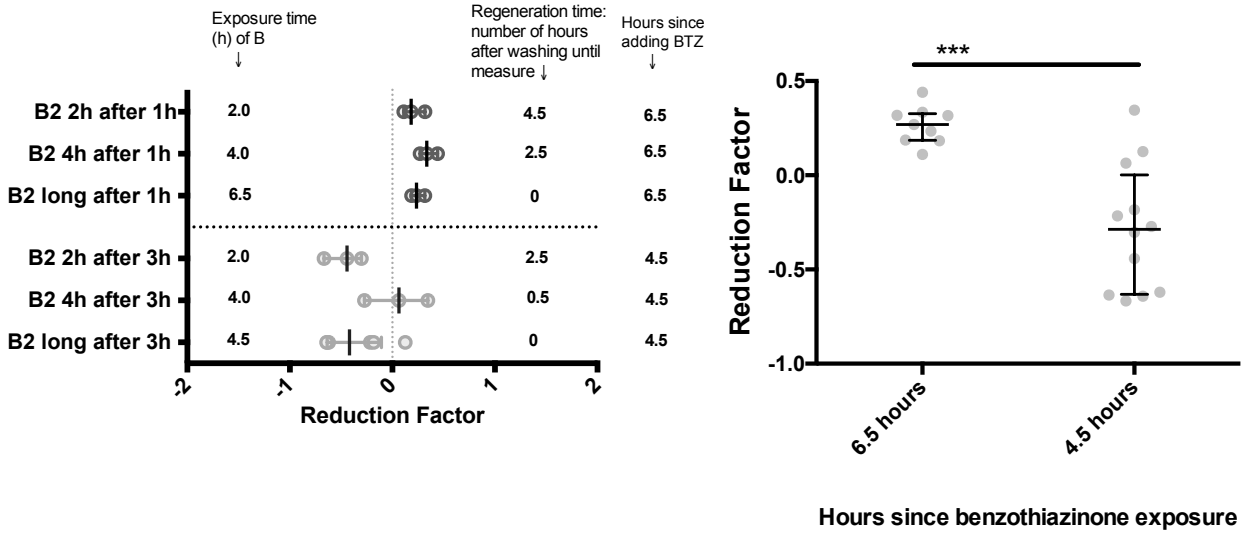

Figure 4-15: Benzothiazinone applied as a single agent after 7.5 hours

Left: The reduction factor plotted under various conditions of applied benzothiazinone. The concentration used and indicated in the graph as "B2" was 2 x MIC value, thus c = 9.5 ng/mL. Right: Growth conditions were pooled by their cumulative observation period since adding benzothiazinone. Bars refer to median and interquartile range. Median $RF_{6.5\ hours}$ = 0.27 (*n* = 9); median $RF_{4.5hours}$= -0.29 (*n* = 12). Significant difference among groups was determined using Mann Whitney U test. Three stars*** refer to a *p*-value of < 0.001.

In the pooled group of values where the duration of observation since adding benzothiazinone does not exceed 4.5 hours, the reduction factor of the pooled group is negative (RF = -0.29; *n* = 12). Therefore, in this case a higher number of CFU was found in the benzothiazinone-exposed group compared to the WT. Although this effect of benzothiazinone appears paradox, this phenomenon occurred in multiple experiments with benzothiazinone. The mean reduction factor determined in the pooled groups where the time since *M. smegmatis* exposure to

benzothiazinone was 6.5 hours (exposure duration for either 2 hours, 4 hours, or 6.5 hours, preincubation for 1 hours) demonstrated a mean of 0.27 (n = 9), thus a positive reduction factor. Hence, the CFU count of the pooled group exposed to benzothiazinone was lower than the CFU count of the respective wildtype (WT). Comparing these two groups by Mann Whitney U test demonstrated that the reduction factor in the 4.5-hour observance group is significantly lower (Δ_{mean} = -0.3; p = 0.0007). In the data collection of the following graph, the observation is prolonged in both pooled groups to a total incubation period of 25 hours (under otherwise identical growth conditions). The pooled groups are now named “24 hours” vs. “22 hours”.

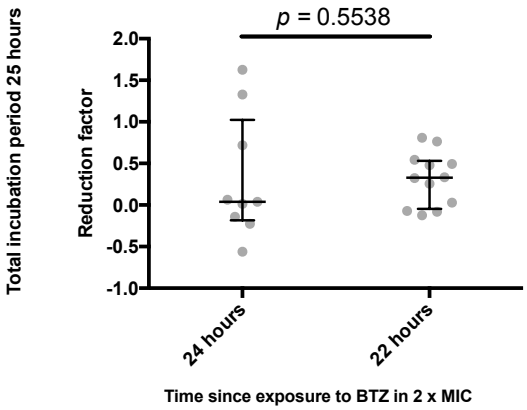

Figure 4-16: Reduction of *M. smegmatis* exposed to benzothiazinone after 25 hours

Reduction factor of either 24 hours or 22 hours observation since exposure to benzothiazinone in 2 x MIC. The number of hours since adding benzothiazinone are pooled as indicated above. 24 hours refers to a pre-incubation period without antibiotic agent of 1 hour, and 22 hours to a pre-incubation period of 3 hours. Median RF $_{24hours}$ = 0.04 (n = 9); median $RF_{22\ hours}$= 0.3 (n = 12); p = 0.5538. Bars indicate median and interquartile range. Groups were compared using Mann Whitney U test.

Prolonging the observation time to 25 hours whilst maintaining identical exposure times to benzothiazinone in the pooled groups, the initial difference in the reduction factor between the pooled groups cannot longer be observed (p = 0.5538, Figure 4-16). The average values of log reductions were 0.3 for 24 hours (95% CI from -0.3 to 0.9) and 0.3 for 22 hours (95% CI of mean ranging from 0.1 to 0.5), in total lack of a significant difference. Moreover, they prove to be highly similar groups. Thus, by this time there is no longer evidence of our previously observed “paradox effect”. From these results, we draw the conclusion that the “paradox effect” of benzothiazinone possibly is a transient phenomenon which appears in the initial phase of exposure and disappears in the course of the experiment. These results will further be discussed.

4.9 The Effect of Benzothiazinone on *M. smegmatis* Morphology

Micrographs of *M. smegmatis* were taken with the SEM after 7.5 hours and 25 hours incubation of *M. smegmatis* with benzothiazinone in 2 x MIC (c = 0.95 ng/mL). The samples were prepared and fixed following the SEM preparation protocol (see 3-31).

4.9.1 Morphology and Examples of *M. smegmatis* Incubated with Benzothiazinone

After an incubation time of 7.5 hours, the bacteria exposed to benzothiazinone (see *a)* and *b)* of Figure 4-17) have a smooth surface, but are shorter than the wild type (compare Figure 4-18). After 25 hours, the surface of the bacteria appears irregular and has dents. The borders between bacteria in multiple cases are not clearly definable. All in all, they are even shorter than after the 7.5-hour incubation period.

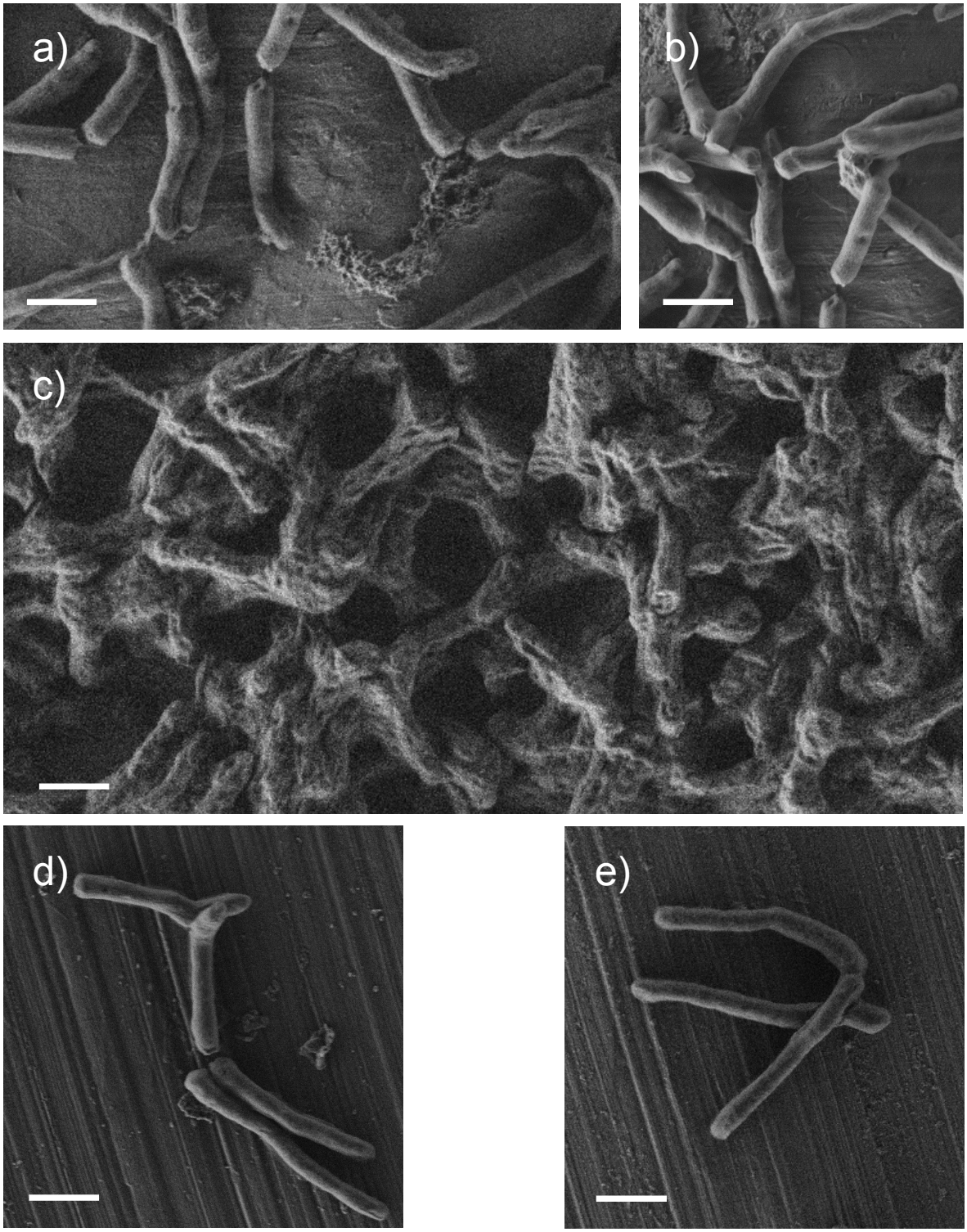

Figure 4-17: *M. smegmatis* under the influence of benzothiazinone

M. smegmatis incubated only with benzothiazinone in 2 x MIC (c = 0.95 ng/mL). *a)* and *b)* are samples after 7.5 hours (mean length = 2.9 µm); *c)* looked at after 25 hours (mean length = 2.3 µm); *d)* and *e)* represent the wildtype. The white bar represents 1 µm.

4.9.2 *M. smegmatis* Length and Width

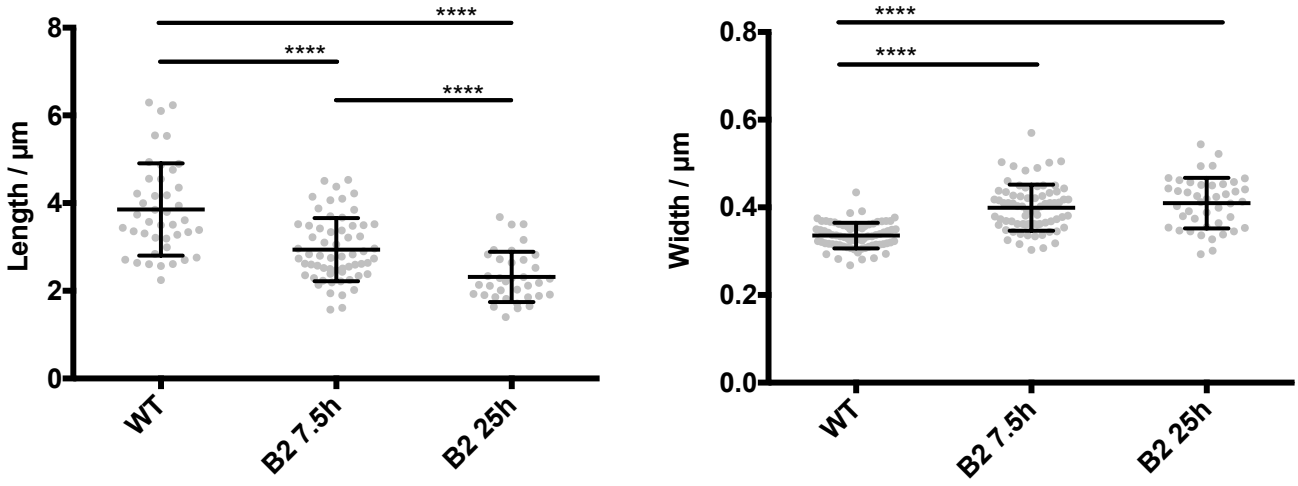

Figure 4-18: *M. smegmatis* length and width under the influence of benzothiazinone.

Left: *M. smegmatis* length; right*: M. smegmatis* width. Images were taken with the scanning electron microscope and mycobacteria were measured in length and width using the program Fiji. We measured the bacteria without antibiotic treatment (WT) and after incubation with benzothiazinone in 2 x MIC ("B2"; c = 0.95 ng/mL) for 7.5 hours and 25 hours. Error bars refer to mean ± SD; *n* ranges from 36 to 74. A gaussian distribution could be assumed for all groups. The length of every group was compared to the wildtype or its respective observation period by using t-tests with Welch's correction. Four stars **** refer to a $p < 0.0001$.

For reference, the mean length of the *M. smegmatis* wild type is depicted in the chart on the left (3.9 µm; 95% CI from 3.5 µm to 4.2 µm; $n = 42$). In contrast, exposure to benzothiazinone demonstrated a significant decrease of the bacterial length to 2.94 µm ($n = 61$; $p < 0.0001$) after 7.5 hours and to 2.3 µm ($n = 36$) after 25 hours incubation time. The difference was found to be significant with $\Delta = -0.6$ µm (95% CI from -0.3 µm to -0.9 µm; $p < 0.0001$).

Mycobacteria treated with benzothiazinone and grown over 7.5 hours have a width of 0.40 µm (95% CI from 0.38 µm to 0.41 µm; $n = 73$) and therefore appear thicker than the wildtype (0.34 µm; $\Delta = 0.064$ µm [0.050 µm to 0.077 µm]; $p < 0.0001$). The width does not significantly increase with a longer growth period to an extent of 25 hours ($p = 0.33$) where the width averaged at 0.41 µm (95% CI from 0.39 µm to 0.43 µm; $n = 43$). Assuming a cylindrical shape, a rough estimate of their surface using mean of length and width projects to 4 µm^2 after 7.5 hours; and to 3 µm^2 after the 25-hour observation period. In both cases, the estimated surface of the mycobacteria incubated with benzothiazinone is smaller than the estimated surface of the WT (estimated surface area 4 µm^2; volume = 0.3 µm^3) and decreases in dependence to the duration of incubation with the compound. The estimated volume amounts to 0.4 µm^3 after 7.5 hours of exposure to benzothiazinone; after 25 hours 0.3 µm^3. These values were assessed

for orientation only, however, they suggest that, in sum, the bacteria become shorter and thicker under the influence of benzothiazinone.

4.10 Combining Linezolid and Benzothiazinone

The effect of the combination of linezolid and benzothiazinone on the CFU count, the reduction factor and on the *M. smegmatis* morphology were studied in different experiments in which the following variables were modified:

1) Length of the pre-incubation period with linezolid, the compound applied first
2) Exposure time of benzothiazinone
3) Concentration of linezolid and benzothiazinone in multiples or fractions of their MIC values

The total growth and observation time were 7.5 hours and 25 hours, respectively. An exemplary experimental setup is shown in Figure 4-19.

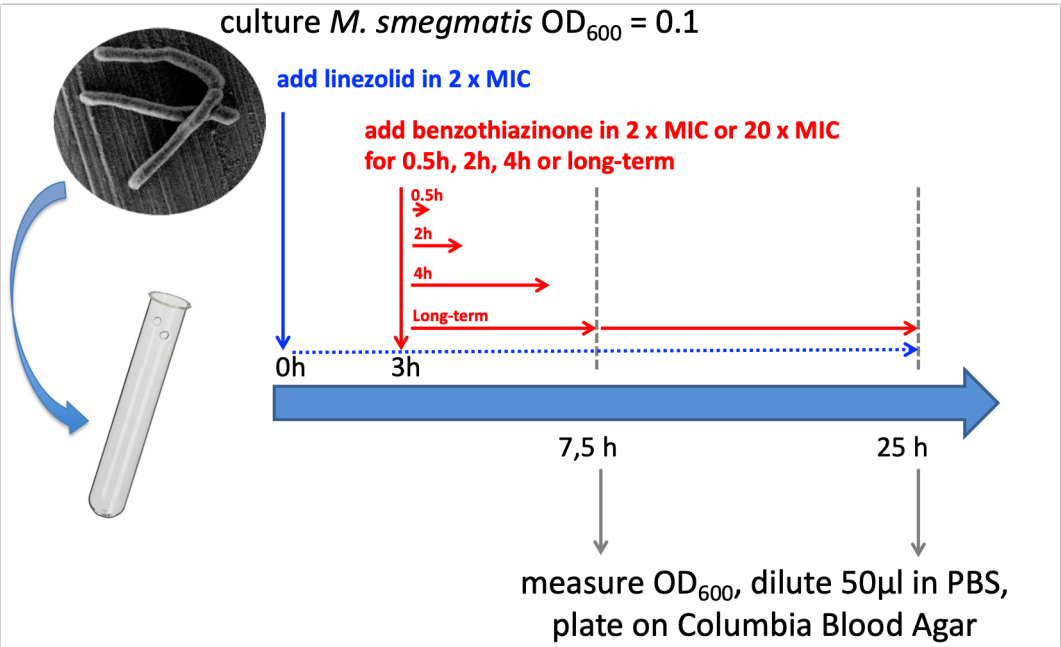

Figure 4-19. Exemplary experimental setup of the combination of linezolid and benzothiazinone.

4.10.1 Increasing the Benzothiazinone Exposure Time

In this experiment, linezolid and benzothiazinone in 2 x MIC were tested in their combination on *M. smegmatis* by observing growth over a total of 25 hours incubation time and calculating the reduction factor. For reference, the effect of linezolid as a single agent is shown in the chart to facilitate the direct comparison to the effect of the combined compounds. Based on the data from carbon isotope traced protein-profiles obtained through MALDI-TOF MS under the influence of linezolid and previous experiments with the single agents (4-42), it could be assumed that linezolid reaches strong effectiveness before three hours (4-37). In coherence to the theory behind the mechanism of both agents, the effect of adding benzothiazinone in 2 x MIC of

increasing exposure duration was tested after a pre-incubation period with linezolid in 2 x MIC of 3 hours. The exposure duration of benzothiazinone was modified by eliminating the benzothiazinone concentration through a specifically developed washing protocol (3-29).

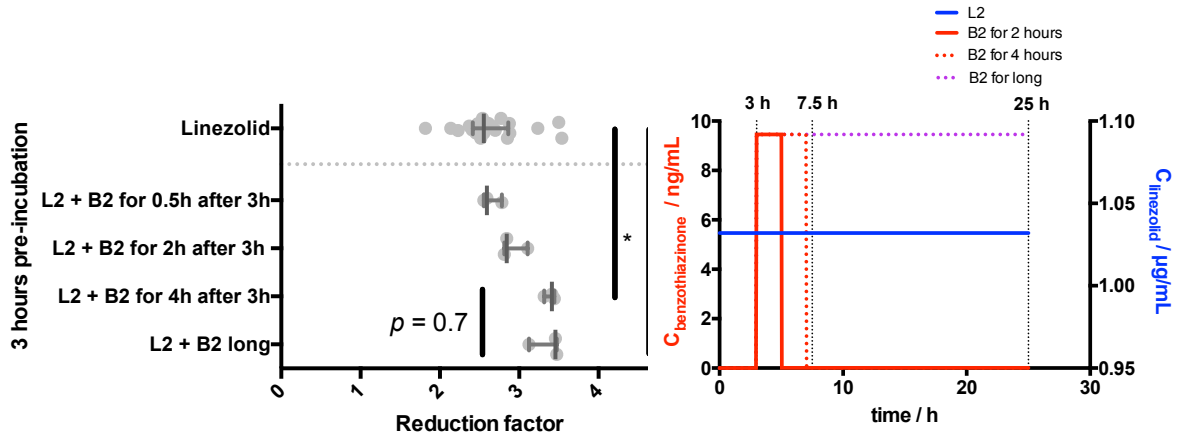

Figure 4-20: 3 hours pre-incubation with linezolid and increasing benzothiazinone exposure times after 25 hours.

Left: Log reductions in dependence to benzothiazinone exposure time (0.5 hours, 2 hours, 4 hours and continuously) after a 3-hour pre-incubation period with linezolid and a total incubation time of 25 hours. Right: Concentration scheme. Compare RF of continuously applied linezolid and combined benzothiazinone when used in constant concentrations but various exposure times. L2 = linezolid used in 2 x MIC (c = 1.032 µg/mL); B2 = benzothiazinone used in 2 x MIC (c = 9.456 ng/mL. Bars refer to median and interquartile range. Median values of the reduction factor: $RF_{Linezolid} = 2.6$ ($n = 21$); $RF_{L2+B2\ for\ 0.5h} = 2.6$ ($n = 3$); $RF_{L2+B2\ for\ 2h} = 2.8$ ($n = 3$); $RF_{L2+B2\ for\ 4h} = 3.4$ ($n = 3$); $RF_{L2+B2\ long} = 3.5$ ($n = 3$). One star * refers to a p-value < 0.05. All combination groups compared and tested for significance by using the Mann-Whitney U test.

The reduction factor in the linezolid control group averaged at 2.6 (95% confidence interval of mean from 2.5 to 2.8; $n = 21$; Figure 4-20). The effect of adding benzothiazinone in 2 x MIC for only half an hour exhibited a nearly identical mean reduction factor of 2.6 (2.3 to 2.9; $n = 3$; $p = 0.68$). Thus, no additional killing could be observed when benzothiazinone (2 x MIC) was added for half an hour. Adding benzothiazinone for 2 hours showed an average reduction factor of 2.9 (95% CI from 2.5 to 3.3; $n = 3$). It did not present significant difference neither to the linezolid control group ($p = 0.17$) nor to the group with half an hour benzothiazinone application ($p = 0.1$). However, a significantly larger reduction compared to the linezolid control group was found when benzothiazinone in 2 x MIC was added to linezolid for 4 hours or for the entire rest of the growth period. The reduction factor averaged at 3.4 (95% CI from 3.2 to 3.6; $n = 3$; $p = 0.023$) and 3.4 respectively (95% CI from 2.9 to 3.8; $n = 3$; $p = 0.031$). For comparison, benzothiazinone applied in the same concentration and for the same duration as a single agent reached a mean reduction factor of 0.05 (95% CI from -0.6 to 0.7; Figure 4-13). A trend in this graph is visible and the two bottom sample groups of the chart determine that combining

benzothiazinone with linezolid for at least 4 hours significantly increases the reduction factor in contrast to the single agent linezolid. The reduction factor in the 4-hour group reaches a mean of 3.4, matching the reduction factor obtained after the additional application of benzothiazinone long-term (also 3.4; p = 0.7). Therefore, adding benzothiazinone for 4 hours to *M. smegmatis* at a concentration level of 2 x MIC did not show less reduction compared to adding benzothiazinone long-term at the same concentration level, in both cases after a previous incubation period of three hours with linezolid.

4.10.2 Peak Benzothiazinone Concentration

We investigated whether a particularly high concentration with benzothiazinone (20 x MIC) and a short exposure would be sufficient to achieve the same effect as a longer, lower-concentrated benzothiazinone exposure when combined with linezolid. To test this, *M. smegmatis* growth was observed after 25 hours of incubation time, the experimental setup being the same as in the previous figure (Figure 4-20), except that benzothiazinone was applied in a concentration *ten times* higher than the previous chart (20 x MIC, c = 94.56 ng/mL).

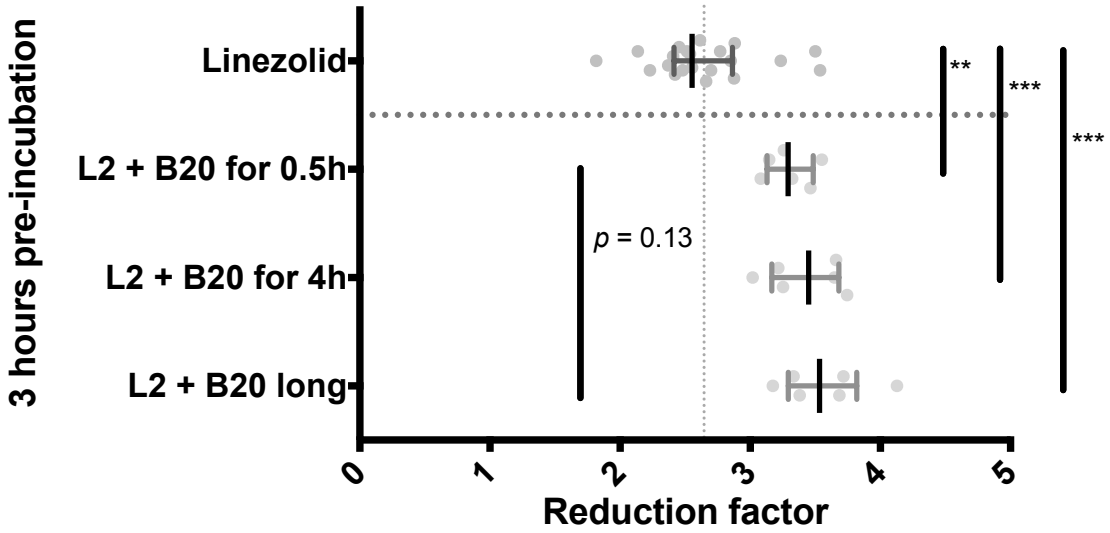

Figure 4-21: Linezolid and benzothiazinone combined activity with benzothiazinone administered in 20 x MIC.

Linezolid was applied in 2 x MIC (c = 1.0 µg/mL) and benzothiazinone in 20 x MIC (c = 94.6 ng/mL) for either 0.5 hours, 2 hours, 4 hours or long-term. The pre-incubation period with linezolid lasted three hours. Total growth time was 25 hours. Bars refer to median and interquartile range. Median values of the reduction factor: $RF_{linezolid}$= 2.6 (n = 21), $RF_{L2+B20\ for\ 0.5h}$= 3.3 (n = 6), $RF_{L2+B20\ for\ 4h}$= 3.5 (n = 6), $RF_{L2+B20\ long}$ = 3.5 (n = 6). One star * refers to a p-value < 0.05; two stars ** to a p-value < 0.01, three stars *** to a p-value of < 0.001. All benzothiazinone groups were compared and tested for significance by using the Mann-Whitney U test.

In this experiment, all combination groups differ significantly from the linezolid control group (Figure 4-21). The data shown in the figure demonstrates that an additional exposure of *M. smegmatis* to benzothiazinone in 20 x MIC for half an hour presents a significantly higher reduction of mycobacteria than incubation with linezolid only. The reduction factor averaged at 3.3 (95 % CI of mean from 3.1 to 3.5; $n = 6$) versus 2.6 with linezolid as a single agent (2.5 to 2.8; $p = 0.0015$; $\Delta_{median} = 0.7$). Benzothiazinone exposure times of 4 hours or for the rest of the incubation period ("long" = continuously) resulted in a mean reduction of 3.4 (3.1 to 3.7; n = 6) and 3.6 (3.2 to 3.9; $n = 6$), respectively. Both reduction factors were significantly higher than the reduction factor of the linezolid control group ($p = 0.0004$ and $p = 0.0003$, respectively). No significant difference could be detected between adding benzothiazinone for half an hour or long-term ($p = 0.13$; $n = 6$ in both groups). Therefore, we can conclude that already half an hour of the additional application of benzothiazinone in 20 x MIC combined to linezolid in 2 x MIC did not show significantly less killing of *M. smegmatis* than adding benzothiazinone at the same concentration continuously, here completing a total exposure time of 22 hours.

4.10.3 Linezolid Pre-Incubation Period

Based on the theory, it was assumed that both the benzothiazinone exposure and the pre-incubation time with linezolid are pivotal parameters for an increased efficiency of both antibiotics. In the following experiment, the pre-incubation period of linezolid was modified to a shorter period of 1 hour (Figure 4-22).

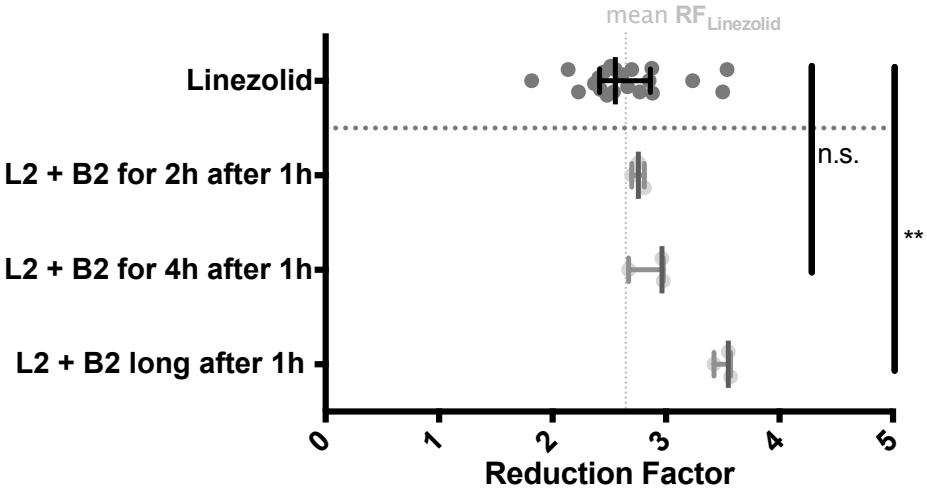

Figure 4-22: 1-hour pre-incubation with linezolid and increasing benzothiazinone exposure times.

M. smegmatis exposed to linezolid and benzothiazinone in 2 x MIC, total observance time 25 hours. Pre-incubation period with only linezolid lasted 1 hour. Bars refer to median and interquartile range. The median values of reduction factor: $RF_{Linezolid} = 2.6$ ($n = 21$); $RF_{L2 + B2\ 2h\ after\ 1h} = 2.8$ ($n = 3$); $RF_{L2+B2\ 4h\ after\ 1h}$=

3.0 (n = 3) and RF $_{L2\ +B2\ long\ after\ 1h}$= 3.6 ($n$ = 3). Two stars ** refer to a p-value < 0.01. All combination groups were tested for significance by using the Mann-Whitney U test.

The reduction factor of *M. smegmatis* exposed to additional benzothiazinone for 2 hours averaged at 2.8 (95 % CI of mean from 2.6 to 2.9; n = 3). The reduction factor averaged at 2.9 (95 % CI from 2.4 to 3.3; n = 3) when benzothiazinone was added for 4 hours. When tested, both groups did not show significant difference compared to the linezolid control group (p = 0.4012 and p = 0.1453). For reference, when benzothiazinone was tested after a 3-hour pre-incubation period with linezolid, as seen in the previous experiment (Figure 4-20), the addition of the compound for 4 hours significantly increased the reduction factor to a mean of 3.4. Here, the 4-hour benzothiazinone exposure time administered after only 1-hour pre-incubation with linezolid did not demonstrate a significant change compared to the linezolid control group (p = 0.1453). Lastly, adding benzothiazinone in 2 x MIC long-term (24 hours, for the rest of the experiment), showed a significantly higher average reduction factor of 3.5 (95 % CI from 3.3 to 3.7; n = 3; Δ_{median}= 1.0; p = 0.004). There is a visible trend for an increase of the reduction factor with increase of benzothiazinone exposure time. The data shown in the graph enables the conclusion that 1 hour of pre-incubation with linezolid is not sufficient for a synergistic effect between both compounds when benzothiazinone is applied for 4 hours in 2 x MIC.

4.10.4 Combination Studies of Linezolid and Benzothiazinone Observed after 7.5 Hours

In the data visualized in Figure 4-23, the reduction factor of *M. smegmatis* after an incubation time of 7.5 hours is blotted. The culture was pre-incubated with linezolid in 2 x MIC for 3 hours and then exposed to benzothiazinone for the duration of 0.5 hours, 2 hours, 4 hours or the rest of the total growth time ("long" = continuously, in this case referring to 4.5 hours).

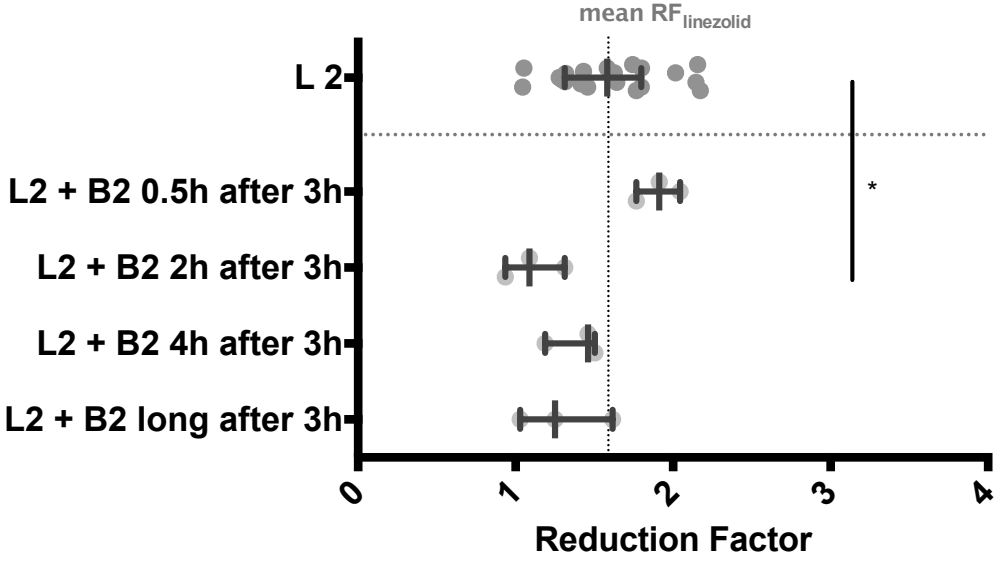

Figure 4-23: 3 hours pre-incubation with linezolid and increasing benzothiazinone exposure times after 7.5 hours.

Total incubation time was 7.5 hours. L2 = linezolid applied in 2 x MIC, B2 = benzothiazinone applied in 2 x MIC. The pre-incubation period with linezolid as a single agent was 3 hours. Error bars refer to median and interquartile range. The median values of reduction: $RF_{linezolid}$ = 1.6 (*n* = 21); $RF_{L2+B2\ 0.5h}$= 1.9 (*n* = 3); $RF_{L2+B2\ for\ 2h}$ = 1.1 (*n* = 3); $RF_{L2+B2for4h}$ = 1.5 (*n* = 3); $RF_{L2+B2\ long}$= 1.3 (*n* = 3). One star * refers to a *p*-value < 0.05. The combination groups had too small *n* values to assume a Gaussian distribution (all *n* = 3) and were thus compared using the Mann-Whitney U test.

Exposing *M. smegmatis* to benzothiazinone for half an hour results in an average reduction factor of 1.9 (95 % CI of mean ranging from 1.6 to 2.3; *n* = 3) and does not present with a significant difference to the incubation with linezolid as a single agent (mean reduction factor 1.6; 95% CI of mean from 1.4 to 1.7; *p* = 0.1215). The reduction factor of the combination sample with the benzothiazinone exposure time of 2 hours (mean reduction factor 1.1; 95 % CI of mean from 0.6 to 1.6; *n* = 3) was significantly lower than that of the linezolid control group (Δ_{median} = - 0.49; *p* = 0.03). Exposure of 4 hours resulted in a reduction factor averaging at 1.4 (95 % CI from 1.0 to 1.8; *n* = 3) and exposing to benzothiazinone for the rest of the experiment the reduction averaged at 1.3 (0.6 to 2.0; *n* = 3). Neither of the two later appeared significantly different from the linezolid control group (*p* = 0.4516 and *p* = 0.1215). Apart from that, the trend shows that the reduction factor in all combination groups with a benzothiazinone exposure time of minimum 2 hours *is lower* than the average of the linezolid control group. The increased antimicrobial effect of adding benzothiazinone compared to linezolid as a single agent that had been observed in a 25-hour incubation period in otherwise identical growth conditions (as pointed out in the paragraph 4.10.1; Figure 4-20), cannot be observed when the total incubation time is limited to 7.5 hours.

In the following, the combination of both compounds was studied in a total growth period of 7.5 hours with 20 x MIC of benzothiazinone (Figure 4-24). The mean reduction factor in combination with half an hour benzothiazinone was 2.2 (95 % CI from 2.0 to 2.5; *n* = 6); for 4 hours 1.6 (95 % CI from 1.3 to 1.9; *n* = 6) and 1.9 in the long-term combination (95 % CI from 1.5 to 2.3; *n* = 6). We observed that the reduction factor was significantly higher when combining linezolid with benzothiazinone for half an hour compared to applying linezolid alone (Δ_{median} = 0.6; *p* = 0.0008). *M. smegmatis* exposed to benzothiazinone for 4 hours had a significantly *lower* reduction factor than *M. smegmatis* exposed to benzothiazinone for only 0.5 hours (*p* = 0.0022). No significant difference was found between the group exposed to benzothiazinone for 4 hours and the linezolid control (*p* = 0.7547). The combination group with

benzothiazinone applied long-term led to a significantly higher reduction factor than linezolid alone (p = 0.0488).

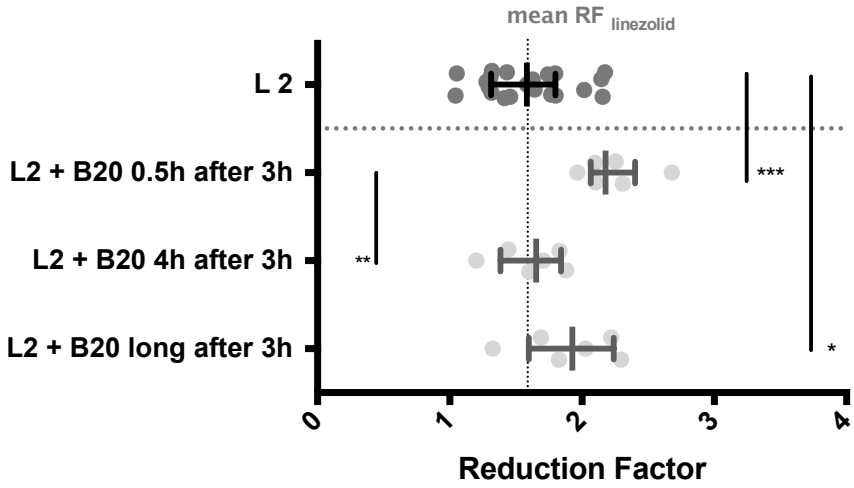

Figure 4-24: 3h pre-incubation with linezolid and benzothiazinone in 20 x MIC after 7.5 hours.

Total growth time was 7.5 hours. L2 = linezolid used in 2 x MIC, B20 = benzothiazinone applied in 20 x MIC after 3 hours. Error bars refer to median and interquartile range. Median values: $RF_{linezolid}$ = 1.6 (n = 21); $RF_{L2+B20for0.5h}$ = 2.2 (n = 6); $RF_{L2+B20\ for\ 4h}$= 1.7 (n = 6); $RF_{L2+B20\ long}$= 1.9 (n = 6). Two stars ** refer to a p-value < 0.01, three stars *** to a p-value of < 0.001. Groups were compared using the Mann-Whitney U test.

No significant difference could be detected between the 4-hour and the continuous exposure (p = 0.2403). In conclusion, at this benzothiazinone concentration (20 x MIC), a significant increase of reduction by the benzothiazinone exposure could be detected when the benzothiazinone exposure time was either 0.5 hours or continuous (here 4.5 hours). Interestingly, in both experimental set-ups with a limited observation time of 7.5 hours (Figure 4-23 and Figure 4-24), we could observe that an additional half-hour exposure to benzothiazinone in 2 x MIC as well as in 20 x MIC led to stronger reduction than the *longer* exposure. This again, appears paradox and will further be discussed (5.4).

In the following graph (Figure 4-25), the combination of linezolid and benzothiazinone in both 2 x MIC is analyzed after an observation period of 7.5 hours and here, *M. smegmatis* was pre-incubated with linezolid for only one hour before benzothiazinone was added. When benzothiazinone was added for 2 hours, the mean reduction was found to be 1.6 (95 % CI from 1.4 to 1.8; n = 3). When it was added for 4 hours, it averaged at 1.7 (95 % CI from 0.8 to 2.5; n =3) and when added long-term, it resulted in an average reduction of 1.1 (95 % CI from 0.8 to 1.4; n = 3).

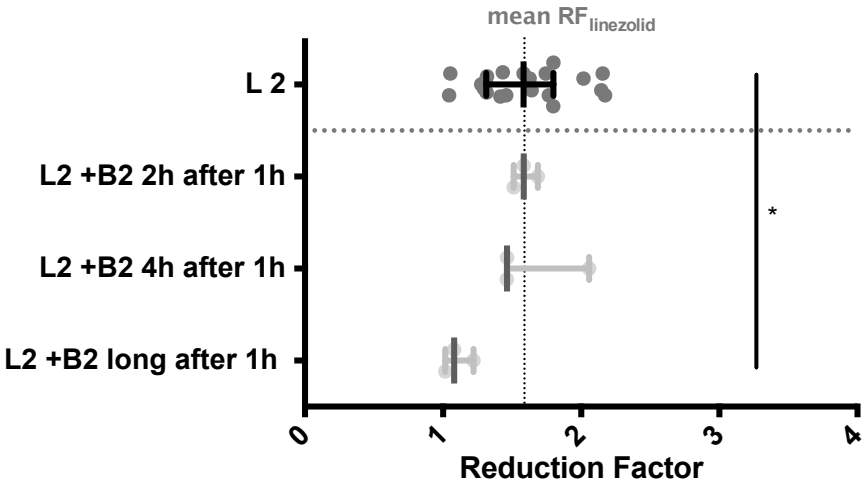

Figure 4-25: 1-hour pre-incubation with linezolid after a total growth period of 7.5 hours.

Total growth time was 7.5 hours. L2 = linezolid applied in 2 x MIC, B2 = benzothiazinone used in 2 x MIC; the pre-incubation with linezolid lasted 1 hour. Error bars refer to median and interquartile range. Median values of reduction: $RF_{linezolid}$ = 1.6 (n = 21); $RF_{L2+B2\ 2h}$= 1.6 (n =3); $RF_{L2+B2\ 4h}$ = 1.5 (n = 3); $RF_{L2+B2\ long}$= 1.1 (n = 3). One star * refers to a p-value < 0.05. The combination groups had n values too small to assume a Gaussian distribution and were thus compared and tested for significance by using the Mann-Whitney U test.

M. smegmatis additionally exposed to benzothiazinone for 2 hours or 4 hours showed no difference in comparison to the control group with only linezolid (p = 0.87 and p = 0.62, respectively). The reduction factor was significantly lower (p = 0.01) when linezolid and benzothiazinone were applied for a long period, meaning that the benzothiazinone concentration was kept at a constant level until the samples were taken for plating. This can be described as the opposite effect from what could be observed in the exact same experiment after 25 hours growth (Figure 4-22) where the reduction factor in the long-termed combination group was significantly higher.

4.10.5 The Effect of Linezolid and Benzothiazinone on *M. smegmatis* Morphology

Exemplary micrographs of *M. smegmatis* exposed to linezolid for 3 hours and four hours in combination with benzothiazinone are shown (Figure 4-26). The top row, *a)* and *b)*, represent the bacteria after 7.5 hours growth, the middle row after 25 hours of growth. After 7.5 hours, the cells have an irregular surface and deep dents on their cell bodies. Also, unclear material is detected in between cells on various images. After 25 hours, the cell bodies appear even more distorted and flattened. At last, *M. smegmatis* grew in the presence of both linezolid and long-term benzothiazinone (identical scheme as shown before in Figure 4-28), the micrographs are visualized in Figure 4-27. The cell bodies have an irregular morphology, appear torn in their surface and provide an aspect as if they had been pealed. After 25 hours growth period with

both compounds, see *d)* and *e)*, it was even harder to find intact cell bodies, concluding that even more cells have lost their integrity, possibly due to lysis. They are not distinguishable in their average length to the compound combination with only four hours of benzothiazinone exposure time (Figure 4-26), and both the bacteria after 7.5 hours and after 25 hours have an average length of 5.8 µm. Their width remains unchanged after 7.5 hours and 25 hours, both averaging at 0.52 µm (results explained on page 4-65). This is thicker than the wildtype and can be compared in *e)* and *f)* of Figure 4-27. From the micrographs alone, it was not possible to distinguish between the group with four-hour benzothiazinone exposure time after 25 hours growth and long-term exposure time after 25 hours growth.

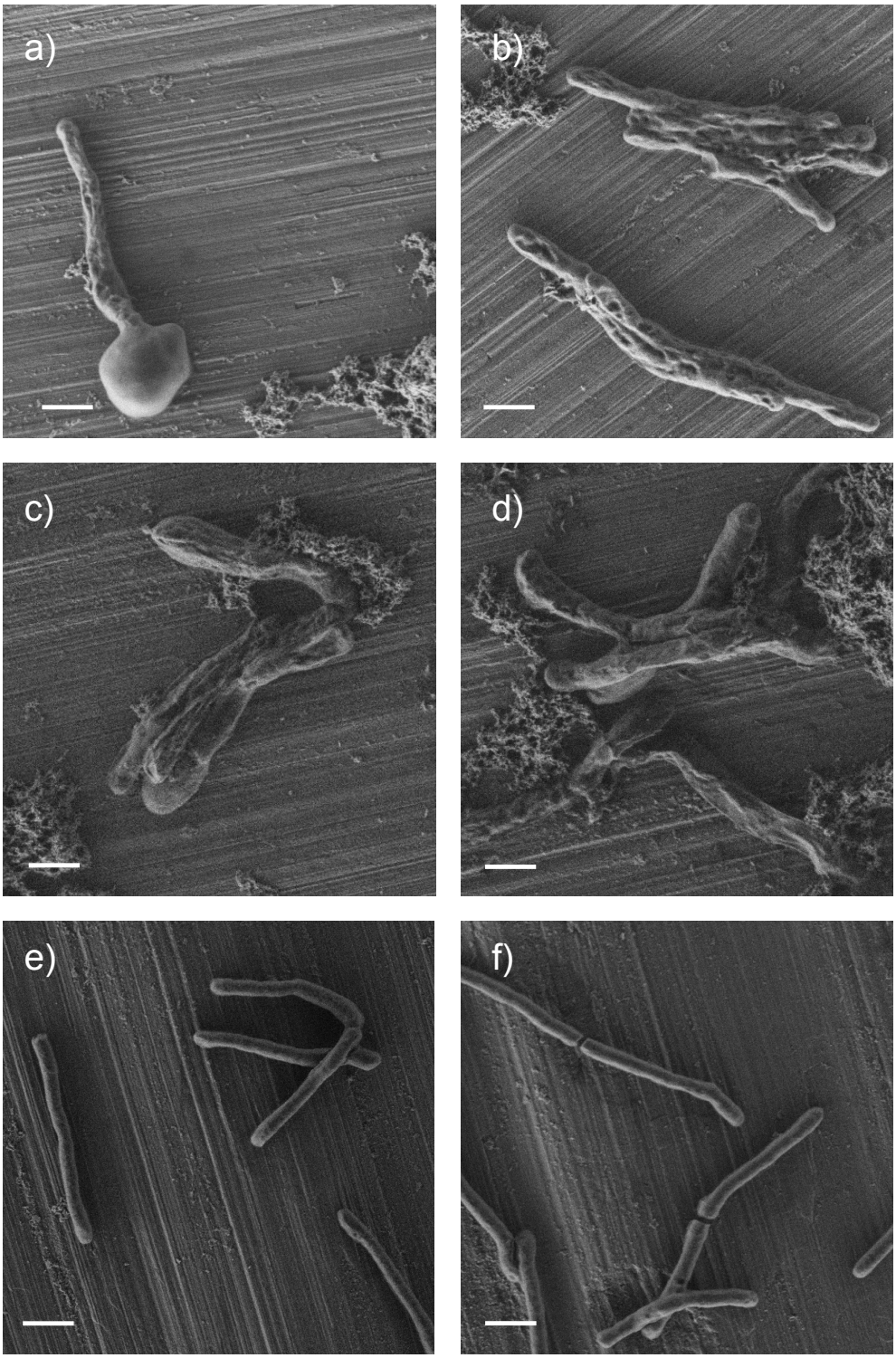

Figure 4-26: *M. smegmatis* after being pre-incubated with linezolid for 3 hours and additionally exposed to benzothiazinone for 4 hours.

Linezolid and benzothiazinone were applied in 2 x MIC, respectively. *a)* and *b)* after 7.5 hours observation period *c)* and *d)* after 25 hours observation period. The bar indicates 1 µm. Mean length of *M. smegmatis* was measured at 5.84 µm in both groups (*n* = 23 and *n*=21). For comparison, the wildtype images are given *e)* and *f)*, mean length 3.9 µm).

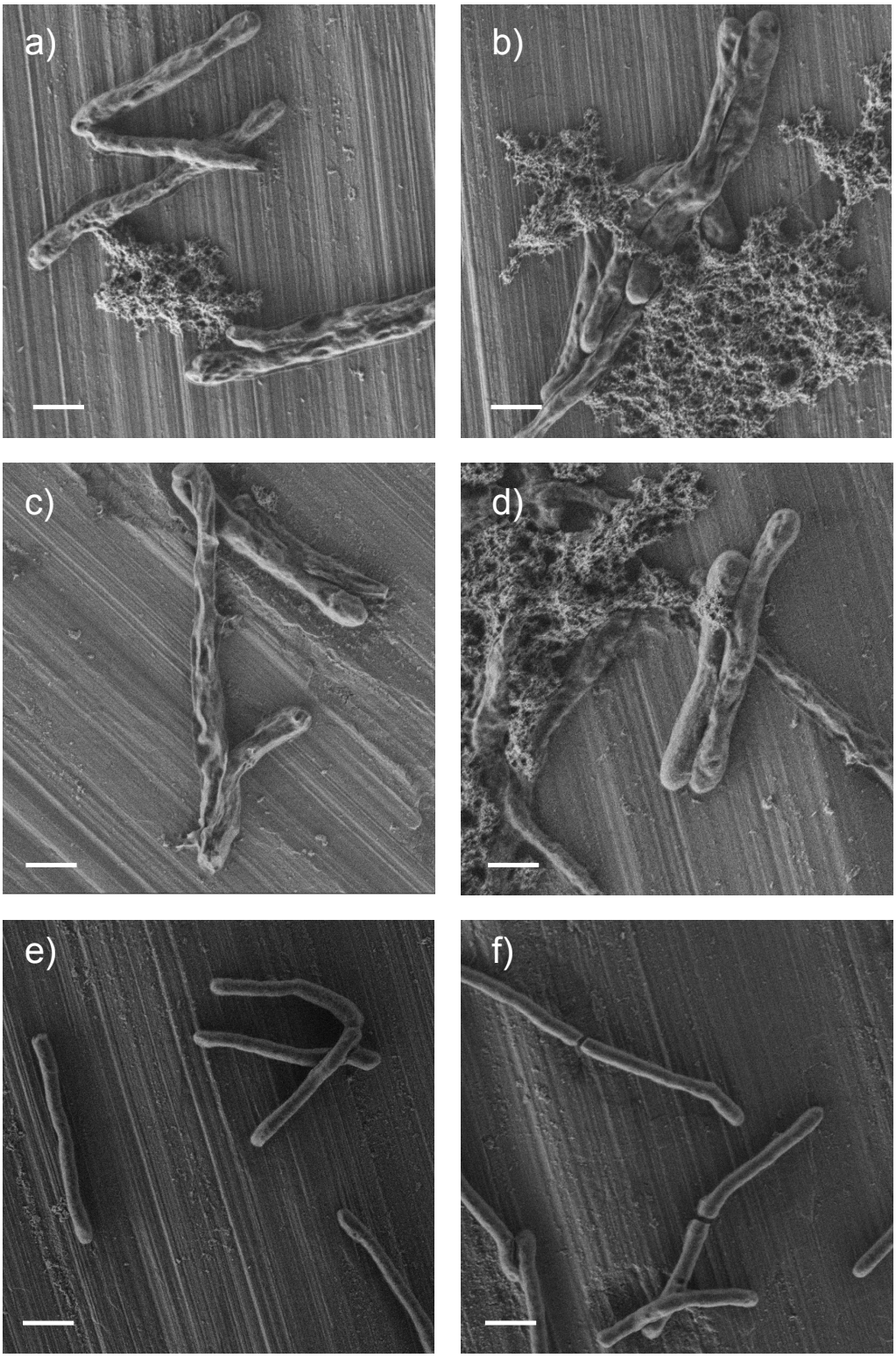

Figure 4-27: *M. smegmatis* after being pre-incubated with linezolid for 3 hours and additionally exposed to benzothiazinone continuously (no washing).

Linezolid and benzothiazinone were applied in 2 x MIC, respectively. *a)* and *b)* after 7.5 hours of growth period; *c)* and *d)* after 25 hours. The bar indicates 1 µm. Mean length were 5.5 µm after 7.5 hours and 5.8 µm after 25 hours. For comparison, the wildtype images are given again in *e)* and *f)*.

M. smegmatis Length and Width

Micrographs were taken with the SEM after 7.5 hours and 25 hours incubation of *M. smegmatis*. The antimicrobials were applied following a scheme with an exposure time of benzothiazinone of 4 hours or long-term after a pre-incubation period with linezolid as a single agent of 3 hours (Figure 4-28, right). The samples were prepared following the SEM preparation protocol (3-31).

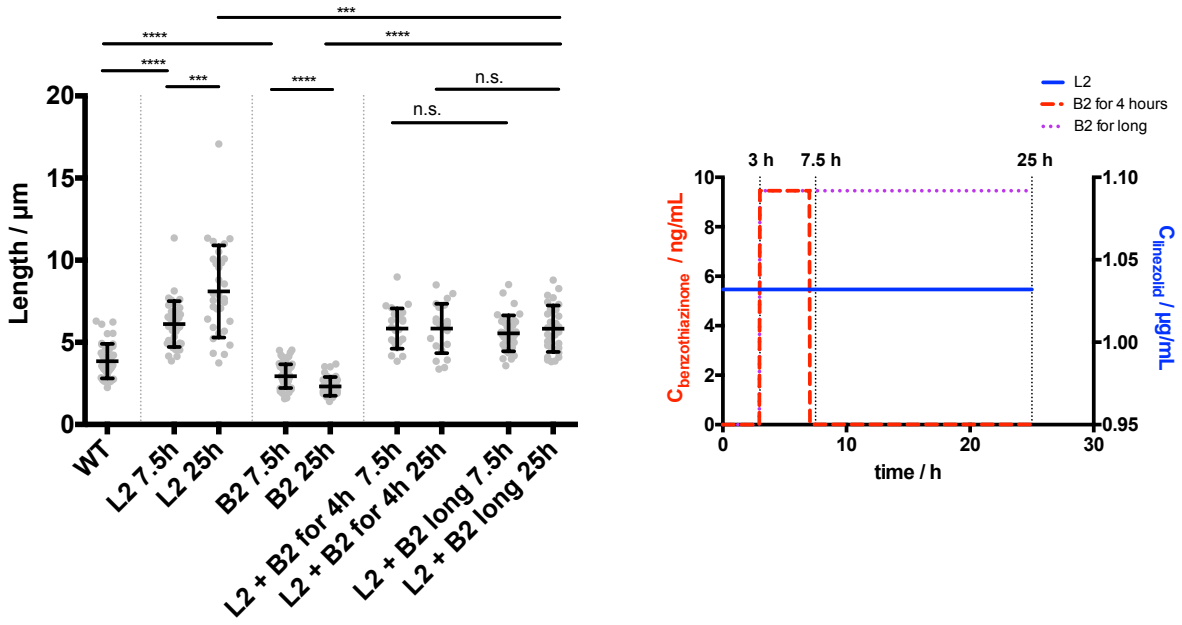

Figure 4-28: *M. smegmatis* length under the influence of combined linezolid and benzothiazinone.

Left: *M. smegmatis* length. Right: Experimental set up. Images were taken with SEM, visualized in Image J and mycobacteria were measured in their longest diameter using the program Fiji. We measured the wildtype and compared it with the other samples after 7.5 and 25 hours: linezolid in 2 x MIC (L2), benzothiazinone in 2x MIC (B2), and the combination of both with a linezolid pre-incubation period of 3 hours; once with a benzothiazinone exposure time of 4 hours and once with a long benzothiazinone exposure time. *n* ranges from 22 to 62. A gaussian distribution could be assumed; the bars refer to mean and SD. The length of every group was compared to the wildtype or its respective observation period by using t-test with Welch's correction. Three stars *** refer to a *p*-value of < 0.001 and four stars **** to a $p < 0.0001$.

The length of the *M. smegmatis* wildtype averaged at 3.9 µm (95 % CI from 3.5 to 4.2; $n = 42$). The length of *M. smegmatis* in the combination groups observed after a total growth time of 25 hours was 5.8 µm (95 % CI from 5.2 to 6.5; $n = 21$) for an exposure time to benzothiazinone of 4 hours and 5.8 µm (5.3 to 6.3; $n = 31$) for the long-termed exposure time. Lengthwise, no difference could be detected among these two groups ($p = 0.97$) and both were significantly longer than the wildtype (both $p < 0.0001$). Comparing the 4-hour exposure and the long exposure time with benzothiazinone after an incubation time of 7.5 hours, we found the length to be 5.8 µm (95 % CI from 5.3 µm to 6.4 µm; $n = 23$) with 4-hour exposure and 5.5 µm (95 % CI

from 5.2 µm to 5.9 µm; *n* = 36), long-term exposure; not to be different from each other (*p* = 0.3379). Hence, neither differing the observation period (whether 7.5 hours or 25 hours) nor prolonging the benzothiazinone exposure time (4 hours vs. long exposure time after three hours of pre-incubation with linezolid) demonstrated a significant change in length in the combination groups. Bacteria of all combination groups are significantly longer than the bacteria that are only incubated with benzothiazinone (mean length 2.9 µm after 7.5 hours and 2.3 µm after 25 hours). All combination groups are still shorter in comparison to the culture that was incubated with linezolid as a single agent for the long period. Regarding only the short observation time of 7.5 hours, no difference in length can be found between using linezolid as a single agent and applying linezolid in combination with benzothiazinone (*p* = 0.45 for 4 hours exposure time, and *p* = 0.056 for long).

The width of *M. smegmatis* exposed to the single agents linezolid and benzothiazinone is depicted for comparison in the following graph (Figure 4-29). It is visible that all mycobacteria presented to a compound appear thicker than the wildtype.

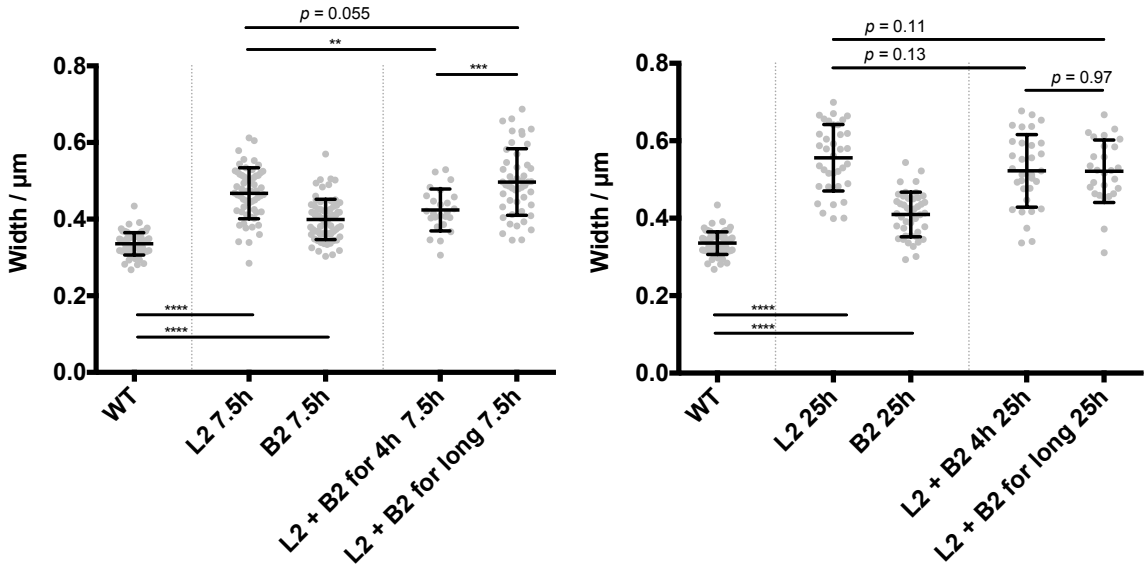

Figure 4-29: *M. smegmatis* width under the influence of linezolid and benzothiazinone.

Micrographs of *M. smegmatis* were measured in their width using the program Fiji. The wildtype was tested after 7.5 hours and all the other samples after 7.5 (left graph) and 25 hours (right graph): linezolid (L2) in 2 x MIC, benzothiazinone (B2) in 2 x MIC, and the combination of both with a respective linezolid pre-incubation period of 3 hours; once with a benzothiazinone exposure time of 4 hours and long-term benzothiazinone exposure time. Bars refer to mean and SD. *n* ranges from 30 to 74. To compare, t-tests with Welch's correction were used. One star * refers to a *p*-value < 0.05; two stars ** to a *p*-value < 0.01, three stars *** to a *p*-value of < 0.001 and four stars **** to a *p* < 0.0001.

For reference, the mean width of the wildtype averaged at 0.34 µm (95 % CI from 0.33 µm to 0.34 µm; *n* = 74). Left graph, total incubation time 7.5 hours: Adding benzothiazinone to

linezolid for 4 hours averages in a width of 0.42 µm (95 % CI from 0.40 µm to 0.45 µm; *n* = 25) and presents with a slight decrease in width compared to application of only linezolid (Δ= - 0.044 µm; *p* = 0.003). Samples incubated with benzothiazinone for the long period have an average width of 0.50 µm (0.47 µm to 0.52 µm; *n* = 49) and are significantly thicker than the combination group with 4 hours of benzothiazinone exposure (0.42 µm; 95 % CI from 0.40 µm to 0.45 µm; *n* = 25; *p* = 0.003). Figure 4-29, right graph: Here, the width of the bacteria after an observation time of 25 hours is visualized (the reference pool is the same wild type growth). No difference could be found between the 4-hour and long exposure time of benzothiazinone in the combination groups (width $_{L2+B2\ for\ 4h}$ = 0.52 µm; 95% CI of mean from 0.49 to 0.56 µm; *n* = 32 and width $_{L2+B2\ for\ long}$= 0.52 µm; 0.49 µm to 0.55 µm; *n* = 27; *p* = 0.97). Simultaneously, this statement could be drawn in regard to the length, as seen in Figure 4-28. In conclusion, there is no detectable morphological difference expressed in length or width between adding benzothiazinone in 2 x MIC to linezolid for a long period or for an exposure limited to 4 hours. The calculated estimate of the surface ranged between 8 µm^2 and 10 µm^2 for all groups of *M. smegmatis* exposed to the combination of linezolid and benzothiazinone. The volume calculated through the average values ranged from 0.8 µm^3 to 1.2 µm^3, thus being twice to three times as voluminous as the wildtype (0.3 µm^3). Again, these values must be treated with caution and are meant for orientation only (limitations are discussed on page 5-95).

5 Discussion

5.1 Linezolid – Antimicrobial Activity against *M. smegmatis*

We determined the IC_{90} value (then defined as MIC) and used its doubled concentration routinely for our experiments. The IC_{90} value was chosen in order to test a slightly larger inhibitory effect than using a MIC classically defined as the IC_{80} value (page 4-33). 2 x MIC refers to a concentration of 1.0 µg/mL for linezolid (in all experiments, the exact value of 1.032 µg/mL was administered), a concentration that has previously been tested as a plasma trough level in a clinical setting (Roger et al., 2018). In humans, linezolid plasma trough concentrations of 2 µg/mL are still tolerable when administered for a duration of *several months* as commonly necessary in second-line treatment of tuberculosis and MDR-TB. With plasma trough concentrations exceeding 2 µg/mL, mitochondrial-related toxicity increases dramatically and severe adverse effects such as polyneuropathy and myelosuppression develop at a supposed 100% probability (Song et al., 2015). The applied linezolid concentration of 1.0 µg/mL is beneath this critical threshold and larger than the 50% mutant prevention concentration (Rodríguez et al., 2004). Patients with 600 mg linezolid daily oral intake reach peak plasma levels of C_{max} = 9 - 12 µg/mL (Boak et al., 2014; Roger et al., 2018). Hence, the applied concentration in our experiments (1.0 µg/mL) is at the minimum threshold that could be administered in humans, leaving air for a temporary increase of the concentration. Therefore, an even stronger antimicrobial activity can be expected once transferred to the clinical setting.

The antimycobacterial efficacy of linezolid has been shown in various studies before (Koh et al., 2009; Rodríguez et al., 2004; Sotgiu et al., 2012; Zhang et al., 2015). Linezolid is an oxazolidinone, which inhibits bacterial growth by binding to the 50S subunit and preventing bacterial protein synthesis (Shinabarger et al., 1997; Swaney et al., 1998). Our experiments demonstrate that linezolid significantly decreases the number of CFU of *M. smegmatis* when used as a single agent. Further, mycobacterial killing correlates with an increase of the incubation period as well as with increasing concentrations of linezolid (page 4-42 and Figure 4-7). This is in agreement with both its previously observed time-dependency when applied in gram-positive pathogens and its limited concentration-dependent killing (Roger et al., 2018). Our findings confirm the antimicrobial activity of linezolid in mycobacteria and are consistent with its relatively new standing as a core treatment option in MDR-TB and XDR-TB (Agyeman & Ofori-Asenso, 2016; Chaiprasert et al., 2014; Dennis Falzon et al., 2017; Sotgiu et al., 2012). Under the given circumstances, linezolid is not able to completely impair *M. smegmatis* growth on an absolute level

(Figure 4-9). This is consistent with our findings of residual protein expression levels in MALDI-TOF MS (Figure 4-5).

M. smegmatis cells exposed to linezolid in 2 x MIC tend to become longer in size (from an average 3.9 µm in the wildtype (95 % CI of mean from 3.5 µm to 4.2 µm) to 6.1 µm after 7.5 hours (95% CI of mean from 5.7µm to 6.6 µm), and 8.1 µm after 25 hours (95 % CI from 7.1 µm to 9.1 µm; 4-44). Based on the mode of action of linezolid, potential reasons for this observation could be considered: Linezolid decreases the production of structural cellular proteins by early blockage of ribosomal translation (Champney & Miller, 2002; Lin et al., 1997; Matassova et al., 1999; Shinabarger et al., 1997; Swaney et al., 1998) and this way inhibits the cell from partition (1-16). Due to deficiency of proteins, when reaching the length where the cell would normally divide, it lacks the ability to form the divisome. Since the cell wall layers consist mostly of peptidoglycan, lipids and mycolic acids (Hett & Rubin, 2008), it can be assumed that the cell wall continues to grow as the existing enzymes are still capable of producing new cell wall. Following this assumption, the integrity of the cell wall would at the beginning be less dependent on a general slow-down in protein production caused by linezolid. It was visible that certain bacteria exposed to linezolid form ballooned tips (Figure 4-10). It is known that mycobacteria grow from their poles (Hett & Rubin, 2008; Thanky et al., 2007). Multiple cell structure proteins are known in the outer mycobacterial membrane (Niederweis, Danilchanka, Huff, Hoffmann, & Engelhardt, 2010) and that may be necessary to maintain their morphology and cell wall integrity. Possibly, the bizarre morphology derives from a linezolid-induced lack of production of cell structure proteins, which eventually leads to failure in maintaining the cell wall structure.

5.2 Benzothiazinone – Antimicrobial Activity against *M. smegmatis*

In previous studies, Benzothiazinone had been tested on *M. tuberculosis* and on various other mycobacteria and its bactericidal effect was often compared to first-line antituberculotic agents (Lechartier et al., 2012; Makarov et al., 2014, 2009). From our experiments with *M. smegmatis*, we can confirm its exceptionally high potency with a MIC value at 4.73 ng/mL (Figure 4-1, Figure 4-8, Figure 4-15). However, in our experiments, the bactericidal efficacy could not be confirmed for benzothiazinone administered in 1 x MIC during the first 25 hours: Exposure of *M. smegmatis* to benzothiazinone at MIC showed an average reduction factor of 0.1 after 7.5 hours and -0.1 after 25 hours of growth (4-49). *M. smegmatis* and benzothiazinone in 2 x MIC showed a reduction factor of 0.25 after 7.5 hours and 1.2 after 25 hours of co-incubation (4-49). A negative reduction factor indicates that the CFU count of the parallel grown

culture without the influence of antimicrobial substances (also named wild type growth = WT) was lower than the number of CFU of the treated group. It is known that *M. smegmatis* naturally expresses the nitroreductase NfnB, an enzyme able to inactivate benzothiazinone by reduction of a critical nitro-group, while *M. tuberculosis* appears to lack nitroreductases with the ability to inactivate the drug (Manina et al., 2010). Furthermore, in previous studies, benzothiazinone had been tested for long periods of time, exceeding ten generation cycles in *M. tuberculosis* (Makarov et al., 2009). In our experiments, the tested incubation period of 25 hours corresponds to six to eight *M. smegmatis* division cycles (Merkov, 2006), which may contribute to why we were not able to observe an equally strong bactericidal effect. Further factors, such as differences in membrane permeability between the two species, yet remain to be evaluated as a potential cause for the differences in MIC.

A trend was visible between the increasing concentration of benzothiazinone and the reduction factor (4-49). To confirm significant evidence of this trend, a larger number of replicates remains to be tested. Furthermore, there was a trend of a negative correlation between CFU count and increasing exposure times to benzothiazinone after a total incubation period of 25 hours (4-50): If benzothiazinone (2 x MIC) is only applied for 2 hours or 4 hours, a reducing effect on *M. smegmatis* CFU cannot (yet) be observed, however, it becomes detectable when *M. smegmatis* is exposed to benzothiazinone continuously. Independently of the concentration, the continuous benzothiazinone exposure always appears superior compared to equally concentrated limited exposure (Figure 4-14). Hereafter, it was concluded that benzothiazinone in the individual application requires a long exposure for efficient killing, which is consistent with previous findings in literature (Makarov et al., 2009). In conclusion, the killing effect of benzothiazinone used as a single agent rises with the increase of its total incubation time.

Short benzothiazinone exposure times (2 hours and 4 hours) are not sufficient to reduce *M. smegmatis* CFU after 25 hours (Figure 4-14). This implies that benzothiazinone has less impact when applied shortly. Benzothiazinone serves as a suicide substrate in a near-quantitative manner (Trefzer et al., 2012), thus, we assume the substance is depleted unless given continuously, given that *M. smegmatis* organism is capable to resynthesize the inhibited molecule DprE1. Therefore, it appears necessary to maintain a continuously high level of benzothiazinone in order to keep DprE1 activity low. From this perspective, a rather time- than dose-dependent behavior of benzothiazinone can be assumed (Makarov et al., 2009). On the other hand, our MALDI-TOF MS results demonstrate a late effect on protein metabolism with the first

detectable change on the selected analytes in a range of 3 hours to 12 hours after application (Figure 5-2). Benzothiazinone inhibits the cell wall synthesis (Makarov et al., 2009) and does not interact with protein synthesis directly.

Based on this information and the theoretical background, we challenge the idea that a sustained high benzothiazinone concentration is required to reach efficient killing. Moreover, we would like to suggest that the killing effect of benzothiazinone appears only after a critical *minimum* point of time since begin of exposure. This theory is further supported by the conclusions drawn from the data shown in Figure 4-15, where samples co-incubated with benzothiazinone in 2 x MIC were pooled by their "time since the start of exposure" to either 6.5 hours or 4.5 hours, independently of their exposure duration. The group pooled to "6.5 hours since the start of exposure" revealed a positive reduction factor that is significantly higher than 0, meaning that inhibition occurred. This leads to the conclusion that the critical point of time was surpassed with 6.5 hours. Pooling the groups to "4.5 hours since exposure" resulted in a *negative* reduction factor that was also significantly lower than the other group ($p = 0.0007$) so that we suggest that this critical point since exposure was not yet reached, moreover, the negative reduction factor appears paradox. We allowed ourselves to pool data based on the theoretical background of the suicide nature of the substrate (Trefzer et al., 2012) assuming that washing off the rest of the substrate does not change the number of already covalently bound Dpre1 molecules unless they are being re-synthesized. This would also explain why after a total observation period of 25 hours, the initially observed difference between the samples grouped to their "time since exposure" is not significant anymore (Figure 4-16): It can be assumed that after six to eight doubling times, the allover quantity of Dpre1 is replicated six to eight times, thus minimizing the effect of BTZ-bound Dpre1. Conclusions of when benzothiazinone in this concentration reaches its maximal efficacy in *M. smegmatis* remain hypothetical, but all in all the results from the CFU count and the MALDI spectra (details 5-82) let us assume that it probably happens *after* an exposure time of 6.5 hours and before 24 hours in *M. smegmatis*.

It remains unknown how benzothiazinone enters *M. smegmatis* to bind to Dpre1 - it could be an active transport, or simply diffusion, which is the closest theory because of its hydrophobic character (Makarov et al., 2009). However, it can be assumed that the diffusion gradient and thus, the concentration of benzothiazinone outside of the cell, play a pivotal role for the accumulation of the compound in the cell. This theory is supported by the results of our combination studies with linezolid where an application of BTZ peak concentration in 20 x MIC

administered for as short as 0.5 hours demonstrated a very good bacterial load reduction (Figure 4-21).

Benzothiazinone (2 x MIC) significantly decreases the length of *M. smegmatis* from an average of 3.9 µm in the wildtype (95% CI from 3.5µm to 4.2 µm) to 2.94 µm after 7.5 hours (95% CI from 2.8µm to 3.1 µm) and finally, to 2.3 µm after 25 hours incubation (95% from 2.1 to 2.5 µm; Figure 4-17). Consistently, the calculated cell surface of *M. smegmatis* decreases compared to the WT. The *M. smegmatis* WT calculated surface was approximately 4 μm^2 (surface/volume ratio approximated a theoretical value of 12). The surface of mycobacteria fed with benzothiazinone approximated 4 μm^2 (surface/volume ratio = 11) after 7,5 hours and 3 μm^2 after 25 hours (surface/volume ratio = 11). Based on the mode of action of benzothiazinone blocking the Arabinan synthesis pathway of the mycobacterial cell wall (Makarov et al., 2009), we assume that the production of the surface components at the site of the growth of the cell is impaired.DprE1, the target molecule of benzothiazinone, was found predominantly in the pole regions of mycobacteria (Sommer et al., 2018). Further, mycobacteria are known to grow from their tips (Thanky et al., 2007). We hypothesized that by slowing/blocking cell wall synthesis, the bacterium grows less membrane while still producing the proteinous divisome. It might thus be still dividing, taking a more rounded shape, reducing the overall volume and surface, while also reducing the surface/volume ratio. As general protein turnover is only slightly inhibited by application of benzothiazinone and proteins are still being *de-novo* synthesized in amounts that are only slightly smaller than in the WT (Figure 5-1), and as the growth of the cell wall suspends or decreases, the quotient of surface in proportion to its cell mass (or volume) should decrease. These observations must be interpreted with care due to technical limitations. However, it is a reasonable possible explanation for the changed *M. smegmatis* morphology.

5.2.1 Paradox Benzothiazinone Effect

Regarding the effect of benzothiazinone applied in 2 x MIC as a single agent in an observation period of 7.5 hours (Figure 4-15), we find higher CFU numbers than in the WT under certain incubation conditions. This paradox effect, defined as the increase of CFU (thus reduction factor lower than 0) occurs when the observance time of *M. smegmatis* exposed to benzothiazinone does not exceed 4.5 hours (median $RF_{4.5hours}$= -0.29 [*n* = 12]). In multiple experiments, we could also observe an increase in the OD compared to the WT, a parallel trend confirming our observations in the CFU counts. We concluded from this data that benzothiazinone in this

concentration, namely 2 x MIC, leads to an increase of CFU within the first 4.5 hours since the beginning of exposure (independently of the final exposure duration) and that its referred antimicrobial effect only starts 6.5 hours after begin of exposure. The initial effect seems paradoxical, as the blockage of the cell wall synthesis would be expected to have the immediate opposite effect. Potentially, the increase of CFU is due to *M. smegmatis* experiencing a stress response upon benzothiazinone exposure. With inhibition of the production of cell wall elements, less mycobacterial cell wall would be produced while the protein synthesis continues, eventually also forming the divisome. At the beginning, this would force *M. smegmatis* into faster partitions producing smaller offspring cells – consistent with the morphological change observed through electron microscopy where mycobacteria exposed to benzothiazinone appeared shorter and thicker (Figure 4-18). An experimental design to further strengthen this theory yet remains to be elaborated.

5.3 The Effect of Linezolid and Benzothiazinone on *M. smegmatis* Protein Metabolism by Carbon Isotopic Labeling in MALDI-TOF MS

5.3.1 General

Matrix-assisted laser desorption/ionization – time of flight mass spectrometry (MALDI-TOF MS) with the support of the tracer nutrient 1,2 ^{13}C-labeled glycerol enables us to observe protein metabolism of *M. smegmatis* from a new perspective. During active metabolism, glycerol as a carbon source is continuously assimilated and incorporated into the organism. Stable isotope labeling causes an m/z shift in the spectra of viable organisms. This can be analyzed using the differential center of gravity (ΔCOG). We received the ΔCOG of eight protein/peptide peaks as a value and measure for incorporation of ^{13}C-traced glycerol into *de-novo* synthesized proteins of *M. smegmatis* (4-40). We found that after a given time, the ΔCOG value of the wildtype (WT) asymptotically approaches a saturation level. Once no additional shift change could be observed, the maximum possible peak shift was defined as ΔCOG = 100% or, maximum contribution. The ratio of ^{13}C-labeled (newly-synthesized) to unlabeled protein reaches the ratio that can maximally be reached in the wildtype under the given circumstances. At this time point, the respective original (unlabeled) mass peak of the eight observed analytes is below detection limit. Thus, new protein can still be synthesized using this intake pathway, but no additional m/z shift is to be expected as the analytes cannot become any heavier. From this moment on, only limited information about *M. smegmatis* metabolism is revealed. We cannot distinguish whether the metabolism has completely come to a halt and *M. smegmatis* got killed, whether

M. smegmatis is still taking up new material using a different pathway, or whether *M. smegmatis* is still synthesizing the same protein but re-using already incorporated ^{13}C-traced material. Conclusions about *M. smegmatis* metabolism can hence primarily be made between timepoint 0 i.e. addition of the tracer and the point in time where the WT value still differs significantly from the asymptotic final value. Hence, after reaching the plateau, the *de-novo* synthesis cannot be further analyzed using this technique and staggered timelines (with later addition of the tracer substance during the course of the experiment) are required to monitor the effect of drugs on *M. smegmatis* expression levels over a longer period of time. Staggered timelines would require to add the tracer nutrient at various points in time in order to align the evaluable data segments in multiple experiments, thereby gathering data points in a continuous manner for a longer time period.

5.3.2 *M. smegmatis* Wild Type Timelines

The timepoint when the contribution of every labeled protein/peptide in not interfered growth in full medium (wild type = WT) reaches a saturation, was defined by T-testing the ΔCOG WT values of the individual analytes at every timepoint to the respective asymptotic value. Seven out of eight analytes could be identified using HPLC-MS/MS (Table 8; 4-35), one analyte remains unidentified and is here referred to as a glycopeptide. The asymptotic value is approached in a range of 7.5 to 25 hours (Table 9, 4-39). Once the ΔCOG is no longer different from the asymptotic value, we can assume that the state of maximum contribution of newly-synthesized to prior existent protein has been reached. This means that either no more unlabeled protein can be found, or that it remains at a constant level. As the allover *M. smegmatis* growth is still exponential over the observed time, unlabeled rests of proteins automatically get diluted to below detection limits. Thus, in the case of the eight analytes investigated here, the unlabeled (original) peak was below detection limit. The WT values of PFAM16525 (peak at m/z 9546) generated from this study are all significantly different from the asymptote which was generated from the timeline determined by preceding experiments of our research group (Figure 4-4). In the graph, there is a visible trend of an approach to a plateau between 7.5 hours and 12 hours. The reasons remain hypothetical, one possible explanation is down-regulation of the protein.

Regarding the wildtype, a ΔCOG value that reaches 50% of the maximum means the contribution of newly synthesized protein in this pathway is 50%. The ratio of *de-novo*-synthesized protein to unlabeled protein can be assumed to be 1:1. For two proteins, this happens between 1

hour and 3 hours. For five proteins (the majority) this occurs between 3 hours and 5 hours. And for one ribosomal protein (50S L33) a little later, between 5 hours and 7.5 hours. In this time, we can assume that the observed analytes have been replicated exactly once. In analogy it can be assumed that the entire proteome of the wildtype has doubled when the majority of the investigated proteins has doubled. The majority of affected proteins reaches the 50% share between 3 hours and 5 hours, which is consistent with the doubling time of *M. smegmatis* being 3 to 4 hours (Merkov, 2006). It appears logical, that certain proteins are produced at higher speed and independent of the state of replication. This would be consistent with the ΔCOG values of the glycopeptide (peak at m/z 2755) and hypothetical protein MSMEG_1770 (peak at m/z 4152), which are *de-novo*-synthesized faster than the other 5 proteins and reach the 50% contribution before the presumed *M. smegmatis* doubling time of 3 hours. Also, a doubling of mass could be observed comparing the ΔCOG at the timepoints of 3 hours and 7.5 hours: Among all analytes, the ΔCOG at the 3-hour and 7.5-hour timepoints were found to be significantly different from each other. The ratio of these values that represent the newly-synthesized protein ranged between 1.32 to 2.56, meaning that the amount roughly doubled (see results 4-37) within 3.5 hours. This is also consistent with *M. smegmatis* generation time.

5.3.3 Percental Contribution over Time and Detectable Onset of Action

The data visualized in Figure 5-1 (5-80) provides an overview of the percental share of the newly synthesized protein/peptide per respective protein/peptide at various points in time. The percental contribution is each shown for the *M. smegmatis* wildtype (WT), *M. smegmatis* exposed to linezolid in 2 x MIC and *M. smegmatis* exposed to benzothiazinone in 2 x MIC. At the timepoint of 12 hours, nearly all synthesized proteins of the WT (six out of eight) are within the top 10% of the asymptotic value that represents the maximum contribution through this synthesis pathway. This is consistent with the results obtained by T-testing the individual values to the asymptotic value where we also perceived that the contribution of the analytes reaches a saturation in a range of 7.5 hours to 25 hours.

The radar chart (Figure 5-2) illustrates from which moment on a significantly smaller share of the *de-novo* synthesized protein/peptide is found in *M. smegmatis* exposed to benzothiazinone or linezolid in 2 x MIC respectively. We identified the timepoint when the ΔCOG of the antibiotic group diverges from the WT timeline for the first time and is significantly smaller than the ΔCOG of the WT. This timepoint was detected through T-testing the ΔCOG value of every antibiotic group (LZD/BTZ) against the WT group at every point in time for every analyte. The timepoint

of the detectable influence on *de-novo* synthesis through linezolid and benzothiazinone was found to be different in every individual protein/peptide. Eight different molecules are plotted and represent a fractional amount of the *M. smegmatis* proteome. Both agents effectuate that PFAM16525 (peak at m/z 9456) is not being *de-novo* synthesized at all anymore at a very early stage (before time point of 1 hour is reached).

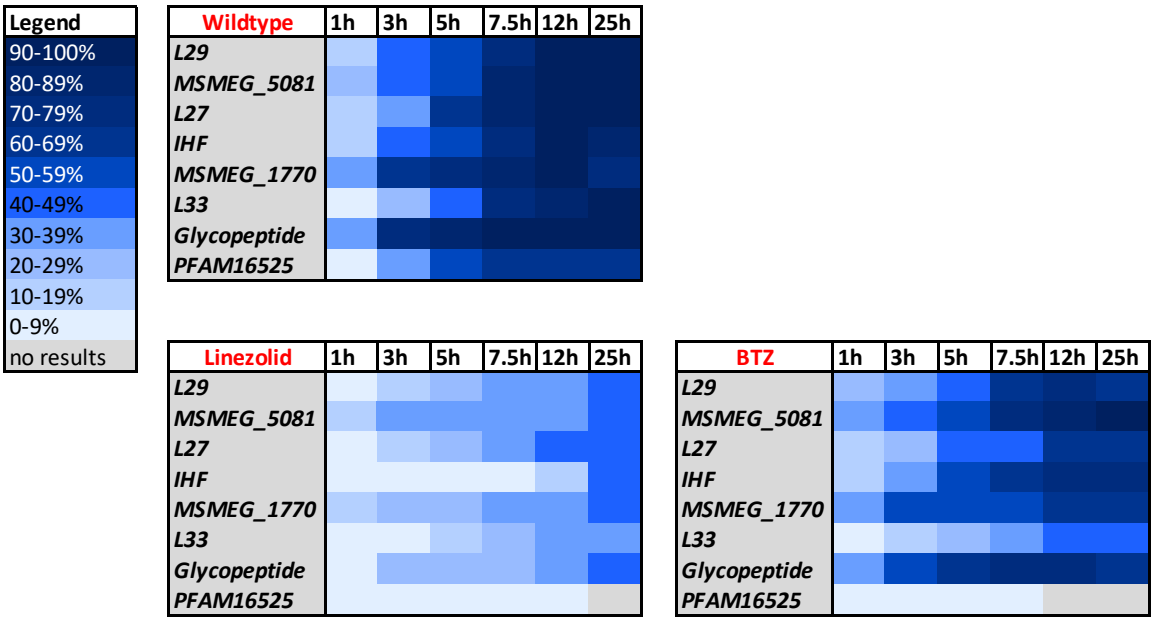

Figure 5-1: Percental contribution over time.

The ratio of ΔCOG of determined time points (1 h, 3 h, 5 h, 7.5 h, 12 h and 25 h) to the asymptotic mean that was received through an exponential curve fit (asymptote visualized in in Figure 4-5 and Figure 4-6). For every respective group of the experiment, the percentage of the ΔCOG of the maximally possible ΔCOG (asymptote) under these circumstances was calculated. Top: wildtype analytes; middle: linezolid applied in 2 x MIC; bottom: "BTZ" – benzothiazinone applied in 2 x MIC.

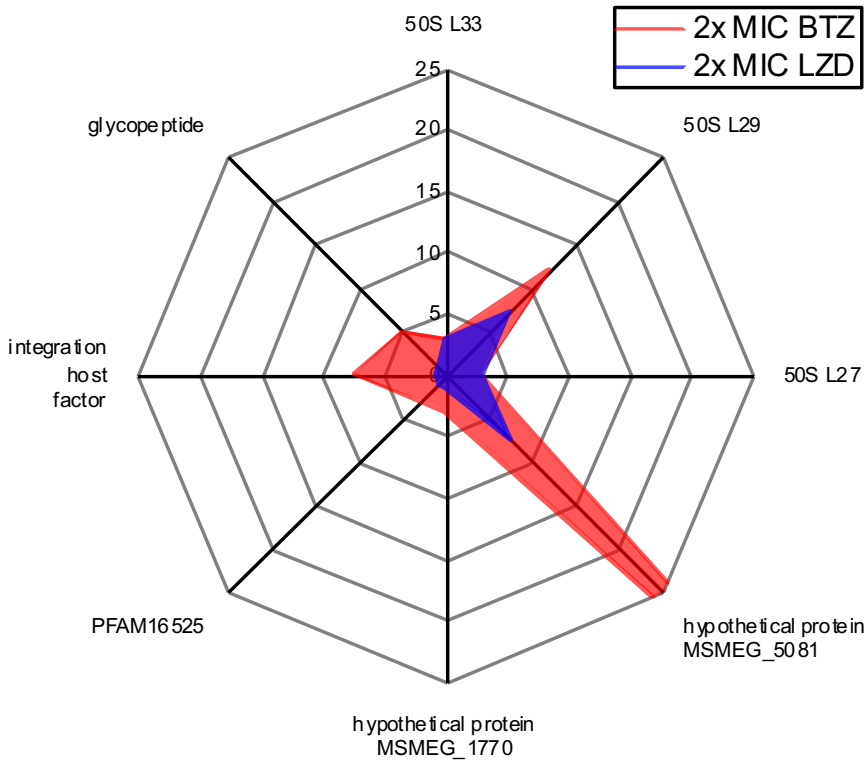

Figure 5-2: Detectable effect of linezolid and benzothiazinone on *de-novo* synthesis.

The respective timepoints were determined through T-tests between the linezolid (LZD, blue) or the benzothiazinone group (BTZ, red) to the WT and provide an idea of when the antimicrobial agents start acting on the mycobacterial proteins/peptide in the respective concentration.

5.3.4 Linezolid

Linezolid in 2 x MIC (c = 1.0 µg/mL; blue) in total, shows an earlier detectable effect, impairing the production of labeled molecules, than benzothiazinone (red; Figure 5-2). Four out of eight observed mycobacterial proteins/peptides have significantly smaller percental amounts of newly-synthesized protein (compared to unlabeled protein) already within the first hour: the molecule categorized as a glycopeptide (peak at m/z 2755), the integration host factor (peak at m/z 5756), PFAM 16525 (peak at m/z 9546) and hypothetical protein MSMEG_1770 (peak at m/z 4152). After 3 hours of incubation, the contribution of ribosomal proteins 50S L27 (peak at m/z 4555) and 50S L33 (peak at m/z 3160) is significantly smaller than in the WT. The two proteins MSMEG_5081 and the ribosomal protein 50S L29 are the last ones to show an effect and are *de-novo*-synthesized in significantly smaller amounts at 7.5 hours. Hence, after 7.5 hours the *de-novo*-synthesis of all the observed proteins/peptides in *M. smegmatis* is significantly inhibited by linezolid. The findings indicate that the effect of linezolid in 2 x MIC on the *M. smegmatis* proteome begins within the first hour after exposure and the majority of proteins is affected within 3 hours. We extrapolated linezolid reaches its full or nearly-full effectiveness by 3 hours. This is consistent with the previously discussed mechanism of action of

linezolid (5-72) and its known direct effect on the ribosome and early inhibition of the translation process (Shinabarger et al., 1997; Swaney et al., 1998).

Regarding *M. smegmatis* cultivated in the presence of linezolid in 2 x MIC (Figure 5-1), at 25 hours after application of linezolid, five out of eight ΔCOG values are not significantly different to the prior timepoint of 12 hours (all $p > 0.05$ except PFAM 16525 [no value]; 50S L27 [$p = 0.0113$]; integration host factor [$p = 0.0048$]). We concluded that the ΔCOG of these peaks does not change anymore and that by this time, a saturation/plateau is reached. Figuratively in the mass spectrum, the mass shift stops and indicates that the ratio between heavy (labeled) and light (unlabeled) versions of the same protein remains constant. This ratio does not change anymore and remains at a level which is less than half the share that the WT would accumulate. It can be assumed that this pathway of synthesis has stopped working and that this may be the point in time when the *de-novo* production of the corresponding protein (or peptide) ceases under the influence of linezolid. By the end of the 25-hour incubation period, the share of freshly-synthesized protein is 40-49% (seven out of eight proteins, one protein has a share between 30-39%), indicating that integrated over the incubation time, at least half the *de-novo*-synthesis in these proteins/peptides was inhibited and that the proteome could not be completely replicated. It is consistent with the data demonstrating that the first effect of linezolid was already detectable within the first hour after application (Figure 5-2). Assuming a doubling time of 3 to 3.5 hours (Merkov, 2006), we can conclude that linezolid applied in c = 1.0 µg/mL inhibits protein synthesis to an extent where *M. smegmatis* does not have enough time for one complete replication, until protein synthesis stops.

5.3.5 Benzothiazinone

On the contrary, when *M. smegmatis* was exposed to benzothiazinone in 2 x MIC (c = 9.5 ng/mL; Figure 5-2), only 3 hours after application the first significant changes could be detected: at 3 hours, 50 S L33, PFAM 16525 and hypothetical protein MSMEG_1770 have significantly lower contributions. The glycopeptide is found in significantly smaller contribution at 5 hours. Integration host factor and ribosomal protein 50 S L27 have significantly lower ΔCOG values at 7.5 hours. And the ΔCOG of the ribosomal protein 50S L29 diverges from the WT timeline at 12 hours. The value for hypothetical protein MSMEG_5081 (peak at m/z 5517) was not found to be significantly different from the WT at any point of time. This leaves open whether the protein synthesis pathway of *M. smegmatis* is not hindered directly or indirectly by benzothiazinone, or whether *de-novo* synthesis of this protein has simply not *yet* been changed by the

effects of benzothiazinone. In the original graph in the results (Figure 4-6) though, there was a visible trend demonstrating smaller average ΔCOG values at 12 hours and 25 hours compared with the wild type. In general, the exposure of *M. smegmatis* to benzothiazinone in 2 x MIC shows contribution timelines of the individual analytes with an approach to a plateau which is much closer to the WT timeline plateau than observed with linezolid (Figure 5-1). After 25 hours, six out of eight ΔCOG values are not significantly different to the prior timepoint at 12 hours (all $p > 0.05$; except glycopeptide [$p = 0.0149$] and PFAM 16525 [no value]). We concluded that a saturation/plateau is reached between 12 hours to 25 hours. At the same time (at 25 hours), in six of the eight observed peaks, the percental contribution of *de-novo* synthesized protein is categorized at least 60-69%. This means that even after 25 hours incubation, the contribution of newly-synthesized protein is larger than its unlabeled pendant. Extrapolating this information to the *M. smegmatis* proteome, it can be understood that *M. smegmatis* under the influence of benzothiazinone has managed to replicate itself at least once.

In conclusion, the earliest detectable onset of action of benzothiazinone in 2 x MIC on *M. smegmatis* protein metabolism was found at 3 hours after application (Figure 5-2). The median value of these defined timepoints when the ΔCOG values of the respective analytes were first detected to significantly diverge from the WT timeline is 6.25 hours. This coincides with the previously discussed results of the reduction factor of *M. smegmatis* under the influence of benzothiazinone: We assumed that only after a critical minimum timepoint which was reached or surpassed at 6.5 hours since exposure, effective killing of benzothiazinone can be observed (5-73). Further, the majority of the *de-novo* synthesis of analytes is affected by benzothiazinone in 2 x MIC within 7.5 hours, suggesting that benzothiazinone reaches full or nearly-full effectiveness at 7.5 hours or later. Hence, the application of benzothiazinone in 2 x MIC as an individual agent leads to a later reduction of protein synthesis of *M. smegmatis* than linezolid in 2 x MIC. This is consistent with the mechanism of action of benzothiazinone, which inhibits production of the crucial cell wall component arabinogalactan by blocking DprE1 (Makarov et al., 2009; Mikušová et al., 2005) and does not directly intervene in protein biosynthesis. Depending on the diffusion gradient as the determining factor for the benzothiazinone uptake into the cell, it is possible that benzothiazinone has a faster onset on the mycobacterial cell wall, which is not represented by the molecules that were analyzed by MALDI-TOF MS here.

5.4 Combination of Linezolid and Benzothiazinone

To summarize the results, the pharmacodynamics of the combination of linezolid and benzothiazinone on *M. smegmatis* were studied based on modification of three variables:

a) Time length of the pre-incubation period with linezolid, the compound applied first

b) Exposure time of benzothiazinone

c) Concentration of linezolid and benzothiazinone in multiples or fractions of their MIC values

In the following, the measurable effects of this combination on the CFU count of *M. smegmatis*, on the reduction factor and on the morphology are discussed in order to evaluate the combined antimicrobial activity. Three conclusions were drawn that are discussed in detail here:

1) The combination of linezolid and benzothiazinone observed after 25 hours significantly increases the killing of *M. smegmatis* compared to the single agents and, applied in a specific scheme, operates in synergy.
2) The synergy of linezolid and benzothiazinone does not depend on a continuously high benzothiazinone concentration level.
3) Pre-incubation period of linezolid is critical in an optimized scheme in combined activity with benzothiazinone.

The combination of linezolid and benzothiazinone observed after 25 hours significantly increases the killing of *M. smegmatis* compared to the single agents and, applied in a specific scheme, operates in synergy.

The results showed that linezolid applied in 2 x MIC (c = 1.0 µg/mL) as a single agent led to a reduction factor of 2.6 after 25 hours (Figure 4-8). Adding benzothiazinone in 2 x MIC after a pre-incubation period with linezolid of 3 hours produced a significantly higher reduction factor of 3.4 ($p < 0.05$). Adding benzothiazinone in 2 x MIC for an exposure duration of 4 hours under otherwise identical conditions, also produced a significantly higher reduction factor (also 3.4; $p < 0.05$) that is equal to the reduction factor under long-termed exposure of benzothiazinone ($p = 0.7$; for details see 4-59; the graph is visualized once more in Figure 5-3). Also, the addition of benzothiazinone in 20 x MIC after a 3-hour pre-incubation period with linezolid showed a significantly higher reduction factor: a combined exposure duration of half an hour was sufficient to significantly increase the reduction factor to an average value of 3.3 ($p < 0.01$), and to 3.5 when the combined exposure lasted for 4 hours or for the rest of the experiment (both

$p < 0.001$; Figure 5-3). In conclusion, an increased killing of *M. smegmatis* compared to the application of the single agents can be observed when benzothiazinone is combined with linezolid under the given circumstances.

In literature, several different definitions of synergy exist (Berenbaum, 1977). Most commonly though, synergy is defined as the combined effect of two different substances resulting in an effect that is larger than predictive by their individual potencies (Greco, Bravo, & Parsons, 1995; Tallarida, 2011). Doern defines the difference between synergy and additivity as the following: "Antimicrobial combinations can act additively, where the cumulative antimicrobial effect is simply the sum total of the two antimicrobials acting together, or they can act synergistically, where the combined activity is greater than the sum of their activities when used individually" (Doern, 2014). One of the most cited models on drug interactions is that of Loewe on pharmacological additivity, graphically represented by the isobole curves (Loewe & Muischnek, 1926). In this case, synergy is defined as when "achieving a stronger effect is easier with a second drug", while additivity is defined as "achieving a stronger effect requires the same increase in drug A or drug B". Various methods have been assessed to test drug interaction and synergy *in vitro*, but there is no true gold standard for synergy testing (Doern, 2014). Literature even suggests that no two methodological approaches produce comparable results (Doern, 2014).

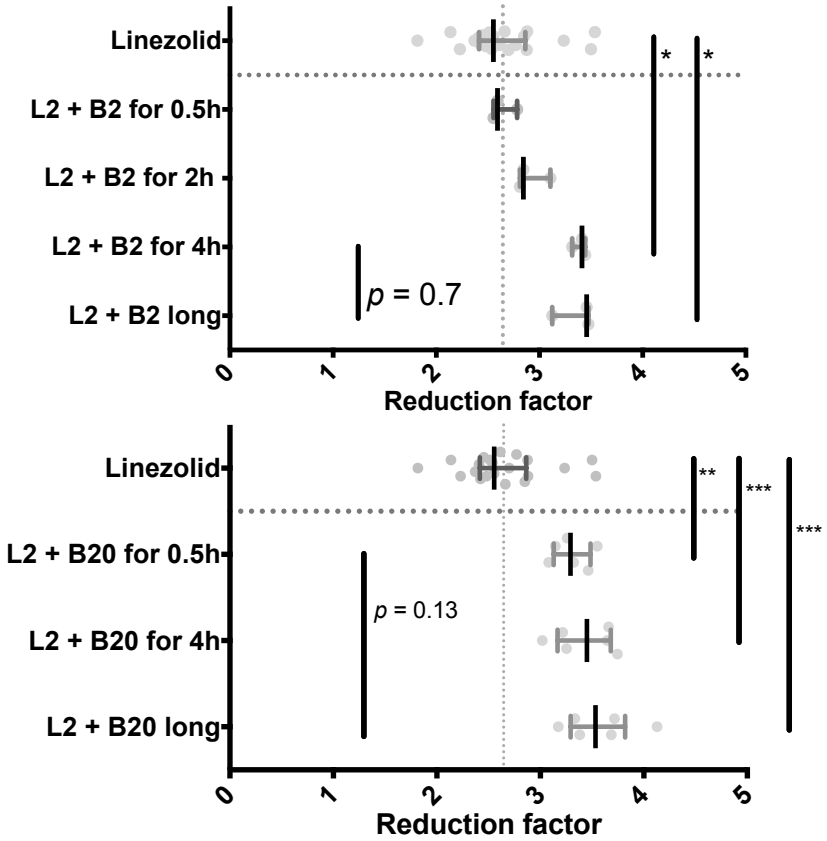

Figure 5-3: Linezolid and benzothiazinone effect.

The pre-incubation with linezolid in 2 x MIC was 3 hours; benzothiazinone applied in 2 x MIC (above) or 20 x MIC (below) in increasing exposure times; total growth time 25 hours. L2 = linezolid used in 2 x MIC (c = 1.0 µg/mL); B2 = benzothiazinone used in 2 x MIC (c = 9.5 ng/mL), B20 = benzothiazinone applied in 20 x MIC (c = 94.6 ng/mL). Bars refer to median and interquartile range. Median values of the reduction factor; upper graph: $RF_{Linezolid}$ = 2.6 (*n* = 21); $RF_{L2+B2\ for\ 0.5h}$ = 2.6 (*n* = 3); $RF_{L2+B2\ for\ 2h}$ = 2.8 (*n* = 3); $RF_{L2+B2\ for\ 4h}$ = 3.4 (*n* = 3); $RF_{L2+B2\ long}$ = 3.5 (*n* = 3). Graph below: $RF_{L2+B20\ for\ 0.5h}$= 3.3 (*n* = 6), $RF_{L2+B20\ for\ 4h}$= 3.5 (*n* = 6), $RF_{L2+B20\ long}$ = 3.5 (*n* = 6). One star * refers to a *p*-value < 0.05; two stars ** to a *p*-value < 0.01, three stars *** to a *p*-value of < 0.001. All combination groups compared and tested for significance by using the Mann-Whitney U test.

In a broader medical perspective, synergy can also be defined as an enhancement of effect between two pharmacological agents. Every analysis demonstrating a significantly larger effect in the combination of both agents compared to linezolid or benzothiazinone in their single application can therefore be called a cooperation. As discussed above, a beneficial interaction between linezolid and benzothiazinone leading to stronger reduction of *M. smegmatis* could be shown in variable constellations and concentrations, mostly with a linezolid base level of 2 x MIC (1.0 µg/mL) and additional benzothiazinone levels in 2 x MIC or 20 x MIC (9.5 ng/mL and 94.7 ng/mL). Following the stricter definition of synergy of Greco et. al, a closer look into the effect of benzothiazinone alone for 2 hours (0.09; 95% CI ranging from -0.4 to 0.6; *n* = 3), 4 hours (0.05; 95 % CI from -0.6 to 0.7; *n* = 3) or long-term (0.6; 95 % CI from 0.3 to 0.8; *n* = 3) is

required. In order to evaluate drug synergism, the predicted effect of the combined individual potencies must be defined which is represented here by the reduction factor of the individually applied agents linezolid and benzothiazinone. Calculating the sum of the mean values of the two reduction factors results in the hypothetical values shown in the following table, followed by the reduction factor ascertained by our trials. The *p*-value refers to the difference between the respective combination group and the linezolid control group. The *p*-values for the benzothiazinone reduction factor, when applied as a single agent for different exposure times, are not shown as the reduction itself did not even exceed 1.

Table 11: Comparing the Hypothetical Sum and the Reduction Factor

Benzothiazinone exposure time (2 x MIC)	Mean reduction benzothiazinone (2 x MIC)	Mean reduction linezolid (2 x MIC)	Hypothetical sum	Actual reduction factor
2 hours	0.09	2.645	2.735	2.92 ($p = 0.17$)
4 hours	0.05	2.645	2.695	3.4 ($p = 0.023$)
Long-term	0.6	2.645	3.245	3.4 ($p = 0.031$)

In Table 11, the observed (actual) reduction is higher than the hypothetical sum in all three cases, but the difference was only significant in the combined benzothiazinone exposure of 4 hours and long-term. Therefore, we concluded linezolid in 2 x MIC and benzothiazinone in 2 x MIC operate in synergy against *M. smegmatis* when applied for 4 hours or long-term.

Table 12: Comparing the Hypothetical Sum and the Reduction Factor

Benzothiazinone exposure time (20 x MIC)	Mean reduction benzothiazinone (20 x MIC)	Mean reduction linezolid (2 x MIC)	Hypothetical sum	Actual reduction factor
4 hours	0.30	2.645	2.945	3.45 ($p = 0.0004$)
Long-term	1.40	2.645	4.045	3.53 ($p = 0.0003$)

When benzothiazinone is added in 20 x MIC (Table 12), the reduction is significantly higher than seen in the individual linezolid application ($p = 0.0004$ and $p = 0.0003$, respectively). However, only the addition of benzothiazinone at 20 x MIC for 4 hours adheres to the stricter definition of synergy. Hence, in this case, we can assume synergy accurately only when the benzothiazinone exposure is limited to a short pulse of concentration.

Further, neither linezolid nor benzothiazinone in *in vitro* conditions as a single agent were capable of impairing mycobacterial growth on an absolute level: the absolute CFU count of *M. smegmatis* exposed to linezolid in 2 x MIC as a single agent still significantly increases between 7.5 hours and 25 hours ($p < 0.01$; from 7.7 x 10^5 CFU/mL to 1.8 x 10^6 CFU/mL; Figure 4-9). This indicates that slow proliferation of *M. smegmatis* exposed to linezolid could still occur. The data of the following graph demonstrates that in combination, the additional 4-hour

benzothiazinone exposure (graph plotted to the left of the dotted line, Figure 5-4) causes a significant decrease of the total CFU count between 7.5 hours to 25 hours incubation (Δ_{Median} = -8.2 x 10^5 CFU/mL; p = 0.026). This indicates that an additional killing occurred between the timepoint of 7.5 hours and 25 hours and demonstrates *in vitro* evidence of the synergy between linezolid and benzothiazinone.

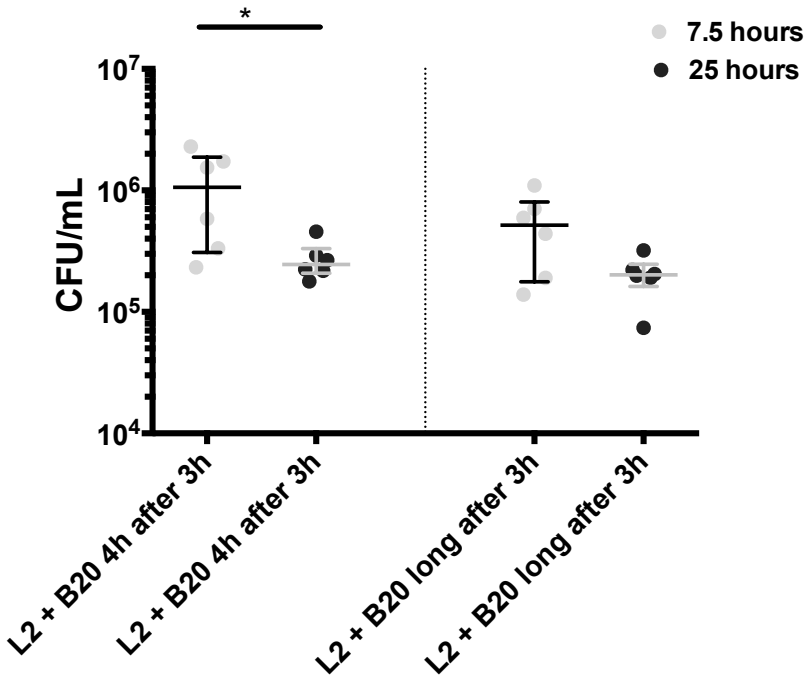

Figure 5-4: Combined efficacy after 7.5 hours versus 25 hours.

Comparing absolute CFU after 7.5 hours (light) versus 25 hours (dark). Left of the dotted line are the CFU counts plotted of combination study with benzothiazinone in 20 x MIC exposure time of 4 hours, on the right we see the long-term application of benzothiazinone. Bars refer to median and interquartile range. Median values for 4 hours benzothiazinone exposure time: 1.1 x 10^6 CFU/mL (7.5 hours) and 2.5 x 10^5 CFU/mL (25 hours); median values for long benzothiazinone exposure: 5.2 x 10^5 CFU/mL (7.5 hours) and 2.0 x 10^5 CFU/mL (25 hours). Groups were compared using Mann Whitney U test. One star * refers to $p < 0.05$.

In contrast, when applying benzothiazinone in 20 x MIC long-term (data shown in the graph right of the dotted line, Figure 5-4), the trend seems similar ($mean_{7.5\ hours}$ = 5.3 x 10^5 CFU/mL and $mean_{25\ hours}$ = 2.0 x 10^5 CFU/mL), but the difference was not significant (p = 0.24), which may be due to a small sample number or to a ceiling effect that is reached earlier when benzothiazinone is applied long-term. Hence, for the group that was exposed to benzothiazinone long-term, we can state that either an additional killing has taken place during the 17.5 hours, or no additional killing has taken place. Nonetheless, *no increase* could be observed between 7.5 hours and 25 hours of growth. This again demonstrates that in contrast to the individual agents, the applied combination of linezolid in 2 x MIC and benzothiazinone in 20 x MIC is able

to impair mycobacterial growth on an absolute level and inhibits proliferation completely, further supporting the hypothesis of synergism between linezolid and benzothiazinone.

Reasons for the synergy between linezolid and benzothiazinone can be based on the following theory. From what is known about both agents, benzothiazinone acts as a suicide substrate by covalently binding to the cell wall synthesis enzyme DprE1 and irreversibly inactivating it (Makarov et al., 2009; Trefzer et al., 2012), and in brief, linezolid blocks the initiation of protein synthesis on ribosomal level (Shinabarger et al., 1997; Swaney et al., 1998). After attaining a certain critical benzothiazinone level, all present molecules of Dpre1 are saturated with benzothiazinone molecules and inactivated. At the same time, protein production is mainly decreased by linezolid, as could be shown through our MALDI-TOF MS results using stable carbon isotope labeling (see results on pages 4-37 and 5-81). If protein synthesis is blocked, the production of new DprE1 will be nearly impossible and functional Dpre1 will be completely depleted. As DprE1 serves as an integral enzyme in cell wall synthesis for mycobacteria (Kolly et al., 2014), *M. smegmatis* is not able to produce new mycolic acids for its cell wall and the concentration of the products of the Arabinan pathway will recede to a certain dilution (whilst other cell wall material still can be produced). This continues until the cell is not anymore capable to produce functional cell wall material. Eventually, this leads to lysis, as could be shown in DprE1-down-regulated mutants (Kolly et al., 2014) and as we can assume from our SEM studies under the combination of linezolid and benzothiazinone (see results and images on page 4-65).

Moreover, comparing the values shown in Figure 5-4 provides no significant difference between a 4-hour exposure time and long-term exposure time of benzothiazinone in 20 x MIC (p = 0.24). This suggests that the combination of linezolid and benzothiazinone in the applied scheme for 25 hours does not require a long, sustained level of benzothiazinone, leading to the next hypothesis: The same effect can be achieved by limiting the combined benzothiazinone exposure to a time period of 4 hours – or even less, if the concentration is higher.

The synergy of linezolid and benzothiazinone does not depend on a continuously high benzothiazinone concentration level.

This hypothesis is further supported by the comparison of the reduction factors achieved in the groups exposed to benzothiazinone at 2 x MIC and 20 x MIC respectively while being also exposed to linezolid 2 x MIC (see Figure 5-5). The reduction factors in both groups average at 3.5

(p = 0.5476). Thus, in combination with linezolid, it is not relevant whether benzothiazinone is applied in 20 x MIC or only in 2 x MIC – the maximum effect in killing *M. smegmatis* is the same.

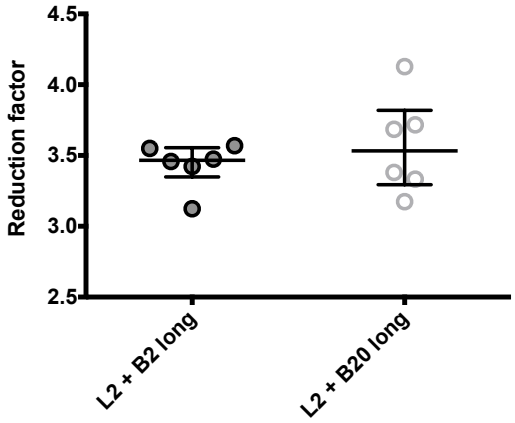

Figure 5-5: Benzothiazinone exposure concentration in combination with linezolid.

The reduction factor shown after a total growth time of 25 hours. Benzothiazinone once applied in 2 x MIC and once in 20 x MIC. N = 6. Bars refer to median and interquartile range. Median values of reduction: $RF_{L2+B2\ long}$ = 3.5; $RF_{B2+B20\ long}$ = 3.5. p = 0.5476.

The results also showed that there is no difference between the 0.5-hour exposure or long-term exposure of benzothiazinone applied in 20 x MIC (Figure 5-3, p = 0.13). In alignment with the reasoning of the first discussed hypothesis we assume that once a critical benzothiazinone level is reached in combination with linezolid, all present DprE1 molecules are saturated and therefore irreversibly inactivated. They cannot be reproduced by synthesis which is inhibited through linezolid, hence no additional effect through increasing the concentration of benzothiazinone is to be expected. The combination has reached its maximum level of killing. We concluded that a continuous administration of linezolid in 2 x MIC combined with a short peak level of benzothiazinone (20 x MIC) is an effective *in-vitro* combination for the reduction of the *M. smegmatis* bacterium. Our results challenge the assumption that the combination of linezolid and benzothiazinone against *M. smegmatis* requires a sustained, high level of benzothiazinone and provide evidence that a pulsed, high benzothiazinone exposure at 20 x MIC is not inferior to a continuous benzothiazinone exposure at 2 x MIC or even 20 x MIC.

The length of the pre-incubation period of linezolid is critical in an optimized scheme in combined activity with benzothiazinone.

In the following figure (Figure 5-6), *M. smegmatis* was incubated with both compounds in 2 x MIC and observed over a period of 25 hours. The only difference was the pre-incubation period of linezolid being either 1 hour or 3 hours (orange dots vs. blue dots). In both groups, benzothiazinone was applied for 2 hours or 4 hours, respectively.

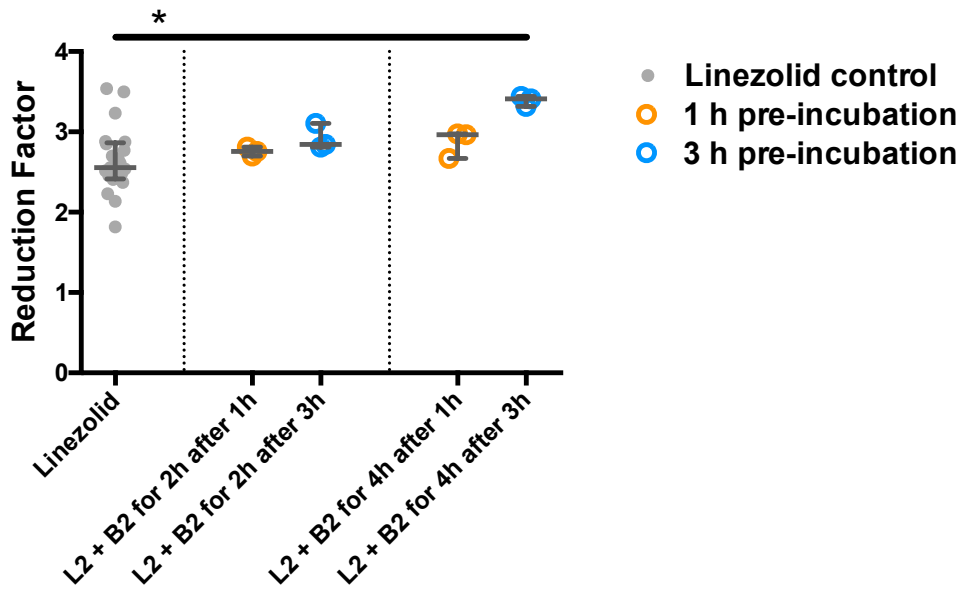

Figure 5-6: The influence of the pre-incubation period.

Linezolid and benzothiazinone combined activity on *M. smegmatis* after 25 hours of growth; 1 hour vs. 3 hours pre-incubation period with linezolid in 2 x MIC. "B2" refers to the benzothiazinone exposure in 2 x MIC and an exposure duration of 2 hours (left) or 4 hours (right), respectively. The bars indicate median and interquartile range. Median values of reduction factor: $RF_{Linezolid} = 2.6$ ($n = 21$); $RF_{L2+B2\ for\ 2h\ after\ 1h} = 2.8$ ($n = 3$); $RF_{L2+B2\ for\ 2h\ after\ 3h} = 2.8$ ($n = 3$); $RF_{L2+B2\ for\ 4h\ after\ 1h} = 3.0$ ($n = 3$); $RF_{L2+B2\ for\ 4h\ after\ 3h} = 3.4$ ($n = 3$). One star * refers to a p-value < 0.05. The groups were compared by Mann-Whitney U test.

The data shown in the graph permits the following conclusion: From all groups, only in the group in which *M. smegmatis* was pre-incubated with linezolid for 3 hours, an exposure time of 4 hours with benzothiazinone was sufficient to create a significant increase in killing effect (median values are 2.6 and 3.4, respectively; $p = 0.0227$). This alone suggests that linezolid has not reached its full effect after 1 hour. As previously discussed, its mode of action as a protein synthesis inhibitor at an early stage of the translation process (Shinabarger et al., 1997; Swaney et al., 1998) directly intervenes in protein metabolism and therefore shows a nearly immediate difference after application in the elected peaks of the mass spectra of *M. smegmatis*. When *M. smegmatis* was exposed to linezolid in this concentration (c = 1.0 µg/mL) the results showed the *de-novo* synthesis rate of the majority of analytes was significantly smaller at a timepoint of 3 hours (Figure 5-2). We extrapolated that the nearly-full effectiveness of linezolid administered in c = 1.0 µg/mL occurs after an incubation period of 3 hours. This led to the assumption that the most efficient combination with benzothiazinone (when benzothiazinone is applied for a restricted period) most likely occurs *after M. smegmatis* is pre-incubated with linezolid for at least 3 hours – potentially causing both compounds to coincide in their maximum response phase. In that given case, the *combination* of linezolid in 2 x MIC and benzothiazinone in 2 x MIC applied for a duration of 4 hours after a 1-hour pre-incubation period with linezolid (as

seen in Figure 4-22 and Figure 5-6) would act at its maximum only for an intersectional phase of 2 hours – and even 2 hours is assumedly overestimated as the addition of benzothiazinone may cause stimulation due to the observed paradox effect in the beginning of the intersectional phase. The reduction factor of *M. smegmatis* exposed to linezolid and benzothiazinone for a duration of 4 hours after a 1-hour pre-incubation period with linezolid as a single agent averages at 2.9 (95% CI of mean ranging from 2.4 to 3.3; $n = 3$). Comparing the results, this value directly corresponds to the killing of *M. smegmatis* exposed to linezolid and benzothiazinone for 2 hours after a 3-hour pre-incubation period with linezolid, where the reduction equally averages at 2.9 (95% CI of mean ranging from 2.5 to 3.3; $n = 3$; $p > 0.999$), revealing that these group values are highly similar. A presumable minimum efficient overlap of the two compounds is exactly 2 hours in both cases. Again, small *n* may be the reason for the lack of possibility to determine significant changes between these groups and further experiments remain to be designed to illuminate this hypothesis. From our MALDI-TOF MS results the maximum response phase of benzothiazinone as an individual agent can be estimated between 7.5 or more hours (5-82). From the results of cultivating *M. smegmatis*, the maximum response phase can be estimated between 6.5 and 22 hours whilst a paradox effect was observed in shorter periods of incubation (5-76). The maximum response phase of benzothiazinone in *combination* remains to be defined more precisely. It is possible that this paradox effect also occurs in the combination, meaning that the maximum intersectional response phase of both agents combined may assumedly be even later than directly after the 3-hour pre-incubation period with linezolid. Nevertheless, due to its nature as a suicide substrate (Trefzer et al., 2012) and the theory previously discussed in combination with linezolid, it is probable that the maximum response phase of benzothiazinone is preponed through the combination with a protein synthesis inhibitor.

The paradox effect of benzothiazinone also occurs in combination with linezolid.

We could initially observe and describe a paradox effect when benzothiazinone was applied as a single agent to *M. smegmatis* and when the observation time since exposure did not exceed 4.5 hours (5-76). We hypothesized that a minimum critical time range needs to be overcome by the benzothiazinone exposure duration in order to surpass the paradox effect and to unfold its antimicrobial effect. When benzothiazinone was added to linezolid after a 3-hour pre-incubation period and if the first sample to count the CFU is seized already after a total growth time of 7.5 hours (Figure 4-23), no additional killing in comparison to the linezolid control group

could be observed. With the time since exposure here being 4.5 hours, potentially, the benzothiazinone application still moves within the critical time range where it supposedly does not yet completely unfold its antimicrobial effect.

In another experiment (Figure 4-25) where benzothiazinone is added in 2 x MIC to linezolid in 2 x MIC after 1-hour preincubation and the bacteria are plated after 7.5 hours, the reduction factor significantly *decreases* (1.6 in the linezolid control group [95% CI of mean ranging from 1.4 to 1.7] and 1.1 in combination; 95% CI of mean ranged from 0.8 to 1.4; $p = 0.0109$). Both examples are consistent with the priorly discussed paradox effect of benzothiazinone applied as a single agent, potentially pushing *M. smegmatis* into faster partition (see page 5-76). In conclusion, we assume that, parallel to its paradox effect as a single agent, benzothiazinone in combination does not work synergistically with linezolid right from the beginning and instead, initially rather increases the CFU count.

Interestingly, we could see in both set-ups with a limited observation time to 7.5 hours (data represented in Figure 4-23 and Figure 4-24) in 2 x MIC as well as in 20 x MIC, a stronger reduction after the 0.5-hour benzothiazinone exposure than after the *longer* exposure. At first sight this doesn't appear logical, but it makes sense when understood as a clue that the paradox effect may begin only after half an hour. However, if waited until the end of the 25-hour observation period, the paradox effect doesn't appear (see Figure 4-20, Figure 4-21) even though the experimental design is otherwise absolutely identical. We concluded that the observed paradox effect is a transient phenomenon, potentially losing its impact when 2-3 *M. smegmatis* growth cycles are exceeded. This may be due to the previously discussed stress response on benzothiazinone exposure (5.2.1) which is compensated with proceeding growth cycles. Therefore, the paradox effect may have not been observed up to now as previous studies have exposed mycobacteria to the benzothiazinone compounds over larger time periods, for example 28 days (Makarov et al., 2009) or 7 days in *M. tuberculosis* (Lechartier et al., 2012) – this refers to 14 to 56 growth cycles in *M. tuberculosis*, whereas we noted the increase of CFU in *M. smegmatis* after an observation period of approximately two growth cycles.

The morphological change of *M. smegmatis* exposed to the combination that was captured by the SEM presented absence of a significant difference between a 4-hour or long-term benzothiazinone exposure (at identical linezolid concentration).

The length of *M. smegmatis* in the combination groups observed after a total growth time of 25 hours was 5.8 µm for a benzothiazinone exposure time of 4 hours and 5.8 µm for the long-termed exposure time (see page 4-65), with no significant difference among these two groups

(p = 0.97). After an incubation time of 7.5 hours, the average lengths were 5.8 µm (4 hours exposure) and 5.5 µm (long-term exposure) and were not found to be significantly different from each other (p = 0.3379). In conclusion, there was neither a significant difference found by increasing the observation period from 7.5 hours to 25 hours nor by prolonging the benzothiazinone exposure time (4 hours vs. long exposure time after three hours pre-incubation with linezolid). No difference in width could be found between the 4-hour and long exposure time of benzothiazinone in the combination groups (width $_{L2+B2\ for\ 4h}$ = 0.52 µm; and width $_{L2+B2\ for\ long}$= 0.52 µm; p = 0.97). We can hereby conclude that there is no morphological difference regarding mycobacterial length or width between adding benzothiazinone long-term or for a 4-hour exposure time to linezolid. The results are consistent with the hypothesis that in combination with linezolid, a long-term benzothiazinone exposure at 2 x MIC is not superior to the 4-hour benzothiazinone exposure.

5.5 Limitations

5.5.1 Technical Limitations

MALDI-TOF MS

In contrast to other mass spectrometry methods, stable isotope labeling in MALDI-TOF MS enables a rapid detection of labeled mycobacterial proteins and peptides in parallel, but the exact quantification of labeled analytes in the MALD-TOF spectra is limited. The imprecise starting conditions of the MALDI (distance from co-crystalized matrix on the target to the laser) as well as competition of ionization cause limited accuracy and limited quantification possibilities for analytes. This impedes direct quantifications of different analytes. The ΔCOG value is a robust tool to quantify the peak shift, but neither can the ΔCOG value be used in an absolute manner. Only ΔCOG values in reference to a maximum contribution in chemically identical analytes permit comparison. Concerning quantification of labeling in newly-synthesized proteins, it must also be considered that of the tracer-glycerol, only 2 of 3 C-atoms are ^{13}C-labeled. Furthermore, full labeling of 2/3 of C-atoms of newly-synthesized proteins cannot be expected either: even though glycerol is the preferred carbon source of mycobacteria, it is not the only carbon source of mycobacteria (Cook et al., 2009) and incorporation of glycerol may vary from one protein to another depending on the amino acid composition. Last, there may be other synthesis pathways, which yet remain to be examined. Time points of 1 hour, 3 hours, 5 hours, 7.5 hours, 12 hours and 25 hours were chosen to detect *de-novo* synthesis of mycobacterial proteins and peptides. The incorporation of labeled glycerol though, is a dynamic process. The method

permits conclusions about the labeling which occurred in the time span between these time points, but does not allow conclusions about what occurs *at* this timepoint.

Eight proteins/peptides of the *M. smegmatis* proteome were chosen to deduce assumptions about the general antimicrobial effect against *M. smegmatis.* The chosen molecules needed to meet certain criteria in their corresponding m/z signals of the mass spectrum to become part of the analysis (defined minimum intensity, no interfering neighboring peaks). Thus, observations on the eight proteins we chose must be regarded very carefully if used for general assumptions on the *M. smegmatis* protein metabolism. On the other hand, it should be expected that effects blocking the protein synthesis pathway should affect all proteins simultaneously and equally. Thus, even few proteins, and especially the proteins that were identified as ribosomal (as we can assume that they are not regulated dramatically), could be enough to monitor protein metabolism.

CFU Counts

All CFU counts were tested in triplicates and by repetition of experiments. To compare CFU counts with more reliability, a number of batches $n > 6$ would be suitable in all CFU counts and reduction factor values in order to receive a larger power when comparing the groups. In a few experiments, a larger sample size is yet required for more accurate evidence (such as in Figure 4-15, Figure 5-4 and Figure 5-5).

Washing

When culturing *M. smegmatis* and going through the specific washing step to reduce the benzothiazinone concentration to a minimum, time was lost to the washing procedure itself. As early washing meant “little pellet loss” and late washing meant “more pellet loss”, to minimize errors, first the linezolid group was washed and then the combination group, followed by all the other controls. Furthermore, choosing 4°C for centrifugation rooted in the aim to inhibit further growth during the washing step, however this may have impaired growth conditions slightly after the washing step as the bacteria needed to regenerate in the incubator. To minimize this effect, we used pre-warmed media after the washing step. To avoid systematic errors, all samples of the same experiment were always washed, even though no change to their media were required.

Scanning Electron Microscope

The micrographs taken with the SEM represent well visible excerpts from a larger sample size. The cell bodies of mycobacteria exposed to the antibiotic compounds appeared flattened, destroyed or irregular. Hence, measuring their width by Image J was difficult and it is possible to

have measured systematically wider mycobacteria with the results that their surface and volume in the manipulated states were potentially slightly overestimated in comparison to the wildtype samples. It must be added that the calculation of the surface and the volume based on a cylindrical shape were an estimation, therefore can be considered for orientation purpose only. Assuming a totally cylindrical shape systematically ignores the rounded shape of the pole region of the mycobacterial cell; further, with increased application of antibiotics, the shape diverged even more from a cylinder. The volume/surface ratio was calculated as a hypothetical value for comparison between exposed mycobacteria. Testing for significance for all above reasons was impossible but numbers were mentioned to demonstrate a tendency.

5.5.2 General Limitations

The project consists of *in vitro* experiments with *M. smegmatis* as a surrogate for *M. tuberculosis*. Even though *M. smegmatis* has routinely been used in the past to draw certain parallels concerning mutations and drug screening (Altaf, Miller, Bellows, & O'Toole, 2010; Lechartier et al., 2012; Makarov et al., 2009) to *M. tuberculosis*, still the behavior of *M. smegmatis* towards linezolid and benzothiazinone is not a 100% predictive to a multi-drug resistant *M. tuberculosis. M. smegmatis* is naturally more resistant to benzothiazinone due to enzymes that have the capability to inactivate benzothiazinone through reduction (Manina et al., 2010). By genomic comparisons it could be approximated that 30% of *M. tuberculosis* proteins lack orthologues in *M. smegmatis* and 50% of compounds that were detected as active against *M. tuberculosis* were not discovered when using *M. smegmatis* as a surrogate for screening (Altaf et al., 2010). Atlaf et al. could precisely show that *M. bovis* BCG serves as a surrogate closer to *M. tuberculosis,* as only 3% of *M. bovis* BCG proteins lack conserved orthologues and only one fifth of compounds that were active against *M. tuberculosis* were not found active when screening with *M. bovis* BCG. Hence, to receive more precise data towards developing a new therapeutic scheme, the next step would be to perform combined linezolid and benzothiazinone studies with specimen of the tuberculosis complex. The synergy that we could observe *in-vitro* then leads to the further step of testing this combination in the *M. tuberculosis* H37rv strain and in infected animal models.

Even if good antimicrobial activity of benzothiazinone against *M. tuberculosis* can be assumed, it still remains unknown whether patients will tolerate benzothiazinone combined with linezolid and what kind of side effects its pharmacokinetic profile will cause. In the mouse model, no adverse events could be observed by applying benzothiazinone as a single agent (Makarov et

al., 2009) and the cytotoxicity profile on representative cell lines remained low in a recent study (Tiwari, Miller, Cho, Franzblau, & Miller, 2015). This may be due to its specificity to mycobacteria or, to still too little comparative studies at disposition. All in all, for safety, tolerability and compliance of patients, it appears logical that patients might benefit from consuming benzothiazinone in a dose and duration as small and short as possible, underlining the importance of this project.

Furthermore, our results of *in vitro* experiments of the combination of linezolid and benzothiazinone against mycobacteria leave us without conclusions about the variables of human pharmacokinetics. If good tolerability, efficacy and safety of the combined compounds were given, there still remain risks: Application of these antibiotics as a drug regime in humans require strong compliance as the continuous linezolid concentration level and hence, non-stop blockage of protein bio-synthesis, appears an indispensable condition to applying benzothiazinone in the manner of a short peak exposure (page 5-90). Generally, consequent compliance is crucial to minimize chance of conversion into resistant strains (Mitchison, 1998). Prolonged administration of linezolid provides an increase of adverse events – specific adverse events such as optic or peripheral neuropathy, anemia or thrombocytopenia due to myelosuppression, serotonin syndrome and lactic acidosis were reported to show up more with a trough level exceeding 2 µg/mL over at least three weeks (Boak et al., 2014; Kenreigh et al., 2016; Kishor et al., 2015; Leader et al., 2018; Roger et al., 2018; Song et al., 2015; Zhang et al., 2015). Our data suggests that in *M. smegmatis* a linezolid concentration level of 1.0 µg/mL is sufficient for an efficient combination with benzothiazinone at peak concentration *in vitro*. Yet, based on our theory that mycobacteria start resynthesizing Dpre1 once protein biosynthesis is no longer inhibited, it appears crucial to not go below a critical linezolid level (which yet remains to be determined).

From our results, we defined a phenomenon with benzothiazinone applied as a single agent which we called the “paradox effect” of benzothiazinone (page 5-73). Implications this effect for the human model may be that once benzothiazinone is added to the regimen, the bacterial number may first rise in the beginning before the bacterial burden drops. In further studies, this needs to be considered. Lastly, it remains questionable whether the combination of a protein synthesis inhibitor and a cell wall blocker are able to have an antimicrobial effect on dormant mycobacterial cultures which are yet one of the largest challenges to face in treating tuberculosis.

5.6 Outlook

Achieving a deeper understanding of linezolid and benzothiazinone and of mycobacteria may reduce tuberculosis treatment duration and open more possibilities to optimize the therapeutic scheme of tuberculosis and MDR-TB in the clinical setting one day. This would alleviate the financial, socioeconomic and health burden of both the individual and the society. Even though antituberculotic agents have been studied since 1944 (Kerantzas & Jacobs, 2017) and possibly even before, it is now that we start questioning increasingly why certain antibiotic combinations act synergistically and investigate to understand combined synergy by the individual mechanisms of action (Lechartier et al., 2012; Zhu, Liu, Hu, Yang, & He, 2018). The treatment of tuberculosis in general poses an enormous challenge to individual patients and health care systems in low- and middle -income countries, given that even the abbreviated treatment scheme requires a minimum drug regimen of four months (in the standard regimen still six months) and an expensive combination drug therapy, and that incidences are especially high in low- and middle-income countries (D Falzon et al., 2011; WHO consolidated guidelines on tuberculosis, 2022; World Health Organization, 2017). MDR-TB or XDR-TB cases require an even more individualized therapy, reserve antibiotics and a prolonged treatment, which can stretch over more than a year (Ahmad et al., 2018; Lee et al., 2012). An increasingly important aspect to treating tuberculosis appears the question of drug penetration in the tuberculotic lesion (described on page 1-3): It seems pivotal that the combination of linezolid and benzothiazinone arrives in the granuloma (Prideaux et al., 2015) as mycobacteria appear to resist by residing in the lesion (Hoff et al., 2011). Benzothiazinone, especially the compound BTZ043 which we used in our experiments, is a highly lipophilic substance (Makarov et al., 2009). Therefore it constitutes a promising candidate to arriving in the caesum and in its antimycobacterial effectiveness (Makarov et al., 2009). Potentially, its more hydrophilic rival compound, PBTZ169, represents an alternative with an improved pharmacodynamic/pharmacokinetic profile (Makarov et al., 2014) but may provide less penetration into the caesum.

It could be shown that strain resistance patterns are a determinant factor in the costs of treatment of MDR-TB or XDR-TB: Applied to the German health care system, mean drug costs of XDR- and MDR-TB ranged between 20,000 € and 95,000 € (Diel, Nienhaus, Lampenius, Rüsch-Gerdes, & Richter, 2014b). The total costs per case including hospitalization and estimation of loss of productivity reached an amount between 82,000 € to 109,000 €. Linezolid took rank 4 of the most expensive drugs on the list, a package of 30 film-coated tablets of 600mg costs

2,673.87 €, one tablet having a value of a little less than 90 € (Diel, Nienhaus, Lampenius, Rüsch-Gerdes, & Richter, 2014a).

Benzothiazinone compound BTZ043 together with the compound PBTZ169 is a leading compound in the new antituberculotic drug pipeline (Makarov et al., 2014). Their pharmacodynamic traits are still being debated and their pharmacokinetic and clinical profiles yet remain to be elucidated. Still, it could be shown that they share the same mechanism of action (Makarov et al., 2014). Following the theory of the combined mode of action between linezolid and BTZ043, it can be assumed that the synergy which we could detect is transferable to the piperazine-version of the benzothiazinone compound. Following our theory, even ethambutol, which is also known to act on the arabinan pathway (Mikusova, Slayden, Besra, & Brennan, 1995), might prove to work in synergy in the combination with linezolid, a protein synthesis inhibitor.

From a scientific perspective it is crucial to comprehend the pharmacodynamics behind synergistic interaction of antimicrobial agents, to investigate their mechanism of action in order to predict and evaluate new efficient combinations. Finding a therapeutic scheme where agents would not have to be applied endlessly but rather prudentially and optimized on their spot, will result in lower costs for health economy, a smaller spectrum of undesired therapeutic side effects for the future patient and a closer step towards ending the global tuberculosis pandemic.

Bibliography

Agyeman, A. A., & Ofori-Asenso, R. (2016). Efficacy and safety profile of linezolid in the treatment of multidrug-resistant (MDR) and extensively drug-resistant (XDR) tuberculosis: a systematic review and meta-analysis. *Annals of Clinical Microbiology and Antimicrobials*, *15*(1), 41. https://doi.org/10.1186/s12941-016-0156-y

Ahmad, N., Ahuja, S. D., Akkerman, O. W., Alffenaar, J. W. C., Anderson, L. F., Baghaei, P., … Menzies, D. (2018). Treatment correlates of successful outcomes in pulmonary multidrug-resistant tuberculosis: an individual patient data meta-analysis. *The Lancet*, *392*(10150), 821–834. https://doi.org/10.1016/S0140-6736(18)31644-1

Akinola, R. O. (2013). A Systems Level Comparison of Mycobacterium tuberculosis, Mycobacterium leprae and Mycobacterium smegmatis Based on Functional Interaction Network Analysis. *Journal of Bacteriology & Parasitology*, *04*(04), 1–11. https://doi.org/10.4172/2155-9597.1000173

Alderwick, L.J., Birch, H. L., Mishra, A. K., Eggeling, L., & Besra, G. S. (2007). Structure, function and biosynthesis of the Mycobacterium tuberculosis cell wall: arabinogalactan and lipoarabinomannan assembly with a view to discovering new drug targets. *Biochemical Society Transactions*, *35*(5), 1325–1328. https://doi.org/10.1042/BST0351325

Alderwick, Luke J., Lloyd, G. S., Lloyd, A. J., Lovering, A. L., Eggeling, L., & Besra, G. S. (2011). Biochemical characterization of the Mycobacterium tuberculosis phosphoribosyl-1-pyrophosphate synthetase. *Glycobiology*, *21*(4), 410–425. https://doi.org/10.1093/glycob/cwq173

Altaf, M., Miller, C. H., Bellows, D. S., & O'Toole, R. (2010). Evaluation of the Mycobacterium smegmatis and BCG models for the discovery of Mycobacterium tuberculosis inhibitors. *Tuberculosis*, *90*(6), 333–337. https://doi.org/10.1016/j.tube.2010.09.002

American Type Culture Collection. (2023). Mycobacterium tuberculosis variant bovis BCG - 35734 | ATCC. Retrieved July 20, 2023, from https://www.atcc.org/products/35734

Andrews, J. R., Morrow, C., Walensky, R. P., & Wood, R. (2014). Integrating Social Contact and Environmental Data in Evaluating Tuberculosis Transmission in a South African Township. https://doi.org/10.1093/infdis/jiu138

Anhalt, J. P., & Fenselau, C. (1975). Identification of Bacteria using Mass Spectrometry. *Analytical Chemistry*, *47*(2), 219–225. https://doi.org/10.1021/ac60352a007

Barrios-Payán, J., Saqui-Salces, M., Jeyanathan, M., Alcántara-Vazquez, A., Castañon-Arreola, M., Rook, G., & Hernandez-Pando, R. (2012). Extrapulmonary locations of mycobacterium tuberculosis DNA during latent infection. *Journal of Infectious Diseases*, *206*(8), 1194–1205. https://doi.org/10.1093/infdis/jis381

Barry, C. E., Boshoff, H., Dartois, V., Dick, T., Ehrt, S., Flynn, J., … Young, D. (2009). The spectrum of latent tuberculosis: rethinking the goals of prophylaxis. *Nat Rev Microbiol*, *7*(12), 845–855. https://doi.org/10.1038/nrmicro2236

Batt, S. M., Jabeen, T., Bhowruth, V., Quill, L., Lund, P. A., Eggeling, L., … Besra, G. S. (2012). Structural basis of inhibition of Mycobacterium tuberculosis DprE1 by benzothiazinone inhibitors. *Proceedings of the National Academy of Sciences of the United States of America*, *109*(28), 11354–11359. https://doi.org/10.1073/pnas.1205735109

Berenbaum, M. C. (1977). Synergy, additivism and antagonism in immunosuppression. A critical review. *Clinical and Experimental Immunology*, *28*(1), 1–18. Retrieved from http://www.ncbi.nlm.nih.gov/pubmed/324671

Boak, L. M., Rayner, C. R., Grayson, M. L., Paterson, D. L., Spelman, D., Khumra, S., … Bulitta, J. B. (2014). Clinical population pharmacokinetics and toxicodynamics of linezolid. *Antimicrobial Agents and Chemotherapy*, *58*(4), 2334–2343. https://doi.org/10.1128/AAC.01885-13

Boehme, C. C., Nabeta, P., Hillemann, D., Nicol, M. P., Shenai, S., Krapp, F., … Perkins, M. D. (2010). Rapid Molecular Detection of Tuberculosis and Rifampin Resistance. *New England Journal of Medicine*, *363*(11), 1005–1015. https://doi.org/10.1056/nejmoa0907847

Boselli, E., Breilh, D., Rimmelé, T., Djabarouti, S., Toutain, J., Chassard, D., … Allaouchiche, B. (2005). Pharmacokinetics and intrapulmonary concentrations of linezolid administered to critically ill patients with ventilator-associated pneumonia. *Critical Care Medicine*, *33*(7), 1529–1533. Retrieved from

http://www.ncbi.nlm.nih.gov/pubmed/16003058

Brennan, P. J. (2003). Structure, function, and biogenesis of the cell wall of Mycobacterium tuberculosis. In *Tuberculosis* (Vol. 83, pp. 91–97). Churchill Livingstone. https://doi.org/10.1016/S1472-9792(02)00089-6

Brennan, Patrick J., & Nikaido, H. (1995). The Envelope of Mycobacteria. *Annual Review of Biochemistry*, *64*(1), 29–63. https://doi.org/10.1146/annurev.bi.64.070195.000333

Brodhun, B., Altmann, D., Hauer, B., Fiebig, L., & Haas, W. (2015). [Current epidemiology of tuberculosis in Germany]. *Pneumologie (Stuttgart, Germany)*, *69*(5), 263–270. https://doi.org/10.1055/s-0034-1391922

Budzikiewicz, H. (1969). H. Kienitz, Herausgeber: Massenspektrometrie. Verfaßt von F. Aulinger, G. Franke, K. Habfast, H. Kienitz und G. Spiteller. Verlag Chemie, GmbH, Weinheim/Bergstr. 1968. XV + 883 Seiten mit 342 Abbildungen und 52 Tabellen im Text und einem Tabellenteil. Pre. In *Berichte der Bunsengesellschaft für physikalische Chemie* (Vol. 73, pp. 114–115). John Wiley & Sons, Ltd. https://doi.org/10.1002/bbpc.19690730123

Cadena, A. M., Fortune, S. M., & Flynn, J. L. (2017, October 27). Heterogeneity in tuberculosis. *Nature Reviews Immunology*. Nature Publishing Group. https://doi.org/10.1038/nri.2017.69

Calmette, A., Guerin, C., & Boquet, A. (1927). *La vaccination préventive contre la tuberculose par le "BCG."* Paris.

Carbonnelle, E., Mesquita, C., Bille, E., Day, N., Dauphin, B., Beretti, J. L., … Nassif, X. (2011). MALDI-TOF mass spectrometry tools for bacterial identification in clinical microbiology laboratory. *Clinical Biochemistry*. https://doi.org/10.1016/j.clinbiochem.2010.06.017

Chaiprasert, A., Srimuang, S., Tingtoy, N., Makhao, N., Sirirudeeporn, P., Tomnongdee, N., … Prammananan, T. (2014). Second-line drug susceptibilities of multidrug-resistant tuberculosis strains isolated in Thailand: an update. *The International Journal of Tuberculosis and Lung Disease*, *18*(8), 961–963. https://doi.org/10.5588/ijtld.13.0197

Champney, W. S., & Miller, M. (2002). Linezolid is a specific inhibitor of 50S ribosomal subunit formation in Staphylococcus aureus cells. *Current Microbiology*, *44*(5), 350–356. https://doi.org/10.1007/s00284-001-0023-7

Chaturvedi, V., Dwivedi, N., Tripathi, R. P., & Sinha, S. (2007). Evaluation of Mycobacterium smegmatis as a possible surrogate screen for selecting molecules active against multi-drug resistant Mycobacterium tuberculosis. *The Journal of General and Applied Microbiology*, *53*(6), 333–337. https://doi.org/10.2323/jgam.53.333

Cherkaoui, A., Hibbs, J., Emonet, S., Tangomo, M., Girard, M., Francois, P., & Schrenzel, J. (2010). Comparison of Two Matrix-Assisted Laser Desorption Ionization-Time of Flight Mass Spectrometry Methods with Conventional Phenotypic Identification for Routine Identification of Bacteria to the Species Level. *Journal of Clinical Microbiology*, *48*(4), 1169–1175. https://doi.org/10.1128/JCM.01881-09

Churchyard, G., Kim, P., Shah, N. S., Rustomjee, R., Gandhi, N., Mathema, B., … Cardenas, V. (2017). What We Know about Tuberculosis Transmission: An Overview. *Journal of Infectious Diseases*, *216*(Suppl 6), S629–S635. https://doi.org/10.1093/infdis/jix362

Conte, J. E., Golden, J. A., Kipps, J., & Zurlinden, E. (2002). Intrapulmonary pharmacokinetics of linezolid. *Antimicrobial Agents and Chemotherapy*, *46*(5), 1475–1480. Retrieved from http://www.ncbi.nlm.nih.gov/pubmed/11959585

Cook, G. M., Berney, M., Gebhard, S., Heinemann, M., Cox, R. A., Danilchanka, O., & Niederweis, M. (2009). Physiology of Mycobacteria. *Advances in Microbial Physiology*. https://doi.org/10.1016/S0065-2911(09)05502-7

Cosma, C. L., Humbert, O., & Ramakrishnan, L. (2004). Superinfecting mycobacteria home to established tuberculous granulomas. *Nature Immunology*, *5*(8), 828–835. https://doi.org/10.1038/ni1091

Daniel, R. A., & Errington, J. (2003). Control of cell morphogenesis in bacteria: two distinct ways to make a rod-shaped cell. *Cell*, *113*(6), 767–776. Retrieved from http://www.ncbi.nlm.nih.gov/pubmed/12809607

De Vriese, A. S., Van Coster, R., Smet, J., Seneca, S., Lovering, A., Van Haute, L. L., … Boelaert, J. R. (2006). Linezolid-Induced Inhibition of Mitochondrial Protein Synthesis. *Clinical Infectious Diseases*, *42*(8), 1111–1117. https://doi.org/10.1086/501356

Dehghanyar, P., Burger, C., Zeitlinger, M., Islinger, F., Kovar, F., Muller, M., … Joukhadar, C. (2005). Penetration of Linezolid into Soft Tissues of Healthy Volunteers after Single and Multiple Doses. *Antimicrobial Agents and Chemotherapy*, *49*(6), 2367–2371. https://doi.org/10.1128/AAC.49.6.2367-2371.2005

Dheda, K., Booth, H., Huggett, J. F., Johnson, M. A., Zumla, A., & W Rook, G. A. (2005). *Lung Remodeling in Pulmonary Tuberculosis*. Retrieved from https://academic.oup.com/jid/article/192/7/1201/2191669

Dheda, K., Schwander, S. K., Zhu, B., Van Zyl-Smit, R. N., & Zhang, Y. (2010, April 1). The immunology of tuberculosis: From bench to bedside. *Respirology*. John Wiley & Sons, Ltd. https://doi.org/10.1111/j.1440-1843.2010.01739.x

Diel, R., Nienhaus, A., Lampenius, N., Rüsch-Gerdes, S., & Richter, E. (2014a). Cost of multi drug resistance tuberculosis in Germany. *Respiratory Medicine*, *108*(11), 1677–1687. https://doi.org/10.1016/j.rmed.2014.09.021

Diel, R., Nienhaus, A., Lampenius, N., Rüsch-Gerdes, S., & Richter, E. (2014b). Cost of multi drug resistance tuberculosis in Germany. *Respiratory Medicine*, *108*(11), 1677–1687. https://doi.org/10.1016/j.rmed.2014.09.021

Dodd, P. J., Yuen, C. M., Sismanidis, C., Seddon, J. A., & Jenkins, H. E. (2017). The global burden of tuberculosis mortality in children: a mathematical modelling study. *The Lancet Global Health*, *5*(9), e898–e906. https://doi.org/10.1016/S2214-109X(17)30289-9

Doern, C. D. (2014, December 1). When does 2 plus 2 equal 5? A review of antimicrobial synergy testing. *Journal of Clinical Microbiology*. American Society for Microbiology. https://doi.org/10.1128/JCM.01121-14

Dorman, S. E., Nahid, P., Kurbatova, E. V., Phillips, P. P. J., Bryant, K., Dooley, K. E., … Chaisson, R. E. (2021). Four-Month Rifapentine Regimens with or without Moxifloxacin for Tuberculosis. *New England Journal of Medicine*, *384*(18), 1705–1718. https://doi.org/10.1056/nejmoa2033400

Ehlers, S., & Schaible, U. E. (2013). The granuloma in tuberculosis: dynamics of a host-pathogen collusion. https://doi.org/10.3389/fimmu.2012.00411

EPA. (2012). Product Performance Test Guidelines Disinfectants for Use on Hard Surfaces — Efficacy Data Recommendations OCSPP 810.2200. *EPA*. Retrieved from http://www.regulations.gov/#!documentDetail;D=EPA-HQ-OPPT-2009-0150-0021

Eurosurveillance editorial Team. (2013). WHO revised definitions and reporting framework for tuberculosis. *Eurosurveillance*, *18*(16), 20455. https://doi.org/WHO/HTM/TB/2013.2

Falzon, D, Jaramillo, E., Schünemann, H. J., Arentz, M., Bauer, M., Bayona, J., … Zignol, M. (2011). WHO guidelines for the programmatic management of drug-resistant tuberculosis: 2011 update. *European Respiratory Journal*, *38*(3), 516–528. https://doi.org/10.1183/09031936.00073611

Falzon, Dennis, Schünemann, H. J., Harausz, E., González-Angulo, L., Lienhardt, C., Jaramillo, E., & Weyer, K. (2017). World Health Organization treatment guidelines for drug-resistant tuberculosis, 2016 update. *European Respiratory Journal*, *49*(3), 1602308. https://doi.org/10.1183/13993003.02308-2016

Fan, X., Tang, X., Yan, J., & Xie, J. (2014). Identification of idiosyncratic Mycobacterium tuberculosis ribosomal protein subunits with implications in extraribosomal function, persistence, and drug resistance based on transcriptome data. *Journal of Biomolecular Structure and Dynamics*, *32*(10), 1546–1551. https://doi.org/10.1080/07391102.2013.826143

Finn, R. D., Coggill, P., Eberhardt, R. Y., Eddy, S. R., Mistry, J., Mitchell, A. L., … Bateman, A. (2016). The Pfam protein families database: towards a more sustainable future. *Nucleic Acids Research*, *44*(D1), D279–D285. https://doi.org/10.1093/nar/gkv1344

Flynn, J. A. L. (2004). Mutual attraction: Does it benefit the host or the bug? *Nature Immunology*, *5*(8), 778–779. https://doi.org/10.1038/ni0804-778

Flynn, J. L., Chan, J., & Lin, P. L. (2011, May). Macrophages and control of granulomatous inflammation in tuberculosis. *Mucosal Immunology*. NIH Public Access. https://doi.org/10.1038/mi.2011.14

Fox, G. J., Barry, S. E., Britton, W. J., & Marks, G. B. (2013, January 1). Contact investigation for tuberculosis: A systematic review and meta-analysis. *European Respiratory Journal*. European Respiratory Society. https://doi.org/10.1183/09031936.00070812

Fox, W., Ellard, G. A., & Mitchison, D. A. (1999). Studies on the treatment of tuberculosis undertaken by the British Medical Research Council Tuberculosis Units, 1946-1986, with relevant subsequent publications, *3*(10 SUPPL. 2), undefined-undefined. Retrieved from https://www.mendeley.com/catalogue/a2217642-bec4-3b96-b68e-a174b7ee439c/?utm_source=desktop&utm_medium=1.19.8&utm_campaign=open_catalog&userDocumentId=%7B9e5e909b-8419-3ecb-8972-de12589a6a0c%7D

Fuchs, G., Eitinger, T., Heider, J., Kemper, B., Kothe, E., Overmann, J., … Unden, G. (2014). Allgemeine Mikrobiologie. In G. Fuchs & H.-G. Schlegel (Eds.) (10. Auflag, pp. 564–568). Stuttgart. New York.: Georg Thieme Verlag. https://doi.org/10.1055/b-002-95260

Fullam, E., Pojer, F., Bergfors, T., Jones, T. A., & Cole, S. T. (2012). Structure and function of the transketolase from *Mycobacterium tuberculosis* and comparison with the human enzyme. *Open Biology*, *2*(1), 110026. https://doi.org/10.1098/rsob.110026

Garrabou, G., Soriano, À., Pinós, T., Casanova-Mollà, J., Pacheu-Grau, D., Morén, C., … Cardellach, F. (2017). Influence of Mitochondrial Genetics on the Mitochondrial Toxicity of Linezolid in Blood Cells and Skin Nerve Fibers. *Antimicrobial Agents and Chemotherapy*, *61*(9). https://doi.org/10.1128/AAC.00542-17

Gill, W. P., Harik, N. S., Whiddon, M. R., Liao, R. P., Mittler, J. E., & Sherman, D. R. (2009). A replication clock for Mycobacterium tuberculosis. *Nature Medicine*, *15*(2), 211–214. https://doi.org/10.1038/nm.1915

Gillespie, S. H., Crook, A. M., McHugh, T. D., Mendel, C. M., Meredith, S. K., Murray, S. R., … Nunn, A. J. (2014). Four-month Moxifloxacin-based regimens for drug-sensitive tuberculosis. *New England Journal of Medicine*, *371*(17), 1577–1587. https://doi.org/10.1056/NEJMoa1407426

Golden, M. P. (2005). *Extrapulmonary Tuberculosis: An Overview - American Family Physician*. *American Family Physician* (Vol. 72). Retrieved from www.aafp.org/afpAmericanFamilyPhysician1761

Greco, W. R., Bravo, G., & Parsons, J. C. (1995). The search for synergy: a critical review from a response surface perspective. *Pharmacological Reviews*, *47*(2).

Hajdas, I., Ascough, P., Garnett, M. H., Fallon, S. J., Pearson, C. L., Quarta, G., … Yoneda, M. (2021). Radiocarbon dating. *Nature Reviews Methods Primers 2021 1:1*, *1*(1), 1–26. https://doi.org/10.1038/s43586-021-00058-7

Hermans, S., Horsburgh, C. R., & Wood, R. (2015). A century of tuberculosis epidemiology in the northern and southern hemisphere: The differential impact of control interventions. *PLoS ONE*, *10*(8). https://doi.org/10.1371/journal.pone.0135179

Hett, E. C., & Rubin, E. J. (2008). Bacterial Growth and Cell Division: a Mycobacterial Perspective. *Microbiology and Molecular Biology Reviews*, *72*(1), 126–156. https://doi.org/10.1128/MMBR.00028-07

Hillemann, D., Rüsch-Gerdes, S., & Richter, E. (2008, February). In vitro-selected linezolid-resistant Mycobacterium tuberculosis mutants [4]. *Antimicrobial Agents and Chemotherapy*. American Society for Microbiology (ASM). https://doi.org/10.1128/AAC.01189-07

Hillenkamp, F., & Karas, M. (1990). Mass spectrometry of peptides and proteins by matrix-assisted ultraviolet laser desorption/ionization. *Methods in Enzymology*, *193*(C), 280–295. https://doi.org/10.1016/0076-6879(90)93420-P

Hoff, D. R., Ryan, G. J., Driver, E. R., Ssemakulu, C. C., de Groote, M. A., Basaraba, R. J., & Lenaerts, A. J. (2011). Location of intra- and extracellular M. tuberculosis populations in lungs of mice and guinea pigs during disease progression and after drug treatment. *PLoS ONE*, *6*(3), e17550. https://doi.org/10.1371/journal.pone.0017550

Horsburgh, C. R. (2014). Tuberculosis. *European Respiratory Review : An Official Journal of the European Respiratory Society*, *23*(131), 36–39. https://doi.org/10.1183/09059180.00008213

Huang, H., Scherman, M. S., D'Haeze, W., Vereecke, D., Holsters, M., Crick, D. C., & McNeil, M. R. (2005). Identification and active expression of the Mycobacterium tuberculosis gene encoding 5-phospho-α-D-ribose-1-diphosphate: Decaprenyl-phosphate 5-phosphoribosyltransferase, the first enzyme committed to decaprenylphosphoryl- D-arabinose synthesis. *Journal of Biological Chemistry*, *280*(26), 24539–24543. https://doi.org/10.1074/jbc.M504068200

James, B. W., Williams, A., & Marsh, P. D. (2000). The physiology and pathogenicity of Mycobacterium

tuberculosis grown under controlled conditions in a defined medium. *Journal of Applied Microbiology*, *88*(4), 669–677. https://doi.org/10.1046/j.1365-2672.2000.01020.x

Johnson, J. L., Hadad, D. J., Dietze, R., Maciel, E. L. N., Sewali, B., Gitta, P., … Boom, W. H. (2009). Shortening treatment in adults with noncavitary tuberculosis and 2-month culture conversion. *American Journal of Respiratory and Critical Care Medicine*, *180*(6), 558–563. https://doi.org/10.1164/RCCM.200904-0536OC

Jung, J. S., Eberl, T., Sparbier, K., Lange, C., Kostrzewa, M., Schubert, S., & Wieser, A. (2014). Rapid detection of antibiotic resistance based on mass spectrometry and stable isotopes. *European Journal of Clinical Microbiology & Infectious Diseases*, *33*(6), 949–955. https://doi.org/10.1007/s10096-013-2031-5

Kanai, K. (1966). Experimental studies on host-parasite equilibrium in tuberculous infection, in relation to vaccination and chemotherapy. *Japanese Journal of Medical Science and Biology*, *19*(4), 181–199. https://doi.org/10.7883/yoken1952.19.181

Karas, M., Bachmann, D., & Hillenkamp, F. (1985). Influence of the Wavelength in High-Irradiance Ultraviolet Laser Desorption Mass Spectrometry of Organic Molecules. *Analytical Chemistry*, *57*(14), 2935–2939. https://doi.org/10.1021/ac00291a042

Karas, M., Glückmann, M., & Schäfer, J. (2000). Ionization in matrix-assisted laser desorption/ionization: Singly charged molecular ions are the lucky survivors. *Journal of Mass Spectrometry*, *35*(1), 1–12. https://doi.org/10.1002/(SICI)1096-9888(200001)35:1<1::AID-JMS904>3.0.CO;2-0

Kenreigh, C., Vazquez, J. A., Arnold, A., Swanson, R., Biswas, P., & Bassetti, M. (2016). Safety of long-term use of linezolid: results of an open-label study. *Therapeutics and Clinical Risk Management*, *Volume 12*, 1347–1354. https://doi.org/10.2147/TCRM.S109444

Kerantzas, C. A., & Jacobs, W. R. (2017). Origins of combination therapy for tuberculosis: Lessons for future antimicrobial development and application. *MBio*. https://doi.org/10.1128/mBio.01586-16

King, H. C., Khera-Butler, T., James, P., Oakley, B. B., Erenso, G., Aseffa, A., … Courtenay, O. (2017). Environmental reservoirs of pathogenic mycobacteria across the Ethiopian biogeographical landscape. *PLOS ONE*, *12*(3), e0173811. https://doi.org/10.1371/journal.pone.0173811

Kishor, K., Dhasmana, N., Kamble, S. S., & Sahu, R. K. (2015). Linezolid Induced Adverse Drug Reactions - An Update. *Current Drug Metabolism*, *16*(7), 553–559. https://doi.org/10.2174/1389200216666151001121004

Koh, W. J., Kwon, O. J., Gwak, H., Chung, J. W., Cho, S. N., Kim, W. S., & Shim, T. S. (2009). Daily 300 mg dose of linezolid for the treatment of intractable multidrug-resistant and extensively drug-resistant tuberculosis. *Journal of Antimicrobial Chemotherapy*, *64*(2), 388–391. https://doi.org/10.1093/jac/dkp171

Kolly, G. S., Boldrin, F., Sala, C., Dhar, N., Hartkoorn, R. C., Ventura, M., … Cole, S. T. (2014). Assessing the essentiality of the decaprenyl-phospho-d-arabinofuranose pathway in Mycobacterium tuberculosis using conditional mutants. *Molecular Microbiology*, *92*(1), 194–211. https://doi.org/10.1111/mmi.12546

Lange, C., Abubakar, I., Alffenaar, J.-W. W. C., Bothamley, G., Caminero, J. A., Carvalho, A. C. C., … Cirillo, D. M. (2014). Management of patients with multidrug-resistant/extensively drug-resistant tuberculosis in Europe: a TBNET consensus statement. *The European Respiratory Journal*, *44*(1), 23–63. https://doi.org/10.1183/09031936.00188313

Larsen, M. H., Biermann, K., & Jacobs, W. R. (2007). Laboratory Maintenance of *Mycobacterium tuberculosis*. *Current Protocols in Microbiology*, *6*(1), 10A.1.1-10A.1.8. https://doi.org/10.1002/9780471729259.mc10a01s6

Leader, R., Hackett, J., Allan, A., & Carter, P. (2018). Linezolid-induced pancytopenia. *BMJ Case Reports*, *2018*, bcr-2018-225480. https://doi.org/10.1136/bcr-2018-225480

Lechartier, B., Hartkoorn, R. C., & Cole, S. T. (2012). In vitro combination studies of benzothiazinone lead compound BTZ043 against mycobacterium tuberculosis. *Antimicrobial Agents and Chemotherapy*, *56*(11), 5790–5793. https://doi.org/10.1128/AAC.01476-12

Lee, M., Lee, J., Carroll, M. W., Choi, H., Min, S., Song, T., … Barry, C. E. (2012). Linezolid for Treatment of Chronic Extensively Drug-Resistant Tuberculosis. *New England Journal of Medicine*, *367*(16), 1508–1518. https://doi.org/10.1056/NEJMoa1201964

Libby, W. (1955). Radiocarbon Dating.

Lienhardt, C., Raviglione, M., Spigelman, M., Hafner, R., Jaramillo, E., Hoelscher, M., … Gheuens, J. (2012, May 15). New drugs for the treatment of tuberculosis: Needs, challenges, promise, and prospects for the future. *Journal of Infectious Diseases*. https://doi.org/10.1093/infdis/jis034

Lin, A. H., Murray, R. W., Vidmar, T. J., & Marotti, K. R. (1997). The oxazolidinone eperezolid binds to the 50S ribosomal subunit and competes with binding of chloramphenicol and lincomycin. *Antimicrobial Agents and Chemotherapy*, *41*(10), 2127–2131. Retrieved from http://www.ncbi.nlm.nih.gov/pubmed/9333036

Loewe, S., & Muischnek, H. (1926). XXIV. Aus dem Pharmakologischen Institut der Universit~it Tartu-Dorpat. t~ber Kombinationswirkungen. I. M i t t e i l u n g : H i l f s m i t t e l d e r F r a g e s t e l l u n g .

Log and Percent Reductions in Microbiology and Antimicrobial Testing | Microchem Laboratory. (n.d.). Retrieved October 7, 2020, from https://microchemlab.com/information/log-and-percent-reductions-microbiology-and-antimicrobial-testing

Lu, T., & Drlica, K. (2003). In vitro activity of C-8-methoxy fluoroquinolones against mycobacteria when combined with anti-tuberculosis agents. *Journal of Antimicrobial Chemotherapy*, *52*(6), 1025–1028. https://doi.org/10.1093/jac/dkg480

Lucarelli, A. P., Buroni, S., Pasca, M. R., Rizzi, M., Cavagnino, A., Valentini, G., … Chiarelli, L. R. (2010). Mycobacterium tuberculosis phosphoribosylpyrophosphate synthetase: Biochemical features of a crucial enzyme for mycobacterial cell wall biosynthesis. *PLoS ONE*, *5*(11). https://doi.org/10.1371/journal.pone.0015494

Maartens, G., & Benson, C. A. (2015). Linezolid for Treating Tuberculosis: A Delicate Balancing Act. *EBioMedicine*. https://doi.org/10.1016/j.ebiom.2015.10.014

Mack, U., Migliori, G. B., Sester, M., Rieder, H. L., Ehlers, S., Goletti, D., … Lange, C. (2009). LTBI: Latent tuberculosis infection or lasting immune responses to M. tuberculosis? A TBNET consensus statement. In *European Respiratory Journal* (Vol. 33, pp. 956–973). European Respiratory Society. https://doi.org/10.1183/09031936.00120908

Maguire, B. A., Beniaminov, A. D., Ramu, H., Mankin, A. S., & Zimmermann, R. A. (2005). A protein component at the heart of an RNA machine: The importance of protein L27 for the function of the bacterial ribosome. *Molecular Cell*, *20*(3), 427–435. https://doi.org/10.1016/j.molcel.2005.09.009

Makarov, V., Lechartier, B., Zhang, M., Neres, J., van der Sar, A. M., Raadsen, S. A., … Cole, S. T. (2014). Towards a new combination therapy for tuberculosis with next generation benzothiazinones. *EMBO Molecular Medicine*, *6*(3), 372–383. https://doi.org/10.1002/emmm.201303575

Makarov, V., Manina, G., Mikusova, K., Möllmann, U., Ryabova, O., Saint-Joanis, B., … Cole, S. T. (2009). Benzothiazinones Kill Mycobacterium tuberculosis by blocking Arabinan synthesis. *Science*, *324*(5928), 801–804. https://doi.org/10.1126/science.1171583

Manina, G., Bellinzoni, M., Pasca, M. R., Neres, J., Milano, A., De Jesus Lopes Ribeiro, A. L., … Riccardi, G. (2010). Biological and structural characterization of the Mycobacterium smegmatis nitroreductase NfnB, and its role in benzothiazinone resistance. *Molecular Microbiology*, *77*(5), 1172–1185. https://doi.org/10.1111/j.1365-2958.2010.07277.x

Mann, M. (2006, December 8). Functional and quantitative proteomics using SILAC. *Nature Reviews Molecular Cell Biology*. Nat Rev Mol Cell Biol. https://doi.org/10.1038/nrm2067

Martinez, L., Shen, Y., Mupere, E., Kizza, A., Hill, P. C., & Whalen, C. C. (2017). Transmission of Mycobacterium Tuberculosis in Households and the Community: A Systematic Review and Meta-Analysis. *American Journal of Epidemiology*, *185*(12), 1327–1339. https://doi.org/10.1093/aje/kwx025

Matassova, N. B., Rodnina, M. V, Endermann, R., Kroll, H. P., Pleiss, U., Wild, H., & Wintermeyer, W. (1999). Ribosomal RNA is the target for oxazolidinones, a novel class of translational inhibitors. *RNA*, *5*(7), 939–946. https://doi.org/10.1017/S1355838299990210

Meija, J., Coplen, T. B., Berglund, M., Brand, W. A., De Bièvre, P., Gröning, M., … Prohaska, T. (2016, March 1). Isotopic compositions of the elements 2013 (IUPAC Technical Report). *Pure and Applied Chemistry*. Walter de Gruyter GmbH. https://doi.org/10.1515/pac-2015-0503

Menzies, D., Pai, M., & Zwerling, A. (2008). Systematic review: T-cell-based assays for the diagnosis of latent tuberculosis infection: an update. *Annals of Internal Medicine*, *149*(3), 177–184. Retrieved from

http://www.ncbi.nlm.nih.gov/pubmed/18593687

Merkov, L. N. (2006). *Glyoxylate Metabolism In Mycobacterium smegmatis*. Rockefeller University.

Metcalfe, J. Z., Everett, C. K., Steingart, K. R., Cattamanchi, A., Huang, L., Hopewell, P. C., & Pai, M. (2011). Interferon-γ release assays for active pulmonary tuberculosis diagnosis in adults in low-and middle-income countries: Systematic review and meta-analysis. *Journal of Infectious Diseases*. https://doi.org/10.1093/infdis/jir410

Mikušová, K., Huang, H., Yagi, T., Holsters, M., Vereecke, D., D'Haeze, W., … Crick, D. C. (2005). Decaprenylphosphoryl arabinofuranose, the donor of the D-arabinofuranosyl residues of mycobacterial arabinan, is formed via a two-step epimerization of decaprenylphosphoryl ribose. *Journal of Bacteriology*, *187*(23), 8020–8025. https://doi.org/10.1128/JB.187.23.8020-8025.2005

Mikusova, K., Slayden, R. A., Besra, G. S., & Brennan, P. J. (1995). Biogenesis of the mycobacterial cell wall and the site of action of ethambutol. *Antimicrobial Agents and Chemotherapy*, *39*(11), 2484–2489. https://doi.org/10.1128/AAC.39.11.2484

Mitchison, D. A. (1998). How drug resistance emerges as a result of poor compliance during short course chemotherapy for tuberculosis. *International Journal of Tuberculosis and Lung Disease*.

Moreno, L. Z., Matajira, C. E. C., Poor, A. P., Mesquita, R. E., Gomes, V. T. M., Silva, A. P. S., … Moreno, A. M. (2018). Identification through MALDI-TOF mass spectrometry and antimicrobial susceptibility profiling of bacterial pathogens isolated from sow urinary tract infection. *Veterinary Quarterly*, *38*(1), 1–8. https://doi.org/10.1080/01652176.2017.1397302

Muñoz-Elías, E. J., Timm, J., Botha, T., Chan, W. T., Gomez, J. E., & McKinney, J. D. (2005). Replication dynamics of Mycobacterium tuberculosis in chronically infected mice. *Infection and Immunity*, *73*(1), 546–551. https://doi.org/10.1128/IAI.73.1.546-551.2005

Nagiec, E. E., Wu, L., Swaney, S. M., Chosay, J. G., Ross, D. E., Brieland, J. K., & Leach, K. L. (2005). Oxazolidinones Inhibit Cellular Proliferation via Inhibition of Mitochondrial Protein Synthesis. *Antimicrobial Agents and Chemotherapy*, *49*(9), 3896–3902. https://doi.org/10.1128/AAC.49.9.3896-3902.2005

Neres, J., Pojer, F., Molteni, E., Chiarelli, L. R., Dhar, N., Boy-Röttger, S., … Binda, C. (2012). Structural basis for benzothiazinone-mediated killing of Mycobacterium tuberculosis. *Science Translational Medicine*, *4*(150), 150–121. https://doi.org/10.1126/scitranslmed.3004395

Niederweis, M., Danilchanka, O., Huff, J., Hoffmann, C., & Engelhardt, H. (2010, March 1). Mycobacterial outer membranes: in search of proteins. *Trends in Microbiology*. Elsevier Current Trends. https://doi.org/10.1016/j.tim.2009.12.005

Niederweis, M., Ehrt, S., Heinz, C., Klöcker, U., Karosi, S., Swiderek, K. M., … Benz, R. (1999). Cloning of the mspA gene encoding a porin from Mycobacterium smegmatis. *Molecular Microbiology*, *33*(5), 933–945. https://doi.org/10.1046/j.1365-2958.1999.01472.x

O'Garra, A., Redford, P. S., McNab, F. W., Bloom, C. I., Wilkinson, R. J., & Berry, M. P. R. (2013, March 21). The immune response in tuberculosis. *Annual Review of Immunology*. Annual Reviews . https://doi.org/10.1146/annurev-immunol-032712-095939

Orme, I. M., & Basaraba, R. J. (2014). The formation of the granuloma in tuberculosis infection. *Seminars in Immunology*, *26*(6), 601–609. https://doi.org/10.1016/j.smim.2014.09.009

Pai, M., Denkinger, C. M., Kik, S. V., Rangaka, M. X., Zwerling, A., Oxlade, O., … Banaei, N. (2014). Gamma interferon release assays for detection of Mycobacterium tuberculosis infection. *Clinical Microbiology Reviews*, *27*(1), 3–20. https://doi.org/10.1128/CMR.00034-13

Pai, M., & Menzies, D. (2007). Interferon-γ release assays: What is their role in the diagnosis of active tuberculosis? *Clinical Infectious Diseases*. https://doi.org/10.1086/509927

Pankey, G. A., & Sabath, L. D. (2004, March 15). Clinical relevance of bacteriostatic versus bactericidal mechanisms of action in the treatment of gram-positive bacterial infections. *Clinical Infectious Diseases*. Oxford Academic. https://doi.org/10.1086/381972

Pasca, M. R., Degiacomi, G., Lopes Ribeiro, A. L. D. J., Zara, F., De Mori, P., Heym, B., … Riccardi, G. (2010). Clinical isolates of Mycobacterium tuberculosis in four European hospitals are uniformly susceptible to benzothiazinones. *Antimicrobial Agents and Chemotherapy*, *54*(4), 1616–1618.

https://doi.org/10.1128/AAC.01676-09

Prideaux, B., Via, L. E., Zimmerman, M. D., Eum, S., Sarathy, J., O'Brien, P., … Dartois, V. (2015). The association between sterilizing activity and drug distribution into tuberculosis lesions. *Nature Medicine*, *21*(10), 1223–1227. https://doi.org/10.1038/nm.3937

Rees, R. J., & Hart, P. D. (1961). Analysis of the host-parasite equilibrium in chronic murine tuberculosis by total and viable bacillary counts. *British Journal of Experimental Pathology*, *42*(1), 83–88. Retrieved from https://www-ncbi-nlm-nih-gov.emedien.ub.uni-muenchen.de/pmc/articles/PMC2083177/

Riccardi, G., Pasca, M. R., & Buroni, S. (2009, June). Mycobacterium tuberculosis: Drug resistance and future perspectives. *Future Microbiology*. https://doi.org/10.2217/fmb.09.20

Rodríguez, J. C., Cebrián, L., López, M., Ruiz, M., Jiménez, I., & Royo, G. (2004). Mutant prevention concentration: Comparison of fluoroquinolones and linezolid with Mycobacterium tuberculosis. *Journal of Antimicrobial Chemotherapy*, *53*(3), 441–444. https://doi.org/10.1093/jac/dkh119

Roger, C., Roberts, J. A., & Muller, L. (2018, May 23). Clinical Pharmacokinetics and Pharmacodynamics of Oxazolidinones. *Clinical Pharmacokinetics*. Springer International Publishing. https://doi.org/10.1007/s40262-017-0601-x

Roos, A. K., Andersson, C. E., Bergfors, T., Jacobsson, M., Karlén, A., Unge, T., … Mowbray, S. L. (2004). Mycobacterium tuberculosis ribose-5-phosphate isomerase has a known fold, but a novel active site. *Journal of Molecular Biology*, *335*(3), 799–809. https://doi.org/10.1016/j.jmb.2003.11.021

Roos, A. K., Mariano, S., Kowalinski, E., Salmon, L., & Mowbray, S. L. (2008). d-Ribose-5-Phosphate Isomerase B from Escherichia coli is Also a Functional d-Allose-6-Phosphate Isomerase, While the Mycobacterium tuberculosis Enzyme is Not. *Journal of Molecular Biology*, *382*(3), 667–679. https://doi.org/10.1016/j.jmb.2008.06.090

Sakula, A. (1982). Robert Koch: Centenary of the discovery of the tubercle bacillus, 1882. *Bulletin of the International Union against Tuberculosis*, *57*(2), 111–116. Retrieved from /pmc/articles/PMC1790283/?report=abstract

Sander, P., Belova, L., Kidan, Y. G., Pfister, P., Mankin, A. S., & Böttger, E. C. (2002). Ribosomal and non-ribosomal resistance to oxazolidinones: Species-specific idiosyncrasy of ribosomal alterations. *Molecular Microbiology*, *46*(5), 1295–1304. https://doi.org/10.1046/j.1365-2958.2002.03242.x

Sarah M. Batt, Talat Jabeen, Veemal Bhowruth, Lee Quill, Peter A. Lund, Lothar Eggeling, Luke J. Alderwick, Klaus Fütterer, and G. S. B. (2012). Structural basis of inhibition of Mycobacterium tuberculosis DprE1 by benzothiazinone inhibitors. *PNAS*, *109*(28), 11354–11359. https://doi.org/10.1021/acsinfecdis.5b00065

Schaberg, T., Bauer, T., Brinkmann, F., Diel, R., Feiterna-Sperling, C., Haas, W., … Stahlmann, R. (2017). Tuberculosis guideline for adults: Guideline for diagnosis and treatment of tuberculosis including LTBI testing and treatment of the German Central Committee (DZK) and the German Respiratory Society (DGP). *Pneumologie*. https://doi.org/10.1055/s-0043-105954

Scherman, M. S., Kalbe-Bournonville, L., Bush, D., Xin, Y., Deng, L., & McNeil, M. (1996). Polyprenylphosphate-pentoses in mycobacteria are synthesized from 5- phosphoribose pyrophosphate. *Journal of Biological Chemistry*, *271*(47), 29652–29658. https://doi.org/10.1074/jbc.271.47.29652

Schurz, H., Daya, M., Möller, M., Hoal, E. G., & Salie, M. (2015). TLR1, 2, 4, 6 and 9 Variants Associated with Tuberculosis Susceptibility: A Systematic Review and Meta-Analysis. *PloS One*, *10*(10), e0139711. https://doi.org/10.1371/journal.pone.0139711

Seng, P., Drancourt, M., Gouriet, F., La Scola, B., Fournier, P., Rolain, J. M., & Raoult, D. (2009). Ongoing Revolution in Bacteriology: Routine Identification of Bacteria by Matrix-Assisted Laser Desorption Ionization Time-of-Flight Mass Spectrometry. *Clinical Infectious Diseases*, *49*(4), 543–551. https://doi.org/10.1086/600885

Shah, N. S., Yuen, C. M., Heo, M., Tolman, A. W., & Becerra, M. C. (2013). Yield of Contact Investigations in Households of Patients With Drug-Resistant Tuberculosis: Systematic Review and Meta-Analysis. https://doi.org/10.1093/cid/cit643

Sharadamma, N., Harshavardhana, Y., Ravishankar, A., Anand, P., Chandra, N., & Muniyappa, K. (2015). Molecular Dissection of *Mycobacterium tuberculosis* Integration Host Factor Reveals Novel Insights into

the Mode of DNA Binding and Nucleoid Compaction. *Biochemistry*, *54*(26), 4142–4160. https://doi.org/10.1021/acs.biochem.5b00447

Shinabarger, D. L., Marotti, K. R., Murray, R. W., Lin, A. H., Melchior, E. P., Swaney, S. M., … Buysse, J. M. (1997). Mechanism of action of oxazolidinones: Effects of linezolid and eperezolid on translation reactions. *Antimicrobial Agents and Chemotherapy*, *41*(10), 2132–2136. Retrieved from http://aac.asm.org/

Skeiky, Y. A. W., & Sadoff, J. C. (2006). Advances in tuberculosis vaccine strategies. *Nature Reviews Microbiology*, *4*(6), 469–476. https://doi.org/10.1038/nrmicro1419

Snapper, S. B., Melton, R. E., Mustafa, S., Kieser, T., & Jr, W. R. J. (1990). Isolation and characterization of efficient plasmid transformation mutants of Mycobacterium smegmatis. *Molecular Microbiology*, *4*(11), 1911–1919. https://doi.org/10.1111/J.1365-2958.1990.TB02040.X

Sommer, R., Neres, J., Piton, J., Dhar, N., Van Der Sar, A., Mukherjee, R., … Cole, S. T. (2018). Fluorescent Benzothiazinone Analogues Efficiently and Selectively Label Dpre1 in Mycobacteria and Actinobacteria. *ACS Chemical Biology*, *13*(11), 3184–3192. https://doi.org/10.1021/acschembio.8b00790

Song, T., Lee, M., Jeon, H. S., Park, Y., Dodd, L. E., Dartois, V., … Chen, R. Y. (2015). Linezolid Trough Concentrations Correlate with Mitochondrial Toxicity-Related Adverse Events in the Treatment of Chronic Extensively Drug-Resistant Tuberculosis. *EBioMedicine*, *2*(11), 1627–1633. https://doi.org/10.1016/j.ebiom.2015.09.051

Soriano, A., Miró, O., & Mensa, J. (2005). Mitochondrial Toxicity Associated with Linezolid. *New England Journal of Medicine*, *353*(21), 2305–2306. https://doi.org/10.1056/NEJM200511243532123

Sotgiu, G., Centis, R., Ambrosio, L. D. ', Alffenaar, J.-W. C., Anger, H. A., Caminero, J. A., … Migliori, G. B. (2012). Efficacy, safety and tolerability of linezolid containing regimens in treating MDR-TB and XDR-TB: systematic review and meta-analysis. https://doi.org/10.1183/09031936.00022912

Srivastava, S., Magombedze, G., Koeuth, T., Sherman, C., Pasipanodya, J. G., Raj, P., … Gumbo, T. (2017). Linezolid dose that maximizes sterilizing effect while minimizing toxicity and resistance emergence for tuberculosis. *Antimicrobial Agents and Chemotherapy*, *61*(8). https://doi.org/10.1128/AAC.00751-17

Stahl, D. A., & Urbance, J. W. (1990). The division between fast- and slow-growing species corresponds to natural relationships among the mycobacteria. *Journal of Bacteriology*, *172*(1), 116–124. https://doi.org/10.1128/jb.172.1.116-124.1990

Stalker, D. J., & Jungbluth, G. L. (2003). Clinical Pharmacokinetics of Linezolid, a Novel Oxazolidinone Antibacterial. *Clinical Pharmacokinetics*. Springer International Publishing. https://doi.org/10.2165/00003088-200342130-00004

Stock, A. M., & Zhulin, I. B. (2017). Two-Component Signal Transduction: a Special Issue in the Journal of Bacteriology. *J Bacteriol Journal of Bacteriology On*, *199*(18), 443–17. https://doi.org/10.1128/JB

Suárez, I., Fünger, S. M., Rademacher, J., Fätkenheuer, G., Kröger, S., & Rybniker, J. (2019). Übersichtsarbeit Diagnostik und Therapie der Tuberkulose. *Deutsches Arzteblatt International*, *116*(43), 729–735. https://doi.org/10.3238/arztebl.2019.0729

Swaney, S. M., Aoki, H., Ganoza, M. C., & Shinabarger, D. L. (1998). The oxazolidinone linezolid inhibits initiation of protein synthesis in bacteria. *Antimicrobial Agents and Chemotherapy*, *42*(12), 3251–3255. Retrieved from https://www-ncbi-nlm-nih-gov.emedien.ub.uni-muenchen.de/pmc/articles/PMC106030/pdf/ac003251.pdf

Szájli, E., Fehér, T., & Medzihradszky, K. F. (2008). Investigating the quantitative nature of MALDI-TOF MS. *Molecular and Cellular Proteomics*, *7*(12), 2410–2418. https://doi.org/10.1074/mcp.M800108-MCP200

Tallarida, R. J. (2011, November). Quantitative Methods for Assessing Drug Synergism. *Genes and Cancer*. Impact Journals, LLC. https://doi.org/10.1177/1947601912440575

Tan, K. E., Ellis, B. C., Lee, R., Stamper, P. D., Zhang, S. X., & Carroll, K. C. (2012). Prospective evaluation of a matrix-assisted laser desorption ionization-time of flight mass spectrometry system in a hospital clinical microbiology laboratory for identification of bacteria and yeasts: A bench-by-bench study for assessing the impact on ti. *Journal of Clinical Microbiology*, *50*(10), 3301–3308. https://doi.org/10.1128/JCM.01405-12

Tanaka, K., Waki, H., Ido, Y., Akita, S., Yoshida, Y., Yoshida, T., & Matsuo, T. (1988). Protein and polymer analyses up tom/z 100 000 by laser ionization time-of-flight mass spectrometry. *Rapid Communications in Mass*

Spectrometry, *2*(8), 151–153. https://doi.org/10.1002/rcm.1290020802

Tang, S., Yao, L., Hao, X., Zhang, X., Liu, G., Liu, X., … Zhang, Z. (2015). Efficacy, safety and tolerability of linezolid for the treatment of XDR-TB: a study in China. *The European Respiratory Journal*, *45*(1), 161–170. https://doi.org/10.1183/09031936.00035114

Thanky, N. R., Young, D. B., & Robertson, B. D. (2007). Unusual features of the cell cycle in mycobacteria: polar-restricted growth and the snapping-model of cell division. *Tuberculosis (Edinburgh, Scotland)*, *87*(3), 231–236. https://doi.org/10.1016/j.tube.2006.10.004

Tiwari, R., Miller, P. A., Cho, S., Franzblau, S. G., & Miller, M. J. (2015). Syntheses and antituberculosis activity of 1,3-benzothiazinone sulfoxide and sulfone derived from BTZ043. *ACS Medicinal Chemistry Letters*, *6*(2), 128–133. https://doi.org/10.1021/ml5003458

Tran, A., Alby, K., Kerr, A., Jones, M., & Gilligan, P. H. (2015). Cost savings realized by implementation of routine microbiological identification by matrix-assisted laser desorption ionization-time of flight mass spectrometry. *Journal of Clinical Microbiology*, *53*(8), 2473–2479. https://doi.org/10.1128/JCM.00833-15

Trefzer, C., Rengifo-Gonzalez, M., Hinner, M. J., Schneider, P., Makarov, V., Cole, S. T., & Johnsson, K. (2010). Benzothiazinones: prodrugs that covalently modify the decaprenylphosphoryl-β-D-ribose 2'-epimerase DprE1 of Mycobacterium tuberculosis. *Journal of the American Chemical Society*, *132*(39), 13663–13665. https://doi.org/10.1021/ja106357w

Trefzer, C., Škovierová, H., Buroni, S., Bobovská, A., Nenci, S., Molteni, E., … Johnsson, K. (2012). Benzothiazinones are suicide inhibitors of mycobacterial decaprenylphosphoryl-β-d-ribofuranose 2′-oxidase DprE1. *Journal of the American Chemical Society*, *134*(2), 912–915. https://doi.org/10.1021/ja211042r

Trobro, S., & Åqvist, J. (2008). Role of Ribosomal Protein L27 in Peptidyl Transfer †. *Biochemistry*, *47*(17), 4898–4906. https://doi.org/10.1021/bi8001874

Tullius, M. V, Harmston, C. A., Owens, C. P., Chim, N., Morse, R. P., McMath, L. M., … Goulding, C. W. (2011). Discovery and characterization of a unique mycobacterial heme acquisition system. *Proceedings of the National Academy of Sciences of the United States of America*, *108*(12), 5051–5056. https://doi.org/10.1073/pnas.1009516108

Turner, R. D., & Bothamley, G. H. (2014). Cough and the Transmission of Tuberculosis. https://doi.org/10.1093/infdis/jiu625

Vynnycky, E., & Fine, P. E. M. (2000). Lifetime risks, incubation period, and serial interval of tuberculosis. *American Journal of Epidemiology*, *152*(3), 247–263. https://doi.org/10.1093/aje/152.3.247

Wang, R., Prince, J. T., & Marcotte, E. M. (2005). Mass spectrometry of the M-smegmatis proteome: Protein expression levels correlate with function, operons, and codon bias. *Genome Research*, *15*(8), 1118–1126. https://doi.org/10.1101/gr.3994105

Wang, Y., & Xiao, M. (2012). Role of the ribosomal protein L27 revealed by single-molecule FRET study. *Protein Science*, *21*(11), 1696–1704. https://doi.org/10.1002/pro.2149

Welshman, I. R., Sisson, T. A., Jungbluth, G. L., Stalker, D. J., & Hopkins, N. K. (2001). Linezolid absolute bioavailability and the effect of food on oral bioavailability. *Biopharmaceutics & Drug Disposition*, *22*(3), 91–97. Retrieved from http://www.ncbi.nlm.nih.gov/pubmed/11745911

WHO consolidated guidelines on tuberculosis. (2022). *Module 4: Treatment Drug-susceptible tuberculosis treatment*. Geneva: World Health Organization.

Wiegand, I., Hilpert, K., & Hancock, R. E. W. (2008). Agar and broth dilution methods to determine the minimal inhibitory concentration (MIC) of antimicrobial substances. *Nature Protocols*, *3*(2), 163–175. https://doi.org/10.1038/nprot.2007.521

Wieser, A., Schneider, L., Jung, J., & Schubert, S. (2012). MALDI-TOF MS in microbiological diagnostics-identification of microorganisms and beyond (mini review). *Applied Microbiology and Biotechnology*, *93*(3), 965–974. https://doi.org/10.1007/s00253-011-3783-4

Williams, G. T., & Williams, W. J. (1983). Granulomatous inflammation - A review. *Journal of Clinical Pathology*. BMJ Publishing Group. https://doi.org/10.1136/jcp.36.7.723

Wolff, M. M., & Stephens, W. E. (1953). A pulsed mass spectrometer with time dispersion. *Review of Scientific Instruments*, *24*(8), 616–617. https://doi.org/10.1063/1.1770801

Wolucka, B. A. (2008). Biosynthesis of D-arabinose in mycobacteria - a novel bacterial pathway with implications for antimycobacterial therapy. *The FEBS Journal*, *275*(11), 2691–2711. https://doi.org/10.1111/j.1742-4658.2008.06395.x

World Health Organization. (2017). *END TB Global Tuberculosis Report 2017*. https://doi.org/10.1001/jama.2014.11450

World Health Organization. (2019). WHO | Global tuberculosis report 2019. *World Health Organization*. https://doi.org/.1037//0033-2909.I26.1.78

World Health Organization. (2022). *WHO consolidated guidelines on tuberculosis. WHO Press*.

Yajko, D. M., Sanders, C. A., Nassos, P. S., & Hadley, W. K. (1990). In vitro susceptibility of Mycobacterium avium complex to the new fluoroquinolone sparfloxacin (CI-978; AT-4140) and comparison with ciprofloxacin. *Antimicrobial Agents and Chemotherapy*, *34*(12), 2442–2444. https://doi.org/10.1128/AAC.34.12.2442

Yates, T. A., Khan, P. Y., Knight, G. M., Taylor, J. G., McHugh, T. D., Lipman, M., … Abubakar, I. (2016, February 1). The transmission of Mycobacterium tuberculosis in high burden settings. *The Lancet Infectious Diseases*. Lancet Publishing Group. https://doi.org/10.1016/S1473-3099(15)00499-5

Zahedi Bialvaei, A., Rahbar, M., Yousefi, M., Asgharzadeh, M., & Samadi Kafil, H. (2017). Linezolid: a promising option in the treatment of Gram-positives. *Journal of Antimicrobial Chemotherapy*, *72*(2), 354–364. https://doi.org/10.1093/jac/dkw450

Zhang, X., Falagas, M. E., Vardakas, K. Z., Wang, R., Qin, R., Wang, J., & Liu, Y. (2015). Systematic review and meta-analysis of the efficacy and safety of therapy with linezolid containing regimens in the treatment of multidrug-resistant and extensively drug-resistant tuberculosis. *Journal of Thoracic Disease*, *7*(4), 603–615. https://doi.org/10.3978/j.issn.2072-1439.2015.03.10

Zhu, C., Liu, Y., Hu, L., Yang, M., & He, Z.-G. (2018). Molecular mechanism of the synergistic activity of ethambutol and isoniazid against *Mycobacterium tuberculosis*. *Journal of Biological Chemistry*, jbc.RA118.002693. https://doi.org/10.1074/jbc.RA118.002693

Register of Figures

Register of Tables

Abbreviations

BCG – *Mycobacterium bovis* - Bacillus Calmette-Guerin

BTZ; B – here: Benzothiazinone compound BTZ043

COG – Center of Gravity

CFU – Colony Forming Units

C_{max} – Maximum plasma concentration

C_{min} – Trough plasma concentration

DNA – Deoxyribonucleic acid

DprE1 – Decaprenylphosphoryl-beta-D-ribose-Epimerase 1

HPLC-MS/MS – High performance liquid chromatography tandem mass spectrometry (Hoch-leistungsflüssigkeitschromatographie mit Tandem Massenspektrometrie-Kopplung)

IGRA – Interferon-Gamma-Release Assay

KBE – Kolonie Bildende Einheiten

LMU – Ludwig-Maximilians-Universität

LZD; L – Linezolid

LTBI – Latent tuberculosis infection

MALDI-TOF MS – Matrix-assisted laser desorption/ionization time of flight mass spectrometry

MDR-TB – Multi-drug resistant tuberculosis

mRNA – Messenger ribonucleic acid

M. smegmatis – *Mycobacterium smegmatis*

M. tuberculosis – *Mycobacterium tuberculosis*

MIC – Minimal Inhibitory Concentration

M7H9 – Middlebrook 7H9 medium

OADC – Oleic Albumin Dextrose Catalase Middlebrook supplement

OD – Optical Density measured at 600 nm wavelength

p – Probability value or significance

PBS – Phosphate buffered saline

REMA – Resazurin microtiter assay

RF – Reduction factor

RNA – Ribonucleic acid

RR-TB – Rifampin-resistant tuberculosis

SEM – Scanning electron microscope

SILAC – stable isotope labeling by amino acids in cell culture

tRNA - Transfer ribonucleic acid

TST – Tuberculin skin test

TUM – Technische Universität München

T80 – Tween 80

WHO – World Health Organization

XDR-TB – Extensively drug-resistant tuberculosis

Acknowledgements

All names appear in the chronological order to the development of this project.

I heartily thank...

... Fanny Pernice, for the inspiration to an experimental doctoral thesis project.

... Michael Pritsch, for getting me in touch with the Tropical Institute of LMU and personal mentoring along the project.

...my supervisor PD Dr. med. Andreas Wieser, for enabling the entire project, his unstoppable enthusiasm, vision and constant support of my project.

... Dr. Anna-Cathrine Neumann-Cip, for the introduction to the laboratory, her enormous help on analyzing the MALDI-TOF MS data, for all of her figures and support in scientific writing.

.... the Tropical Institute of the LMU under Prof. Dr. med. Hoelscher for physical and material provision.

... Sarah Sternkopf, for her patience and her personal encouragement into my work.

... Gabi Liegl, the good soul of our laboratory.

... Christine Benning and TUM, for the extraordinary opportunity to take pictures with the SEM.

… David Bauer, who mentally supported me with great coffee breaks and the introduction to the program Fiji.

... Boj Friedrich Hoppe, for providing me with a graph pad for my figures.

... Prof. Dr. Christoph Haisch, for the pivotal support of getting my mind into the deeper back-grounds of mass spectrometry.

... to all employees of the Max-von-Pettenkofer-Institute in Großhadern, who have supported my experiments by assisting, advising or helping in any other way.

… Marlene Gertz, for her introduction into formatting my thesis.

... to Viviana Gomez Ramirez as a friend who supported this project personally.

…Philip Werner, for letting me experience that even in stress, trust can win over control.

... my mother, who did not get tired of encouraging me to complete this project.

Affidavit

LMU LUDWIG-MAXIMILIANS-UNIVERSITÄT MÜNCHEN | Promotionsbüro Medizinische Fakultät | MMRS

Eidesstattliche Versicherung

Ich, Alexandra Burger, erkläre hiermit an Eides statt, dass ich die vorliegende Dissertation mit dem Titel:

„Linezolid and BTZ043 Combined Activity against *M. smegmatis* as a Precursor Model for New Combined Antimicrobial Treatment of *M. tuberculosis*"

selbständig verfasst, mich außer der angegebenen keiner weiteren Hilfsmittel bedient und alle Erkenntnisse, die aus dem Schrifttum ganz oder annähernd übernommen sind, als solche kenntlich gemacht und nach ihrer Herkunft unter Bezeichnung der Fundstelle einzeln nachgewiesen habe.

Ich erkläre des Weiteren, dass die hier vorgelegte Dissertation nicht in gleicher oder in ähnlicher Form bei einer anderen Stelle zur Erlangung eines akademischen Grades eingereicht wurde.

Traunstein, 1.12.2025
Ort, Datum

Alexandra Burger
Alexandra Burger